ORNL/M-4997

ornl

OAK RIDGE NATIONAL LABORATORY

LOCKHEED MARTIN

DEVELOPMENT OF LIFETIME TEST PROCEDURE FOR POWDER EVACUATED PANEL INSULATION

Final Report for CRADA Number ORNL 91-0042

K. E. Wilkes
R. S. Graves
K. W. Childs

March 1996

PROTECTED CRADA INFORMATION

This product contains Protected CRADA Information which was produced on March 22, 1996 under CRADA No. ORNL 91-0042 and is not to be further disclosed for a period of three (3) years from the date it was produced except as expressly provided for in the CRADA.

Expired 3/22/1999 per KEW

Prepared by
OAK RIDGE NATIONAL LABORATORY
Oak Ridge, Tennessee 37831
Managed by
LOCKHEED MARTIN ENERGY RESEARCH CORP.
for the
U.S. DEPARTMENT OF ENERGY
under contract DE-AC05-96OR22464

MANAGED AND OPERATED BY
LOCKHEED MARTIN ENERGY RESEARCH CORPORATION
FOR THE UNITED STATES
DEPARTMENT OF ENERGY

ORNL-27 (3-96)

ORNL/M-4997

Metals and Ceramics Division

CRADA Final Report
for CRADA Number ORNL 91-0042

DEVELOPMENT OF LIFETIME TEST PROCEDURE FOR POWDER EVACUATED PANEL INSULATION

K. E. Wilkes, R. S. Graves, and K. W. Childs

Date Published - March 1996

Prepared for the
U. S. Department of Energy
Office of Buildings Energy Research

and

Appliance Research Consortium

Prepared by
OAK RIDGE NATIONAL LABORATORY
Oak Ridge, Tennessee 37831
Managed by
LOCKHEED MARTIN ENERGY RESEARCH CORP.
for the
U.S. DEPARTMENT OF ENERGY
under contract DE-AC05-96OR22464

TABLE OF CONTENTS

LIST OF FIGURES v

LIST OF TABLES vii

ABSTRACT 1

1. OBJECTIVES OF CRADA 1

2. BENEFITS OF CRADA TO DOE 2

3. TECHNICAL DISCUSSION OF RESULTS 2
   - 3.1 Phase I 2
   - 3.2 Phase II 8
   - 3.3 Phase III 9
     - 3.3.1 Accelerated Aging and Determination of Permeance of Barrier Film 11
     - 3.3.2 Measurement of Thermal Resistivity versus Pressure 39
     - 3.3.3 Predictions of Lifetime Aging of PEPs 44
   - 3.4 Phase IV 47
     - 3.4.1 Test Panels 47
     - 3.4.2 Experimental Procedures 49
     - 3.4.3 Results of Tests 50
       - 3.4.3.1 Superinsulation Panels 50
       - 3.4.3.2 Foam Insulation 50
       - 3.4.3.3 Composite Panels with Only Foam Insulation 57
       - 3.4.3.4 Composite Panels Containing Superinsulations 60

4. INVENTIONS 65

5. COMMERCIALIZATION POSSIBILITIES 65

6. PLANS FOR FUTURE COLLABORATIONS 65

7. CONCLUSIONS 66

8. ACKNOWLEDGEMENTS 68

9. REFERENCES 69

APPENDIX A 71

APPENDIX B 91

APPENDIX C 113

LIST OF FIGURES

1. Effect of Pressure on Thermal Resistivity of Powder Evacuated Panel Insulation 3
2. Aging of Powder Evacuated Panel Insulation 4
3. Metal Plate for use in Aging Tests 7
4. Interlaboratory Comparison of PEP Thermal Conductivity Measurements 10
5. Aging Data for Set 1 Panels in Air 23
6. Aging Data for Set 1 Panels in Helium 24
7. Aging Data for Set 2 Panels in Air 25
8. Aging Data for Set 2 Panels in Helium 26
9. Aging Data for Set 3 Panels in Air 27
10. Aging Data for Set 3 Panels in Helium 28
11. Preliminary Analysis of Tyvek Void Volume for Panels in Air 32
12. Preliminary Analysis of Tyvek Void Volume for Panels in Helium 33
13. Analysis of Tyvek Void Volume for Panels in Helium 34
14. Preliminary Analysis of Tyvek Void Volume for Panels in Air 36
15. Analysis of Tyvek Void Volume for Panels in Air 37
16. Probe Pressures Measured on Solid Metal-filledPanel with Known Internal Pressure 41
17. Probe Pressures Measured with Perforated Metal Panel with Known Internal Pressure 42
18. Thermal Resistivity of PEPs for Phase III 43
19. Lifetime Predictions for Internal Pressure for PEPs 45
20. Lifetime Predictions for Thermal Resistivity for PEPs 46
21. Construction of Composite Panels 48
22. Thermal Conductivity of CFC-11 Foam from Thin-Slicing Studies 53
23. Thermal Conductivity of HCFC-141b Foam from Thin-Slicing Studies 54
24. Thermal Conductivity of HCFC-142b/22 Foam from Thin-Slicing Studies 55
25. Thermal Conductivity of Foam Insulation from Composite Panels 59
26. Computer Model of Composite Panels Containing Superinsulations 61

LIST OF TABLES

1. Physical Characteristics of Panels for Lifetime Aging Tests 12
2. Aging Data for Panel 1-A 14
3. Aging Data for Panel 1-B 15
4. Aging Data for Panel 1-C 16
5. Aging Data for Panel 2-A 17
6. Aging Data for Panel 2-B 18
7. Aging Data for Panel 2-C 19
8. Aging Data for Panel 3-A 20
9. Aging Data for Panel 3-B 21
10. Aging Data for Panel 3-C 22
11. Results of Regression Analysis on Aging Data, Using Equation 8. 30
12. Tyvek Void Volumes of Sets of Panels in Air and Helium 38
13. Permeance of Vecat Film 38
14. Thermal Resistivities and Internal Pressures of PEPs for Phase III 40
15. Center-of Panel Thermal Resistivities of Superinsulation Panels 51
16. Regression Analyses of Foam Thermal Conductivity from Thin-Slicing Studies 56
17. Thermal Conductivity of Foam Insulation in Composite Panels 58
18. Thermal Resistance of Composite Panels Containing Superinsulations 63

DEVELOPMENT OF A LIFETIME TEST PROCEDURE FOR POWDER EVACUATED PANEL INSULATION

K. E. Wilkes, R. S. Graves, and K. W. Childs

ABSTRACT

This CRADA is between the Appliance Research Consortium (ARC) of the Association of Home Appliance Manufacturers (AHAM) and the Lockheed Martin Energy Research Corp. A Powder Evacuated Panel (PEP) is a "super" thermal insulation, having a thermal resistivity (R) substantially above that of existing insulation without the environmental problems of some insulations such as Chlorofluorocarbon (CFC) blown foam. For example, the R of a PEP is about 7 times that of fiberglass insulation and about 2.5 times that of CFC-blown foams. Consequently, development of PEPs could enable their use in many energy conservation applications as well as reducing the use of environmentally unacceptable insulation. One of the most promising applications of PEPs is in home refrigerator/freezers (R/Fs). The R/F industry estimates that 6 to 12 percent of the energy used by current R/F models could be saved if they were insulated with PEPs in combination with foamed plastics. A major accomplishment needed for development of PEPs is the determination of their lifetimes, which must exceed 20 years for R/F applications. The R of PEPs decrease with time due to diffusion of air through the PEPs semipermeable vacuum barrier material.

The goal of the CRADA, therefore, was to develop a procedure that will predict the lifetime of a PEP in dry air. The procedure must accelerate the aging processes of a PEP so the test is completed in less than 6 months to yield the lifetime in a reasonable time. Also, the procedure must be relatively inexpensive so that it can be used to screen potential PEP designs at an acceptable cost. It is anticipated that the test procedure could be employed to determine the lifetime in air of PEP designs for applications other than R/Fs.

1. OBJECTIVES OF CRADA

The overall objective of this CRADA was to develop and verify a lifetime test procedure for Powder Evacuated Panel (PEP) insulation in dry air. The CRADA was to be performed in four Phases. Phase I had the objective of developing the lifetime test procedure. Phase II was an interlaboratory comparison of measurements of the thermal resistivity (R) of PEPs by members of the ARC. Phase III was to have been an interlaboratory comparison of the developed lifetime test procedure by members of the ARC. Phase IV had the objective of demonstrating the thermal performance of advanced insulation/foam composite simulated refrigerator doors.

2. BENEFITS OF CRADA TO DOE

A major part of the Building Materials Program, which is funded by the DOE Office of Buildings Energy Research, is the development of PEPs with higher R, lower costs, and longer lifetimes. The procedures and technology learned in developing the lifetime testing procedure will be of direct benefit to the R&D efforts of the Building Materials Program. ORNL will continue to utilize these procedures to evaluate the performance of alternative barrier materials that may result in longer useful lifetimes for PEPs.

3. TECHNICAL DISCUSSION OF RESULTS

3.1 Phase I

The lifetime testing procedure was developed in Phase I. The procedure was motivated by the knowledge that the thermal resistance of powder evacuated panels decreases as the internal pressure is increased, as shown in Figure 1. Since the components of air can permeate through the plastic barrier film, the internal pressure will rise over the lifetime of the panel, as shown schematically in Figure 2. Combining the trends in Figures 1 and 2 results in a curve of thermal resistance versus time, also shown in Figure 2. It is hoped that the pressure rise in a PEP will occur slowly, so that the useful lifetime of a PEP will be on the order of 20 years. In order to assess the useful lifetime of a PEP in a reasonable amount of time, the goal of Phase I was to develop a procedure that would take on the order of six months to perform.

To design an accelerated testing procedure, it is necessary to examine the equations that govern the rise of pressure in a PEP. Consider a PEP with an internal volume V, a surface area A, and initial pressure P_0. If the PEP is surrounded by a gas at pressure P_a and temperature T, the volume flow rate, Q, at which the gas permeates through the surface is given by

$$Q = K A (P_a - P) \qquad (1)$$

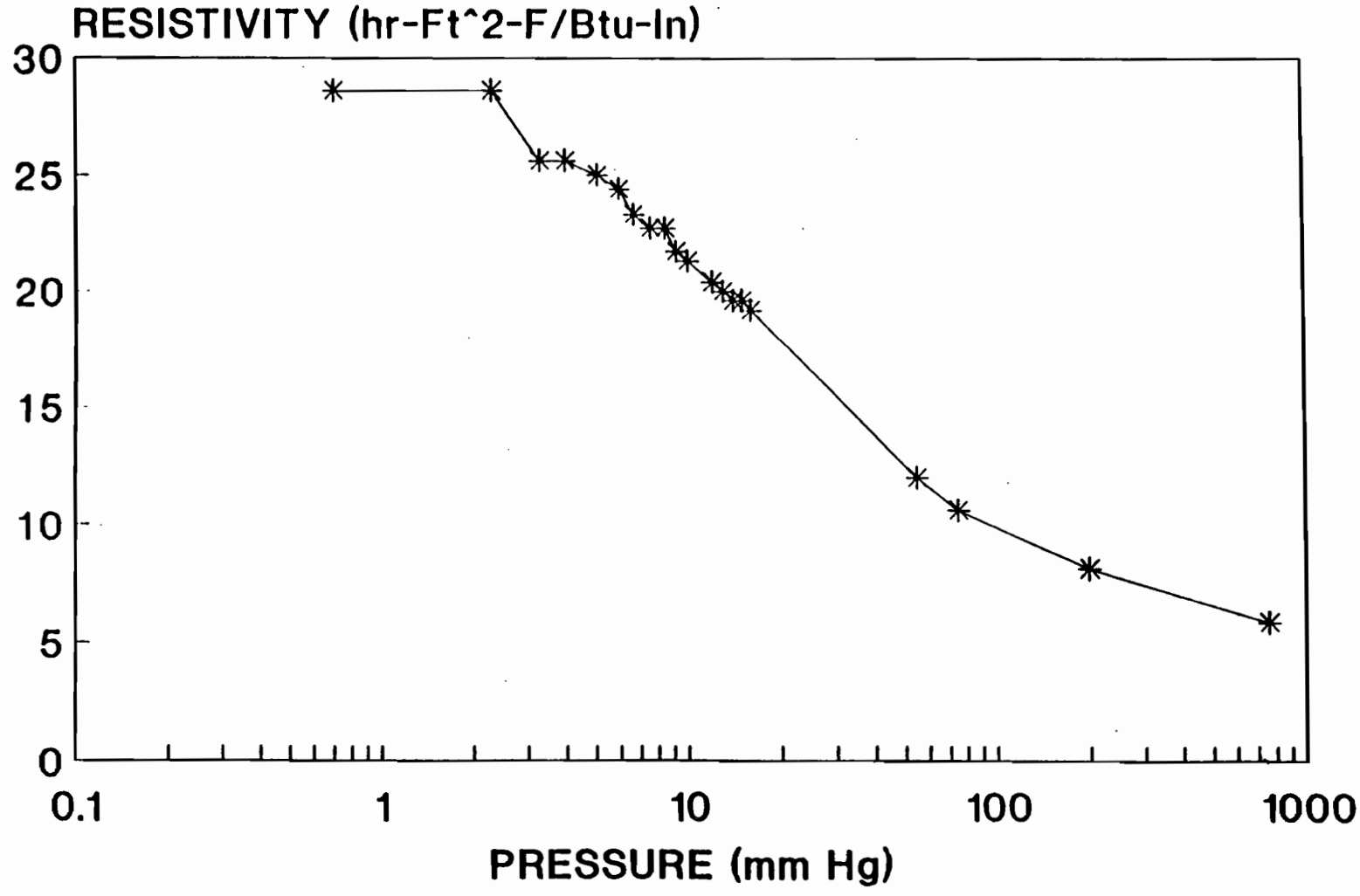

Figure 1. Effect of Pressure on Thermal Resistivity of Powder Evacuated Panel Insulation

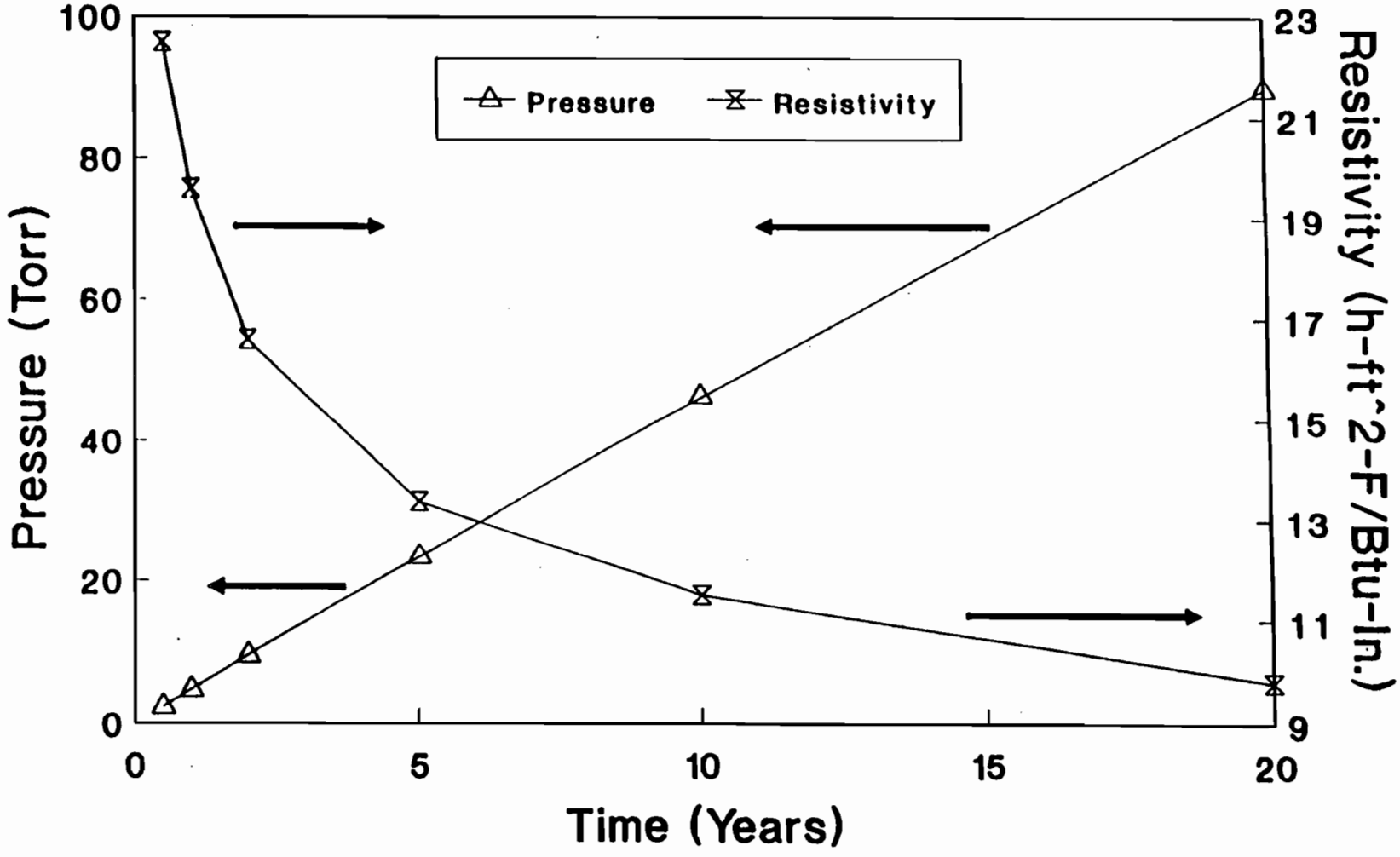

Figure 2. Aging of Powder Evacuated Panel Insulation.
The numbers on this figure are hypothetical and do not represent results on real PEPs.

where K is the permeance of the surface. A common system of units for the permeance is cc(STP)/100 in.^{2}•atm•day. This is the number of cubic centimeters of gas, measured at standard temperature and pressure (0°C and 760 torr), that permeates through 100 square inches of surface per day under a full atmosphere of partial pressure difference. The mass flow rate of gas permeating through the surface is given by

$$\dot{m} = \rho_0 K A (P_a - P) \tag{2}$$

where ρ_0 is the density of the gas at standard temperature and pressure. The mass flow rate into the PEP may also be related to the mass gain inside the PEP by

$$\dot{m} = V \frac{d\rho}{dt} \tag{3}$$

where ρ is the density of the gas inside the PEP. Using the ideal gas law, $P = \rho RT/M$, where R is the universal gas constant and M is the molecular weight of the gas, Equations 2 and 3 may be rearranged to give

$$\rho_0 K A (P_a - P) = \frac{V M}{RT} \frac{dP}{dt} \tag{4}$$

Equation 4 may be integrated to give

$$P = P_a + (P_0 - P_a) \exp\left(- K \frac{A}{V} \frac{\rho_0 RT}{M} t \right) \tag{5}$$

The above equations are all based on the partial pressures of one gas. If the panel initially contains a partial pressure of another gas, then that partial pressure should be added to the pressure from Equation 5 to give a total pressure.

Equation 5 shows the factors that are needed to obtain an accelerated test. In particular, the ratio of surface area to internal volume should be made large. A way to do this is to replace

the powder with a solid filler material or a filler material with a much smaller volume for the gas to occupy. Then as the gas permeates through the barrier film, it will cause a more rapid increase in internal pressure. For this procedure, solid metal plates were chosen as a filler material with no internal volume. The same plates with a series of tiny holes provide fillers with very small and known amounts of internal volume. Figure 3 shows a shop drawing of aluminum plates that were fabricated for use in these tests. The figure also shows the layout of over 1000 small holes that were drilled into some of the plates to produce an internal volume that occupied about 5 percent of the volume of the plate. Since the filler material in a PEP has about 90 percent void volume, the aluminum plates with 5 percent void volume should give an acceleration of aging by a factor of about 18. Thus aging that occurs in a PEP over an 18 year period should occur in a panel made with a metal plate with 5 percent void volume in about one year. With smaller internal volumes in the metal plate, the acceleration should be more rapid.

To perform the aging tests, it is necessary that the ambient conditions surrounding the test panels be maintained at constant temperature and pressure over time periods of many months. To provide for these conditions, three aging chambers were fabricated. These were constructed from 24 inch diameter schedule 10 Type 304 stainless steel pipe. The chambers were 24 inches long and had a door fitted with a rubber O-ring. Internal shelves were added to hold the test panels. The chambers with fitted with a vacuum system and a valve system to allow flushing and filling the chambers with either dry nitrogen, dry air, or helium. The pressures inside the chambers were measured with capacitance manometers. The chambers were fitted with copper coils connected to constant temperature baths so that the chambers could be maintained at a constant temperature.

Briefly, the lifetime testing procedure consists of the following. Three test panels are constructed using a solid aluminum plate, an aluminum plate with 2.5 percent void volume, and an aluminum plate with 5 percent void volume. The plates are encapsulated in a Tyvek film and are then placed in a pouch made of the selected barrier film. These packages are placed in a vacuum packer, pumped down to about 0.5 torr, and then heat-sealed under vacuum. This sequence simulates the construction and fabrication of a PEP, with the only difference being the replacement of the filler powder with an aluminum plate. Internal pressures are measured in the

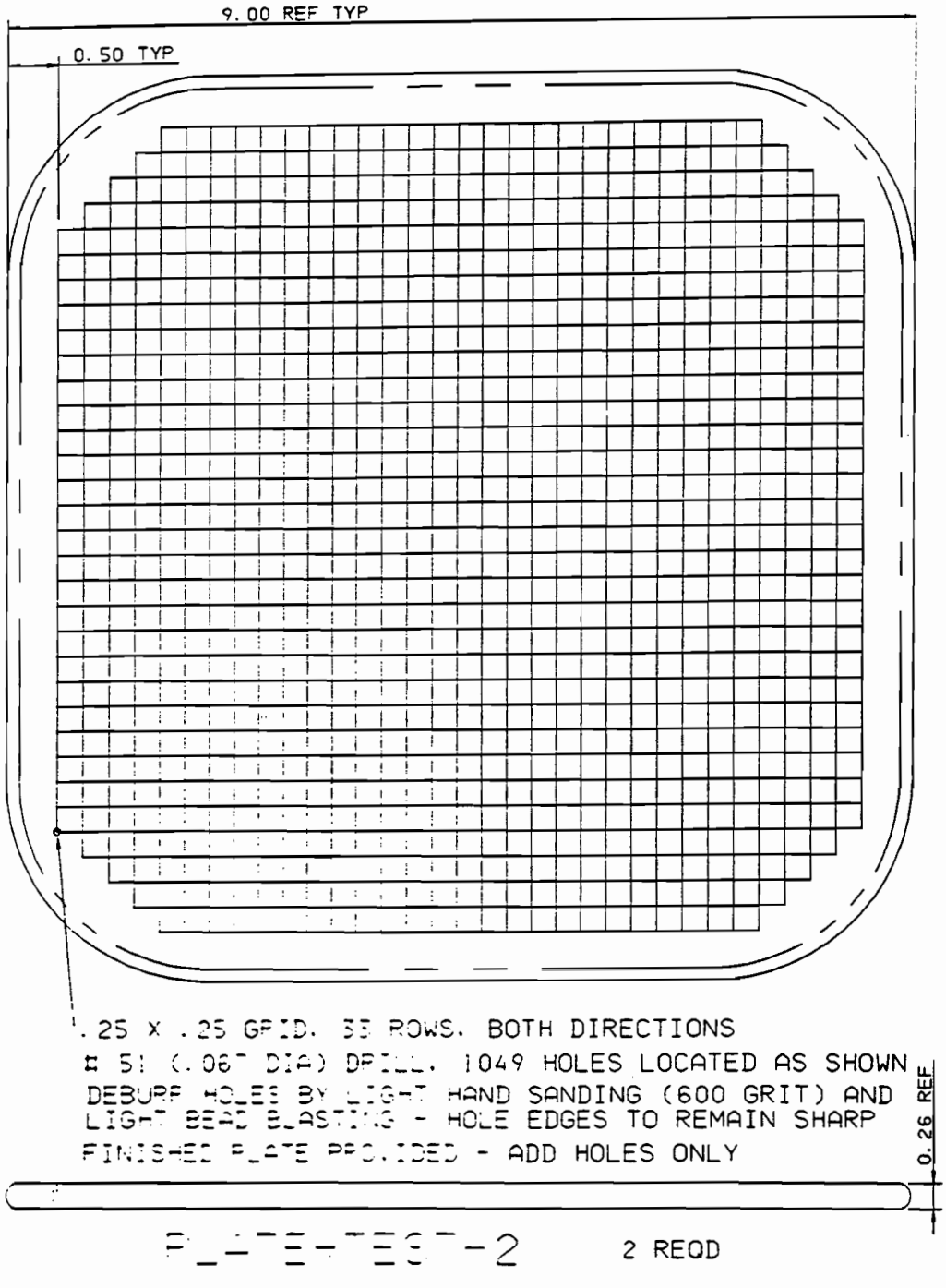

Figure 3. Metal Plate for Use in Aging Tests

panels and then they are placed in the aging chamber filled with dry air. For the tests performed in this study, the aging chamber was maintained at a constant temperature of 90°F and at a constant pressure of 785 torr. This pressure level was chosen to be slightly above atmospheric pressure, but the exact pressure was selected somewhat arbitrarily. The constant temperature corresponds to typical conditions used to test refrigerators.

After aging in air for about two weeks, the panels are removed from the aging chamber and allowed to cool to room temperature. The internal pressures are measured using the patented ORNL hand-held vacuum gauge.[1] The panels are then replaced in the aging chamber, and the above sequence is repeated at about two week intervals over a time period of about five months. After aging in air for about five months, the panels are transferred to the aging chamber fitted with helium. A sequence of pressure measurements is conducted during aging in helium. Since helium permeates through barrier films much more rapidly than does air, the pressure tests are done on a nearly daily basis over a time period of about a week. As will become evident in Section 3.3 on Phase III, the tests in helium are used to obtain an experimental value of the total internal volume of the test panel, including the known volume of the voids in the metal plates as well as the porosity of the Tyvek film.

Appendix A contains a writeup of the procedure that is also an invention disclosure. Appendix A gives results of preliminary tests that show the proof-of-principle of the procedure. Appendix B gives a more detailed step by step procedure for carrying out the procedure. When the procedure was carried in Phase III, additional details were learned and these modifications to the procedure are given in the Section 3.3.

3.2 Phase II

Phase II was an interlaboratory comparison of measurements of the thermal resistivity (R) of PEPs by members of the ARC. This Phase was intended to demonstrate the ability to obtain consistent thermal data on PEPs for constructing the curves of thermal resistance versus internal pressure that are needed, along with the curves of pressure versus time, to establish the thermal performance of PEPs over their lifetimes. A detailed report on this phase was presented at the 22nd International Thermal Conductivity Conference and was published in the proceedings of that

conference.[2] The paper is reproduced in Appendix C, and only a brief summary (taken from the abstract of the paper) will be given here.

The interlaboratory comparison was conducted by eight members of the ARC and by ORNL. Three different sizes of Heat Flow Meter Apparatuses (HFMAs) and specimens were employed in the work. GE Appliances fabricated five each of the three sizes of PEPs from the same materials to approximately the same powder density and internal PEP pressure. The three PEP sizes used were 6 × 6 in., 9.5 × 9.5 in., and 21.5 × 21.5 in. All PEPs were about 0.75 in. thick. To check the calibration of the HFMAs, an expanded polystyrene (EPS) specimen, supplied by ORNL for each size apparatus, was measured before and after measurements on the PEPs. The ASTM C 518 Test Method was employed for these measurements, which resulted in a two standard deviation (2σ) of 5.25% about the mean for the measurement by eight of the nine participating laboratories. Results of the thermal measurements on the PEPs are given in Figure 4. Measurements on the five specimens of the two larger sized PEPs by five other laboratories and ORNL, which measured on both sizes, demonstrate a 2σ of 7.4% about the mean. When the measurements of the other three laboratories and ORNL on the five smallest sized PEPs are included, the 2σ increases to 12.9% about the mean because the thermal conductivities of the smallest PEPs are higher than the other two sizes. The reason that the thermal conductivity of the smallest PEPs was higher than that of the other two sizes is not known. If the small specimen measurements are not included, the measured R-value for the nominally 0.75-inch-thick PEPs is 17.4 h•ft²•°F/Btu, and the average thermal resistivity is 23.2 h•ft²•°F/Btu•in. To within experimental error, the internal pressures in the PEPs did not change during the course of this work. These results demonstrated the ability of the nine laboratories to obtain consistent thermal resistances on PEPs.

3.3 Phase III

Phase III was intended to be an interlaboratory comparison of the aging procedure that was developed in Phase I. Three members of the ARC had originally intended to participate in this phase. However, each of them chose not to participate. Instead, ORNL agreed to perform the procedure in its entirety to gain further confidence in it and to determine the repeatability of

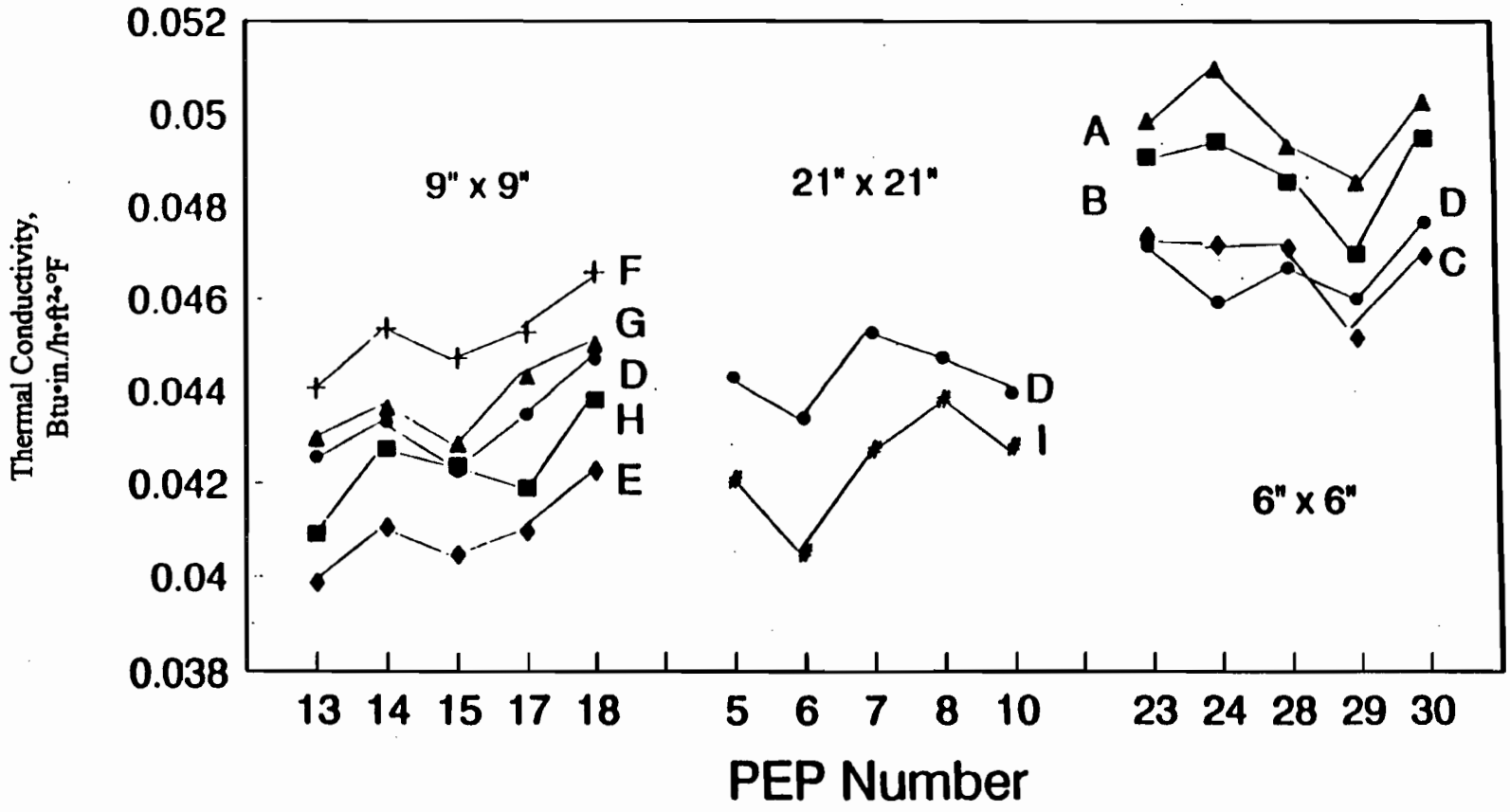

Figure 4. Interlaboratory Comparison of PEP Thermal Conductivity Measurements

the procedure.

3.3.1 Accelerated Aging and Determination of Permeance of Barrier Film

Nine test panels were fabricated for Phase III testing. Solid aluminum plates were machined as described in the Section 3.1. The density of each solid plate was measured by immersion in water and application of Archimedes' principle. Three plates were drilled with 1049 holes to give a void volume of about 5 percent of the plate's volume. Three other plates were similarly drilled to give a void volume of about 2.5 percent. The other three plates were left solid. Actual void volumes within the drilled metal plates were determined from the measured density and the weight loss upon drilling. The plates were cleaned and then baked in an oven at 250°F for one hour. Sheets of Tyvek film were also baked for one hour at 250°F. After baking, the plates were encapsulated in the Tyvek film, the heat sealed edges of which were trimmed to within about 1/8 to 1/4 inch of the metal plate. The Tyvek-encapsulated plates were then placed into pouches made of Vecat film. (Vecat is a multilayer polymer barrier film that is commonly used for PEPs.) This assembly was placed in a vacuum packer, and was pumped to a pressure of 0.5 torr for 1-1/2 hour, after which the open end of the Vecat pouch was heat-sealed under vacuum.

Table 1 gives the void volumes of the metal plates and the areas of the finished panels. Areas are measured to the inside edges of the heat seals, and include the area on both sides of the panels. The panels were divided into three sets, with each set containing one panel of each of the three void volumes. The widths of all Vecat pouches were approximately 10 inches, or just slightly larger than the 9 inch width of the aluminum plates. The lengths of Vecat pouches in Sets 1 and 2 were approximately 16 inches, while the lengths for Set 3 were approximately 10 inches. The original intent of the longer Vecat pouches was to provide a larger area for permeation of gases through the film, which was expected to result in a faster pressure rise. The shorter Vecat pouches were intended to test the hypothesis of acceleration of the testing by using larger area pouches.

After removal from the vacuum packer, the internal pressures of the panels were measured using the hand-held gauge. The panels were then placed in the air aging chamber. The panels were removed from the aging chamber periodically for measurement of the internal pressures in

Table 1. Physical Characteristics of Panels for Lifetime Aging Tests

Panel	Void Volume of Metal Plates, cm^3	Area between Seals, $in.^2$
1-A	0.00	312.5
1-B	7.51	312.8
1-C	15.20	317.8
2-A	0.00	316.4
2-B	7.66	316.0
2-C	15.24	317.0
3-A	0.00	203.0
3-B	7.47	201.0
3-C	15.24	202.8

the panels. After aging in the air chamber for about five months, the panels were transferred to the helium aging chamber. Aging in this chamber took place over a time period of several days. For the aging tests, both the air and helium chambers were maintained at 90°F and 785 torr.

Aging time and internal pressure data obtained on the nine panels are given in Tables 2-10 and are plotted in Figures 5-10. Figures 5-10 also show curves obtained from regression analyses of the data, as described below. These plots show that the pressure rise curves follow the expected trends. The pressure rise is much faster in the panels with very little internal volume, and very slow in the panels with the largest internal volume. Also, the pressure rise with helium is several orders of magnitude faster than with air.

As noted in Section 3.1, the pressure rise versus time is expected to be given by

$$P = P_b + P_a + (P_0 - P_a) \exp\left(- K \frac{A}{V} \frac{R T \rho_0}{M} t \right) \qquad (6)$$

where P is the total internal pressure, P_a is the ambient pressure in the aging chamber, P_0 is the initial partial pressure of the ambient gas in the panel, and P_b is the background partial pressure of other gases in the panel. For the sequence of experiments conducted here, P_0 for aging in air was taken to be the initial pressure reading on the panel and P_b was taken to be zero, since the gas trapped inside the panel immediately after fabrication would be air. For aging in helium, P_0 was taken to be zero, and P_b was taken to be the final pressure measured during aging in air (note that this assumes that very little of the air inside the panel will escape during the few days of aging in helium). It should be noted that the adjustment for the background pressure during aging in helium is a refinement added after the procedures in Appendices A and B were written.

Equation 6 may be rearranged to give

$$\ln\left(\frac{P - P_b - P_a}{P_0 - P_a} \right) = - K \frac{A}{V} \frac{R T \rho_0}{M} t \qquad (7)$$

A plot of the left hand side of this equation versus time should yield a straight line, with a slope that is equal to the factors multiplying the time on the right hand side. The data were transformed to the logarithmic quantity and a linear regression was used to find a and b in the following

Table 2. Aging Data for Panel 1-A

Gas	Time in Gas, hours	Internal Pressure, torr
Air	0.0	8.5*
Air	332.2	17.4
Air	643.7	18.2
Air	972.7	18.3
Air	1308.2	20.8
Air	1604.7	21.3
Air	1965.0	24.7
Air	2854.3	28.1
Air	4453.2	36.2
Helium	0.0	36.2
Helium	6.0	162.1
Helium	26.0	438.8
Helium	51.0	606.5

* Data point not used in regression analysis.

Table 3. Aging Data for Panel 1-B

Gas	Time in Gas, hours	Internal Pressure, torr
Air	0.0	13.6*
Air	360.2	12.2*
Air	1249.6	9.8
Air	2848.5	13.5
Air	3209.5	14.0
Air	3691.0	15.0
Helium	0.0	15.0
Helium	5.0	63.2
Helium	24.2	221.4
Helium	48.9	376.5
Helium	69.9	474.2

* Data points not used in regression analysis.

Table 4. Aging Data for Panel 1-C

Gas	Time in Gas, hours	Internal Pressure, torr
Air	0.0	4.1*
Air	360.2	10.5
Air	1249.6	10.5
Air	2848.5	10.7
Air	3209.5	12.2
Air	3691.0	12.2
Helium	0.0	12.2
Helium	5.0	42.1
Helium	24.2	147.2
Helium	48.9	260.6
Helium	69.9	341.4
Helium	112.3	466.5

* Data point not used in regression analysis.

Table 5. Aging Data for Panel 2-A

Gas	Time in Gas, hours	Internal Pressure, torr
Air	0.0	8.5*
Air	166.5	14.5
Air	478.0	16.7
Air	807.0	18.1
Air	1142.5	19.7
Air	1439.0	22.9
Air	1799.2	25.3
Air	2688.6	29.3
Air	4097.3	36.7
Helium	0.0	36.7
Helium	6.0	145.5
Helium	24.0	395.8
Helium	50.0	577.2

* Data point not used in regression analysis.

Table 6. Aging Data for Panel 2-B

Gas	Time in Gas, hours	Internal Pressure, torr
Air	0.0	5.0*
Air	166.5	4.5
Air	478.0	6.0
Air	807.0	7.2
Air	1142.5	7.8
Air	1439.0	8.5
Air	1799.2	8.3
Air	2688.6	10.2
Air	4097.3	14.0
Helium	0.0	14.0
Helium	6.0	64.9
Helium	24.0	199.8
Helium	50.0	357.1
Helium	98.0	551.5

* Data point not used in regression analysis.

Table 7. Aging Data for Panel 2-C

Gas	Time in Gas, hours	Internal Pressure, torr
Air	0.0	8.3
Air	166.5	8.5
Air	478.0	9.0
Air	807.0	8.7
Air	1142.5	9.3
Air	1439.0	10.5
Air	1799.2	10.8
Air	2688.6	11.4
Air	4097.3	12.5
Helium	0.0	12.5
Helium	6.0	44.3
Helium	24.0	139.2
Helium	50.0	257.6
Helium	98.0	416.5
Helium	162.2	561.5

Table 8. Aging Data for Panel 3-A

Gas	Time in Gas, hours	Internal Pressure, torr
Air	0.0	15.6*
Air	360.2	13.2
Air	1249.6	17.8
Air	2848.5	26.0
Air	3209.5	27.4
Air	3691.0	30.8
Helium	0.0	30.8
Helium	5.0	134.1
Helium	24.2	431.5
Helium	48.9	585.5*

* Data points not used in regression analysis.

Table 9. Aging Data for Panel 3-B

Gas	Time in Gas, hours	Internal Pressure, torr
Air	0.0	4.0*
Air	311.5	7.5
Air	640.5	6.5
Air	976.0	9.3
Air	1272.5	10.5
Air	1632.8	11.0
Air	2522.1	12.2
Air	4121.0	16.6
Air	4482.0	16.6
Air	4963.5	18.3
Helium	0.0	18.3
Helium	5.0	64.4
Helium	24.2	221.4
Helium	48.9	365.5
Helium	69.9	460.5

* Data point not used in regression analysis.

Table 10. Aging Data for Panel 3-C

Gas	Time in Gas, hours	Internal Pressure, torr
Air	0.0	10.2*
Air	360.2	6.0
Air	1249.6	6.3
Air	2848.5	7.1
Air	3209.5	7.7
Air	3691.0	8.7
Air	0.0	8.7
Air	5.0	38.4
Air	24.2	144.2
Helium	48.9	257.3
Helium	69.9	331.4
Helium	112.3	452.8

* Data point not used in regression analysis.

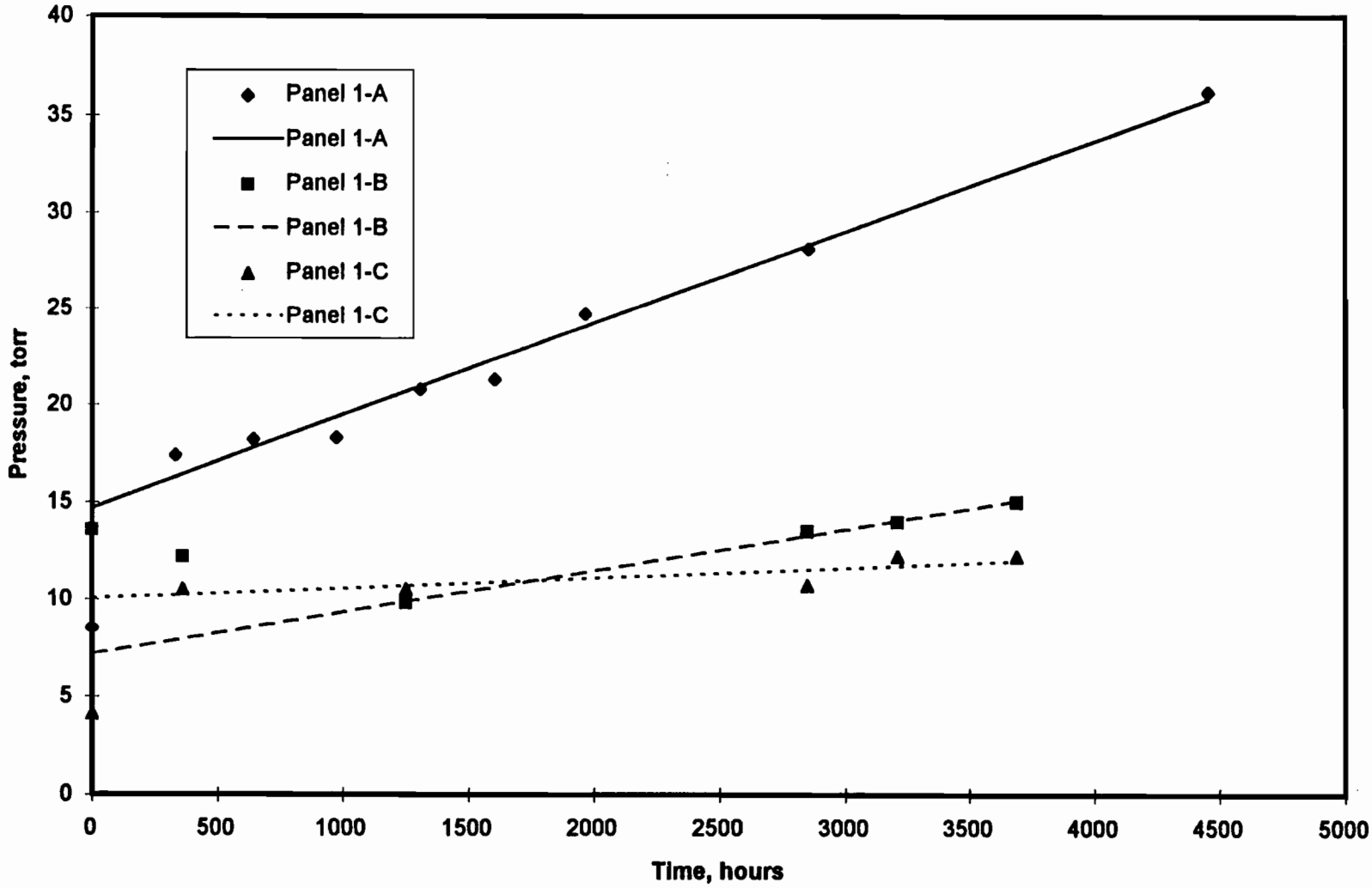

Figure 5. Aging Data for Set 1 Panels in Air

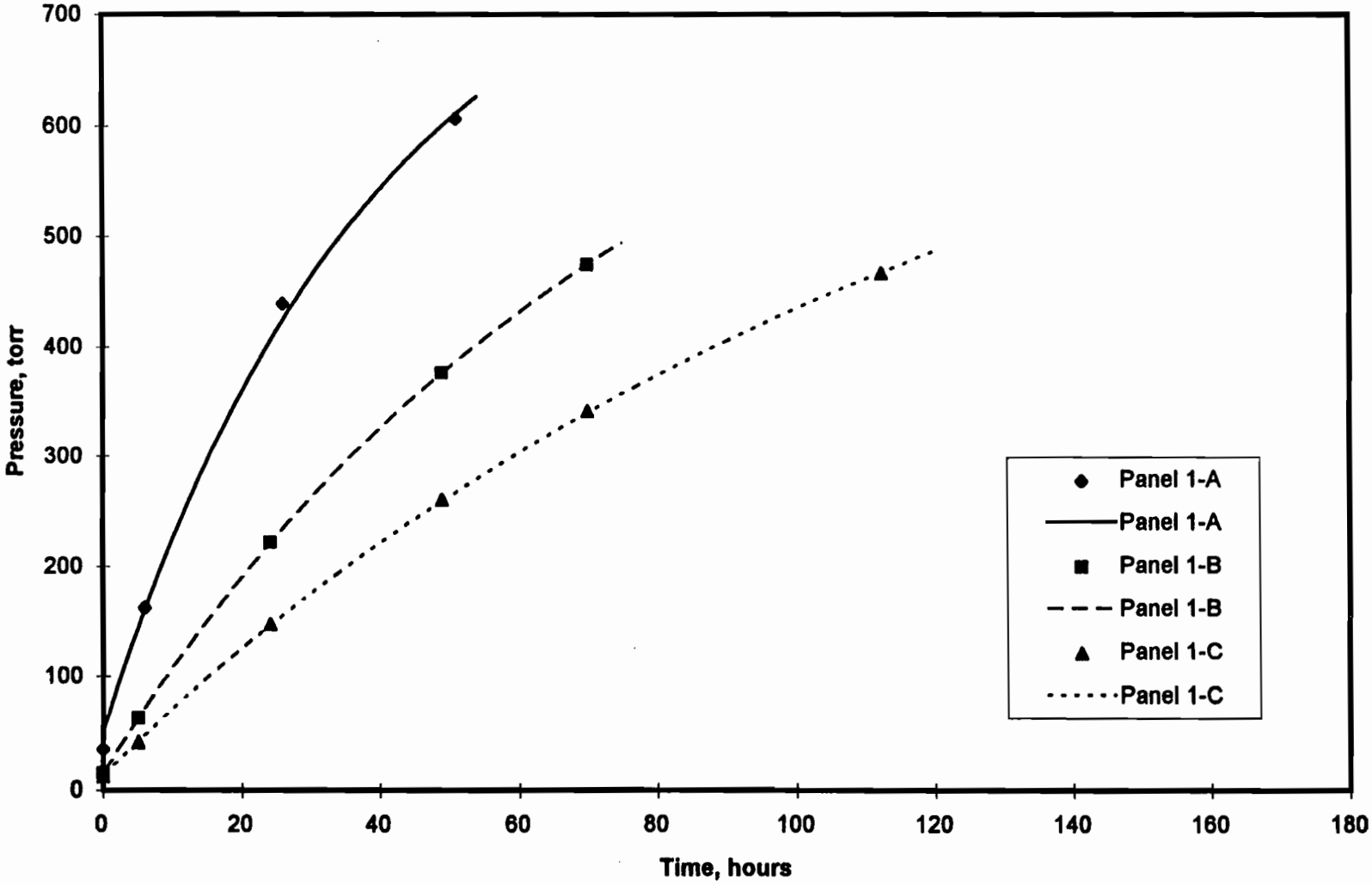

Figure 6. Aging Data for Set 1 Panels in Helium

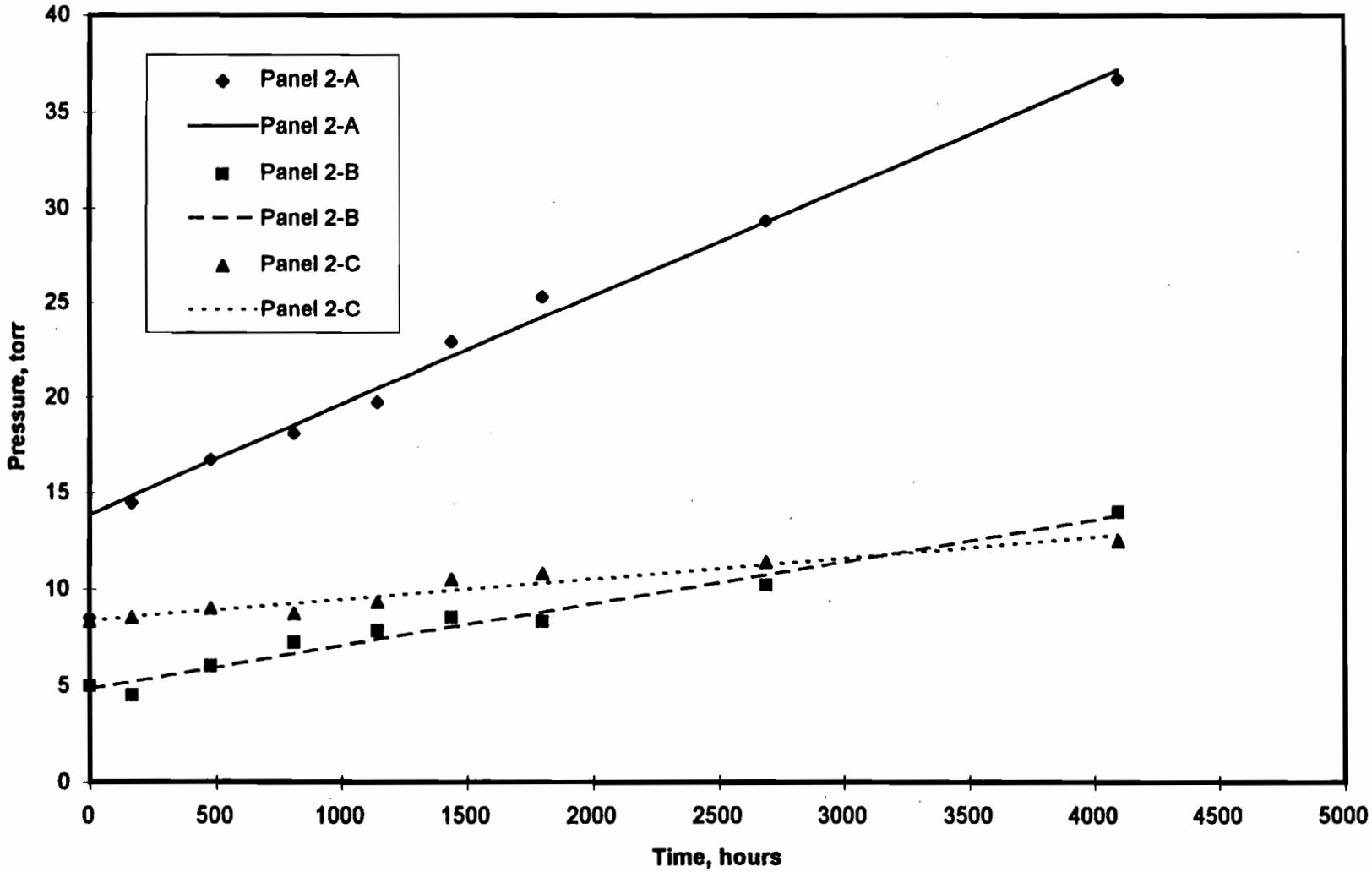

Figure 7. Aging Data for Set 2 Panels in Air

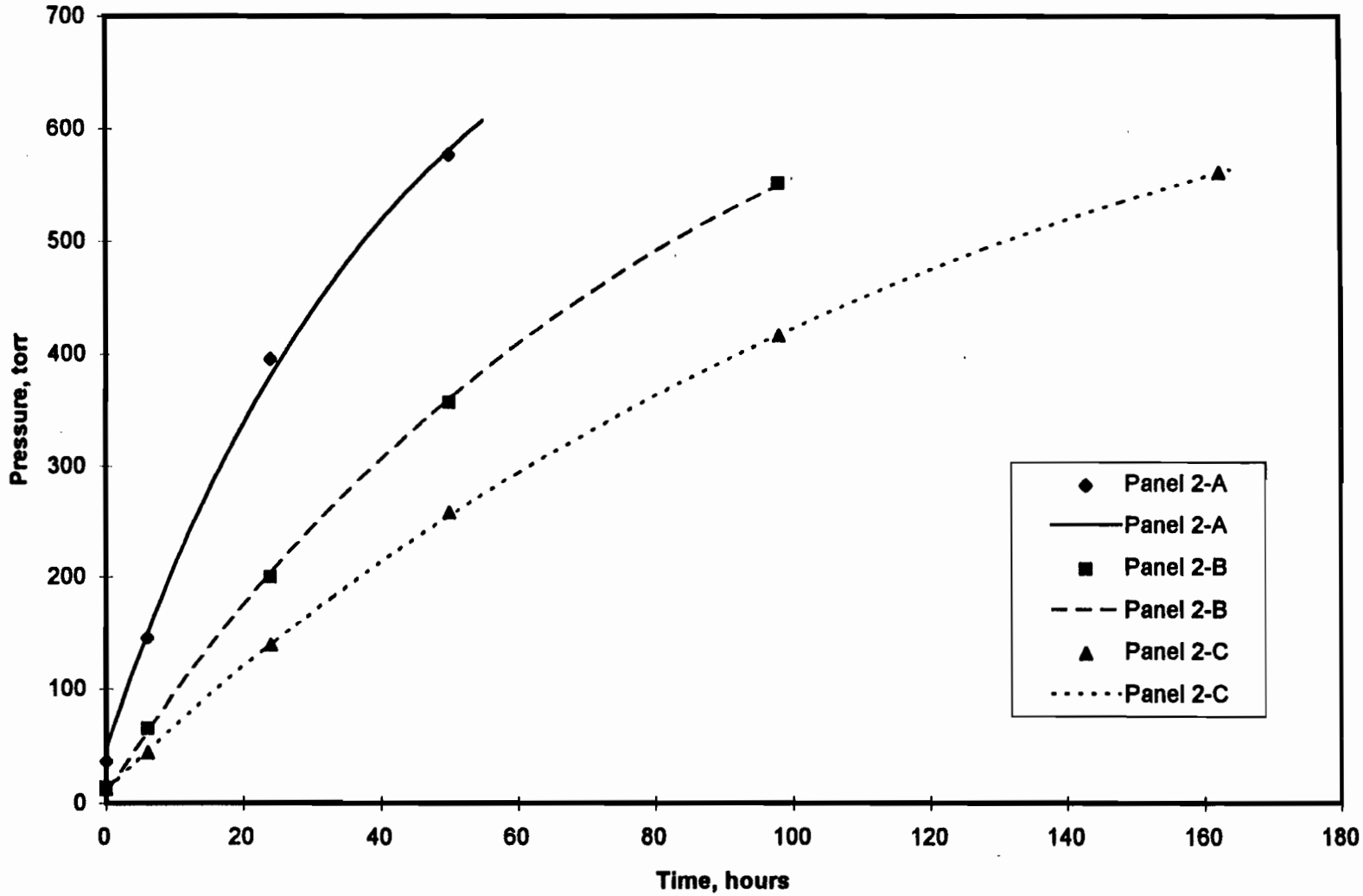

Figure 8. Aging Data for Set 2 Panels in Helium

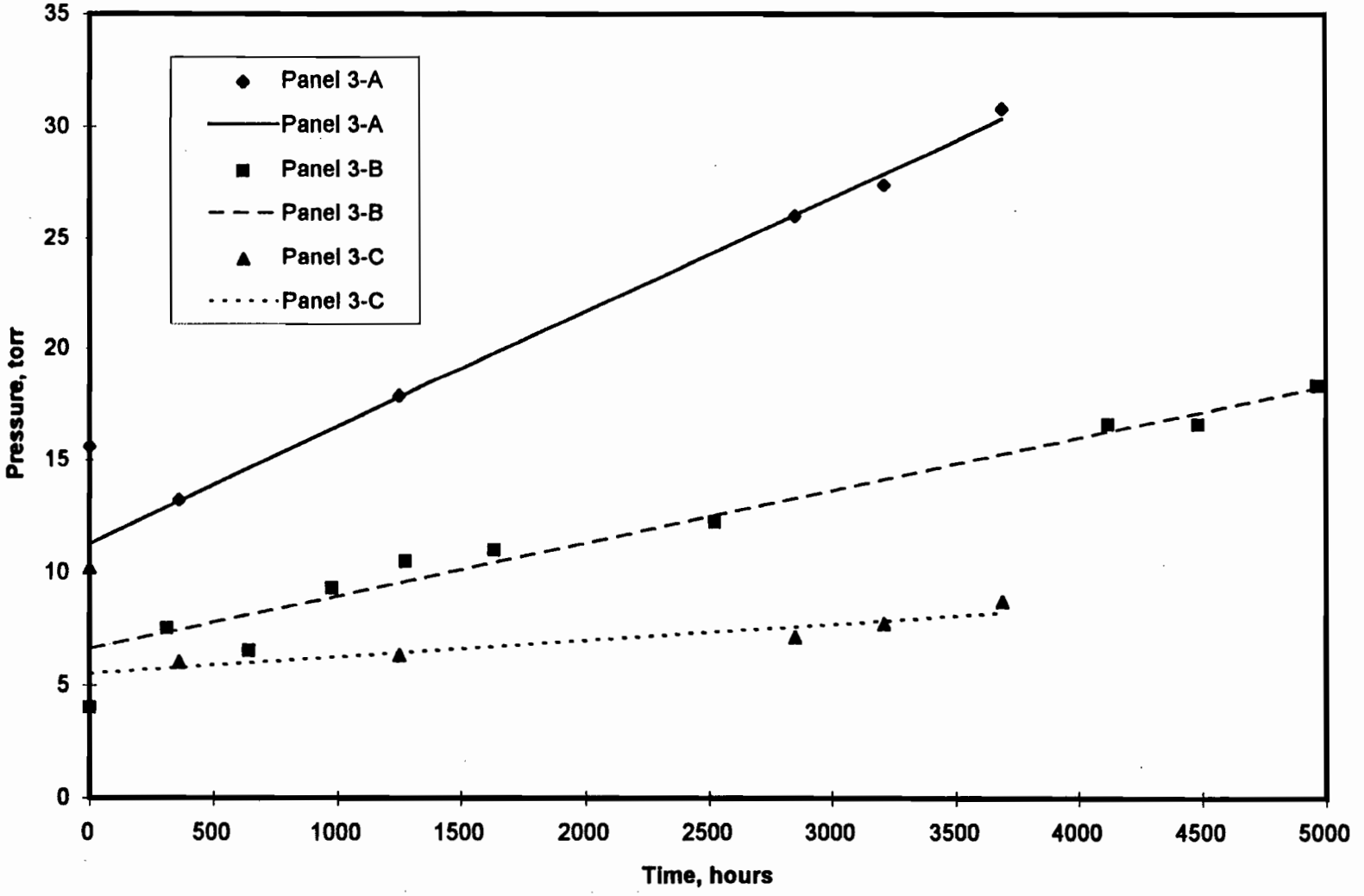

Figure 9. Aging Data for Set 3 Panels in Air

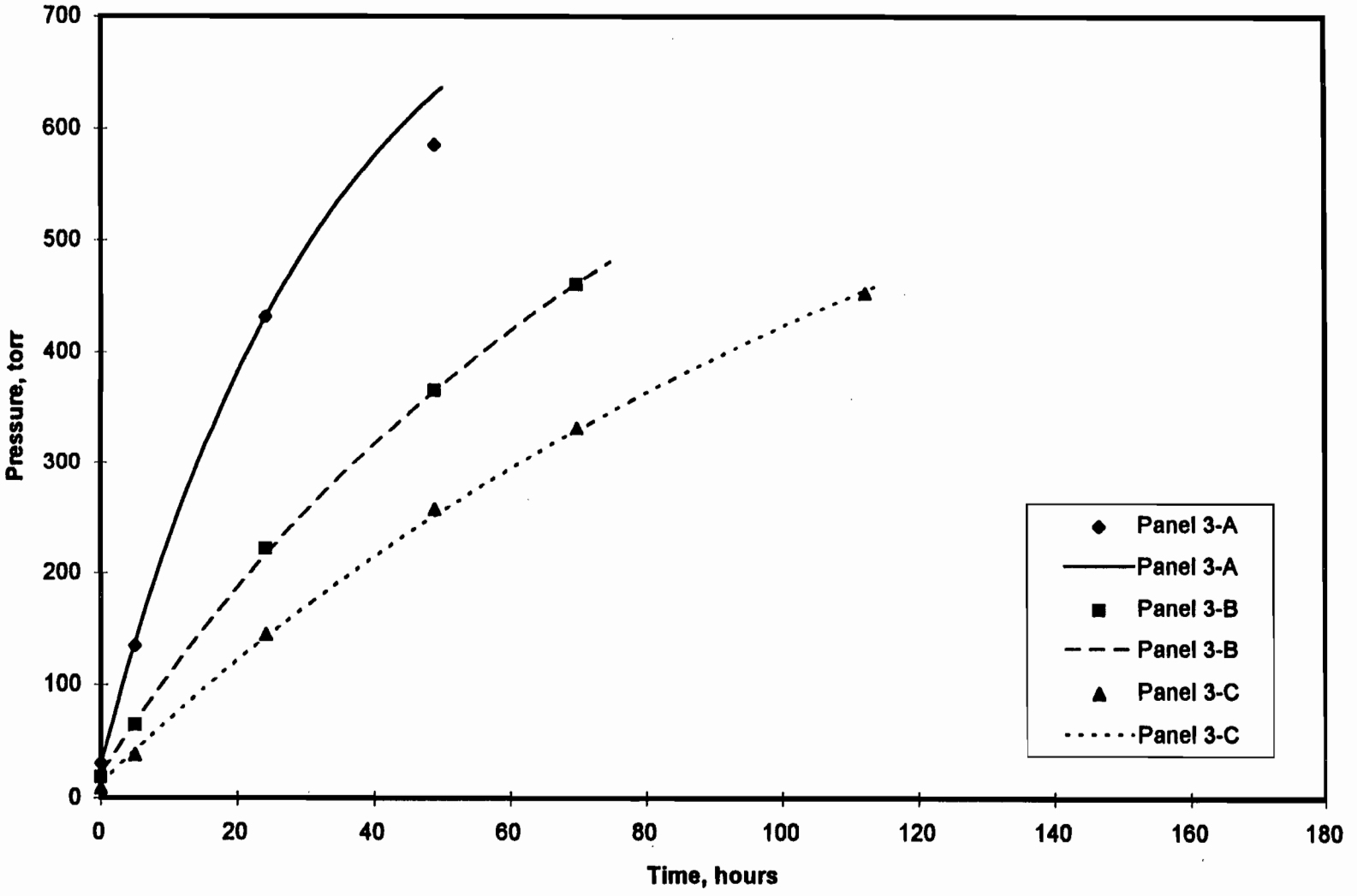

Figure 10. Aging Data for Set 3 Panels in Helium

equation:

$$\ln\left(\frac{P - P_b - P_a}{P_0 - P_a}\right) = a + b\,t \qquad (8)$$

Ideally, the parameter "a" will be close to zero. The constants obtained from these regressions are given in Table 11, along with the coefficients of determination. In many cases, the first data point in air was dropped from the analyses since conditions did not appear to be stable at the beginning of the test; Tables 2-10 note which data points were deleted. When an initial data point was deleted, the next pressure data point was taken as the initial pressure. When such a change in the initial pressure was made, the associated times were not adjusted accordingly; rather, this time shift was absorbed into the parameter "a" of Equation 8. In this way, the regression equations could be plotted directly on the same time scale as was used on the pressure-time plot of the measured data points.

Only one data point in helium was dropped from the analyses. This was the last point obtained on Panel 3-A. The final pressure for this panel was lower than expected. This panel was removed from the helium aging chamber, and, because of a distraction, the pressure was not measured until about one hour later. During this one hour period, enough helium could have permeated out of the envelope to result in this lower pressure. Rather than trying to correct for loss of helium, this data point was simply dropped from the analysis. However, the result does point out the need to measure the pressures quickly after removing the panels from the helium aging chamber.

The regression analyses of data obtained with aging in helium give coefficients of determination of 0.998 or greater, showing that the data do fit the form of Equation 6 extremely well. For aging in air, the coefficients of determination are greater than 0.98 for the panels with no void volume in the metal plates. With 2.5 percent void volume in the metal plates, the coefficients of determination are 0.967 or greater. However, with 5 percent void volume in the metal plates, the coefficients of determination range from 0.938 to as low as 0.664. The lower coefficients of determination with increasing void volume are attributed to the very small pressure rises observed when aging these panels in air.

Table 11. Results of Regression Analysis on Aging Data, Using Equation 8.

Panel	Gas	a	b	r^2
1-A	Air	3.5115×10^{-3}	-6.2425×10^{-6}	0.985
1-A	Helium	-2.0439×10^{-2}	-2.5406×10^{-2}	0.998
1-B	Air	3.3850×10^{-3}	-2.7720×10^{-6}	0.996
1-B	Helium	-4.1162×10^{-4}	-1.2587×10^{-2}	1.000
1-C	Air	5.9672×10^{-4}	-6.7231×10^{-7}	0.664
1-C	Helium	-1.5371×10^{-3}	-7.7098×10^{-3}	1.000
2-A	Air	8.1165×10^{-4}	-7.4905×10^{-6}	0.992
2-A	Helium	-1.4177×10^{-2}	-2.3380×10^{-2}	0.998
2-B	Air	-4.6241×10^{-4}	-2.8151×10^{-6}	0.967
2-B	Helium	6.3720×10^{-3}	-1.1786×10^{-2}	1.000
2-C	Air	-8.9805×10^{-5}	-1.3977×10^{-6}	0.938
2-C	Helium	8.8893×10^{-4}	-7.4125×10^{-3}	1.000
3-A	Air	2.4900×10^{-3}	-6.7660×10^{-6}	0.998
3-A	Helium	3.0748×10^{-3}	-2.9609×10^{-2}	1.000
3-B	Air	1.1626×10^{-3}	-3.0331×10^{-6}	0.970
3-B	Helium	-3.7504×10^{-3}	-1.1849×10^{-2}	1.000
3-C	Air	6.2954×10^{-4}	-9.3343×10^{-7}	0.879
3-C	Helium	-5.9067×10^{-3}	-7.4413×10^{-3}	0.999

If the effective permeating area (A) and total internal volume (V_{tot}) of the panels were known, then the permeance could be calculated directly from:

$$K = -b \frac{V_{tot}}{A} \frac{M}{R\ T\ \rho_0} \tag{9}$$

In general, the total internal volume will be larger than the void volume of the metal plates because of additional volume, such as that associated with the porosity of the Tyvek layer.

Rearranging Equation 9 gives

$$-\frac{A}{b} = \frac{1}{K} \frac{M}{R\ T\ \rho_0} V_{tot} = \frac{1}{K} \frac{M}{R\ T\ \rho_0} \left(V_{plate} + V_{Tyvek} \right) \tag{10}$$

where V_{plate} is the void volume within the metal plate and V_{Tyvek} is the void volume within the Tyvek layer (and also possibly other unidentified sources of extra volume). Assuming the permeance to be nearly the same for all panels, a plot of -A/b versus V_{plate} should give a straight line. If the total internal volume of the panel were equal to the known void volume of the metal plate, then this straight line should pass through the origin. The amount by which the x-intercept is shifted to the left from the origin will be equal to the void volume within the Tyvek layer.

Figures 11 and 12 show plots of -A/b versus V_{plate} for aging of panels in air and helium. The correlation between -A/b and V_{plate} is not very good for either gas. For air, there is a wide scatter in the data points at 5% metal plate void volume. This is due to the uncertainty in b because of the small pressure rises. For helium, the data for panels with the larger area are close together, but the data points for the smaller panels are much lower.

Plotting -1/b (instead of -A/b) versus V_{plate} for helium, as shown in Figure 13, gives a very good correlation. This indicates that the panels all have nearly the same effective permeating area, even though the physical areas are much different. Observation of the panels during aging in helium revealed that blisters formed between the layers of Vecat in regions removed from the aluminum plate. This would indicate that the helium permeates through the plastic film, but does not readily travel in a lateral direction to produce a pressure rise at the aluminum plate. Apparently, only the gas that permeates through the barrier film that is directly over the aluminum

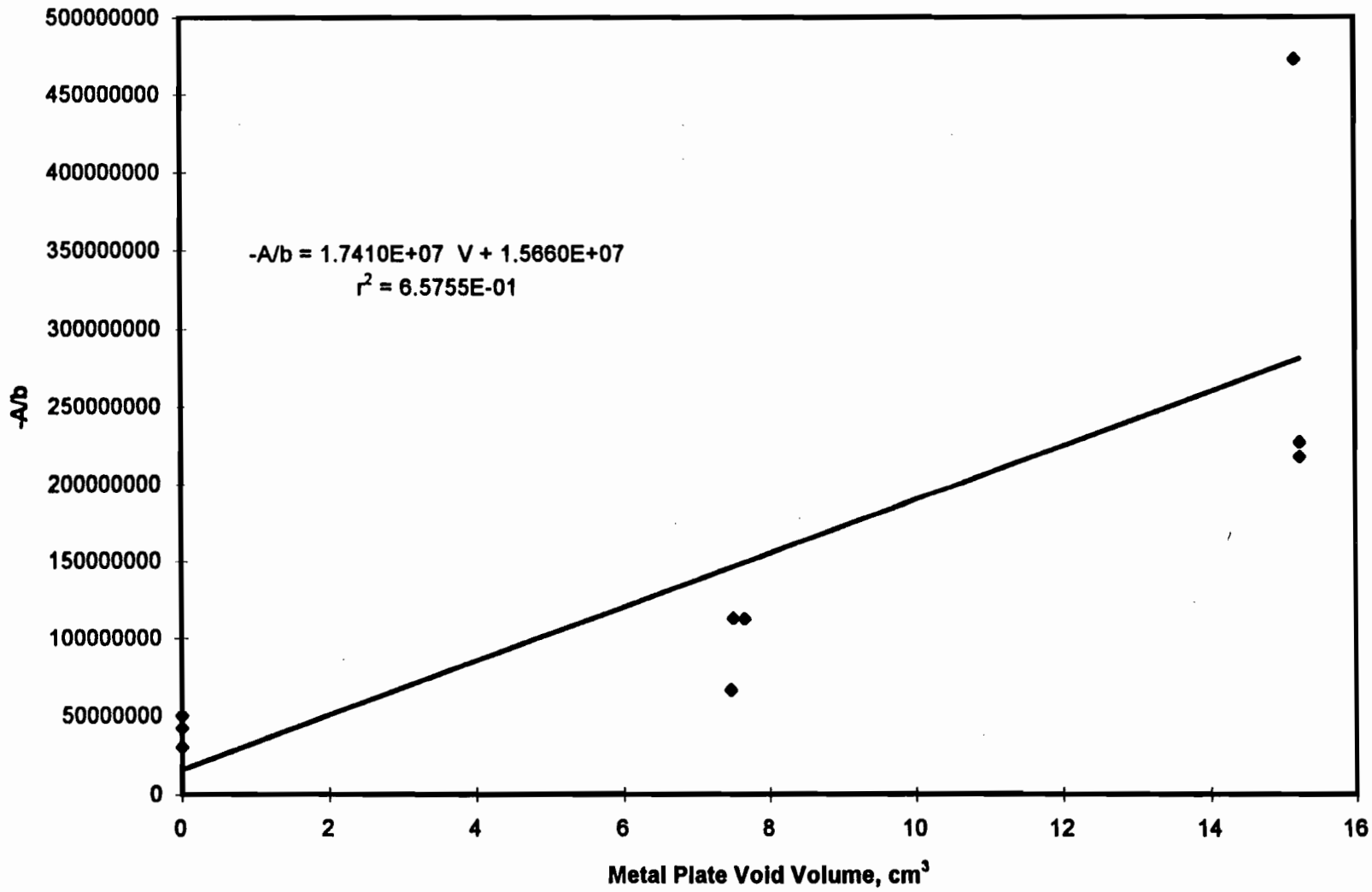

Figure 11. Preliminary Analysis of Tyvek Void Volume for Panels in Air The ordinate is the area between seals divided by the negative of the slope of the logarithm of the pressure ratio v. time.

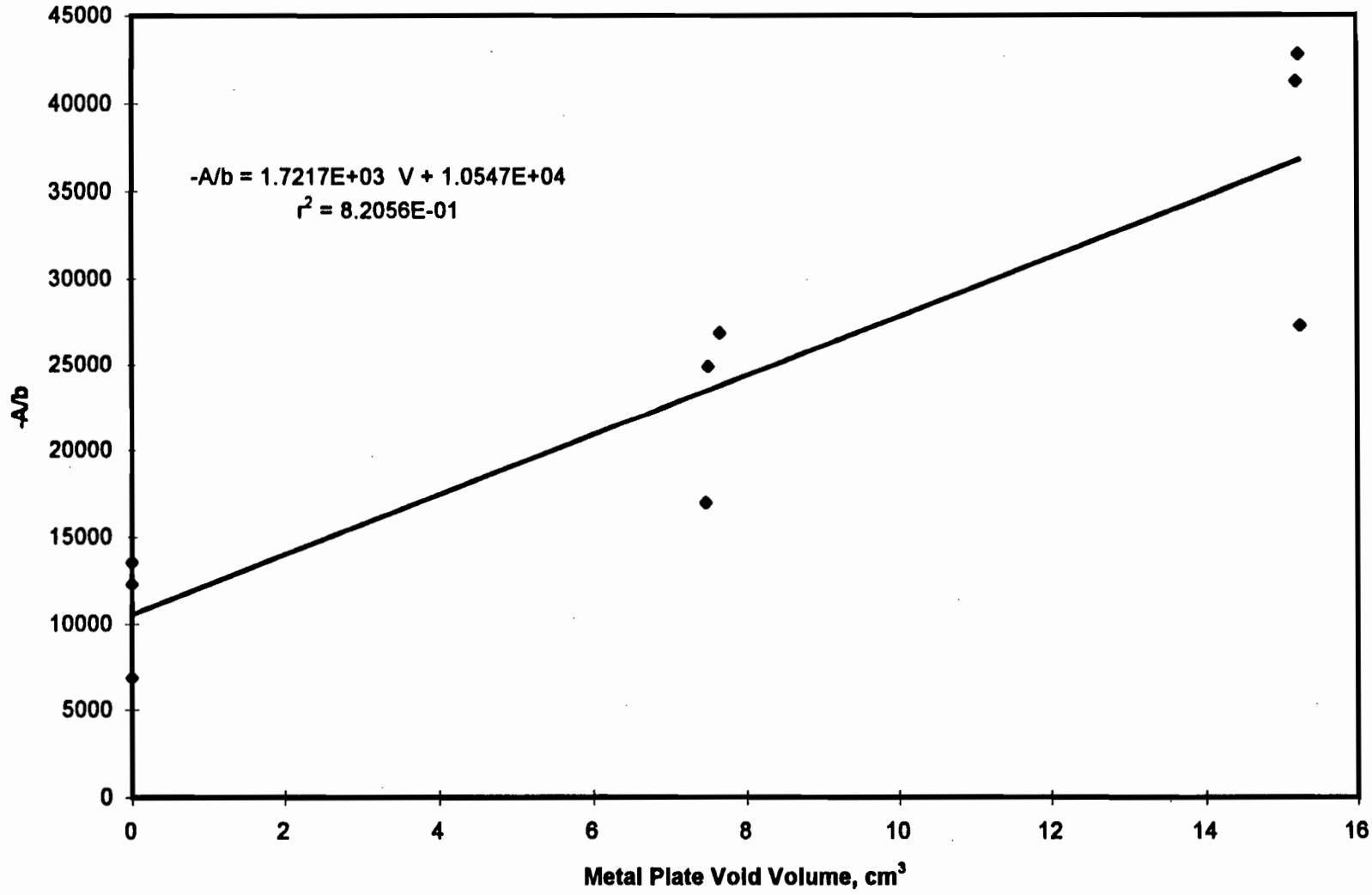

Figure 12. Preliminary Analysis of Tyvek Void Volume for Panels in Helium The ordinate is the area between seals divided by the negative of the slope of logarithm of the pressure ratio v. time.

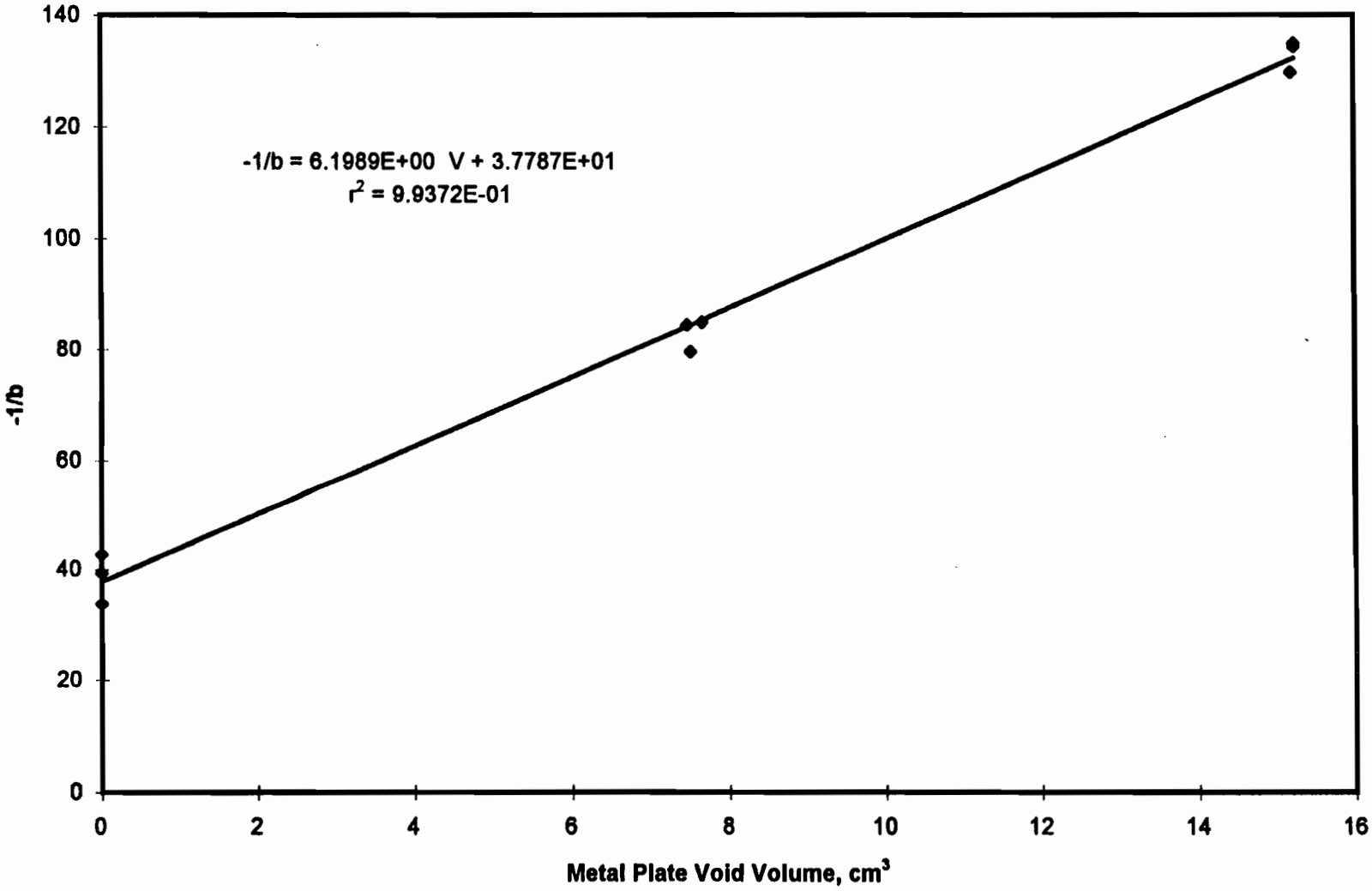

Figure 13. Analysis of Tyvek Void Volume for Panels in Helium The ordinate is the reciprocal of the negative of the slope of the logarithm of the pressure ratio v. time.

plate (and possibly a small fringe area) enters the volume within the plate and contributes to the pressure rise.

Plotting -1/b versus V_{plate} for air, as shown in Figure 14, produces an improvement in the correlation. The scatter is greatly reduced at the two smaller void volumes, but the scatter is not reduced at the large void volume. Ignoring the data at the large void volume, as in Figure 15, produces a very good correlation.

Values of V_{Tyvek} obtained for helium (from Figure 13) and for air (from Figure 15) are 6.10 and 5.51 cm^3. The fact that these two values are within 10 percent of each other gives confidence that the method is yielding the true volume due to the porosity of the Tyvek layer. The Tyvek layer is about 0.003 inches thick and has a total area of slightly more than 160 $in.^2$, or a total volume of about 7.8 cm^3. The calculated free volumes would be consistent with a porosity of about 75 percent, which is a reasonable value for this film.

The procedure of plotting -1/b versus V_{plate} was used separately for each of the three sets of panels. Tyvek void volumes calculated from these analyses are given in Table 12. With estimated values for the total internal volume for each panel, the permeance may be calculated from Equation 9. For these calculations, the permeating area was taken to be the area of the film directly over the aluminum plate, which is 150 square inches (counting both sides of the panel). Calculated permeance values for each panel are given in Table 13. The average value for air is 0.00046 cc(STP)/100 $in.^2$•atm•day and the standard deviation is 0.00014, or 30 percent of the mean. Because of the small pressure rises within the panels with 5 percent void volume, their permeances are subject to more uncertainty than those for the other panels. Eliminating these three panels gives a mean and standard deviation of 0.00054 and 0.000045 cc(STP)/100 $in.^2$•atm•day (8 percent of the mean). These values give a standard error of the mean of 3.4 percent. For helium, the average and standard deviation are 2.31 and 0.12 cc(STP)/100 $in.^2$•atm•day. Here, the standard deviation is about 5 percent of the mean, and the standard error of the mean is 2 percent.

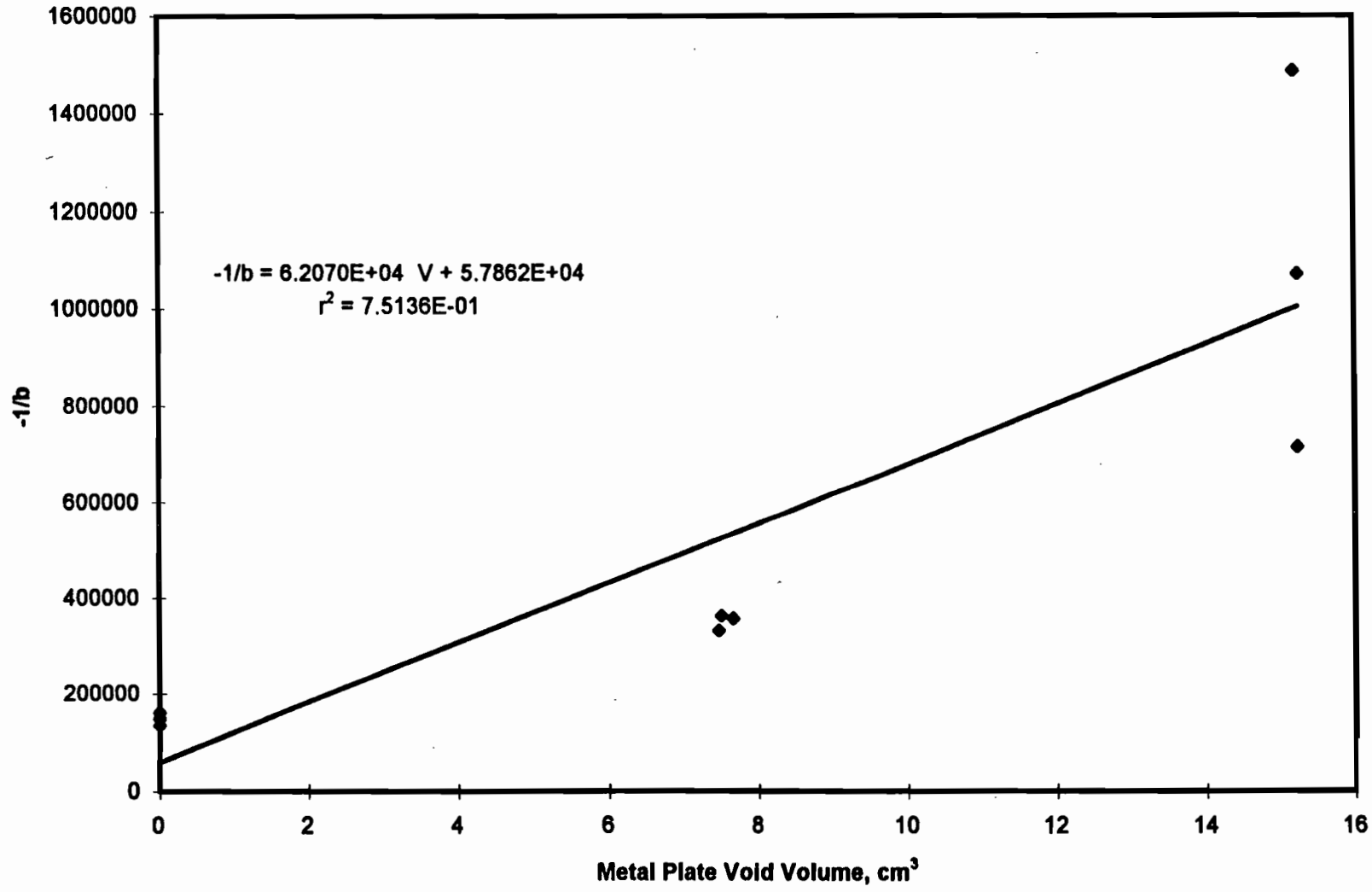

Figure 14. Preliminary Analysis of Tyvek Void Volume for Panels in Air
The ordinate is the reciprocal of the negative of the slope of the logarithm of the pressure ratio v. time.

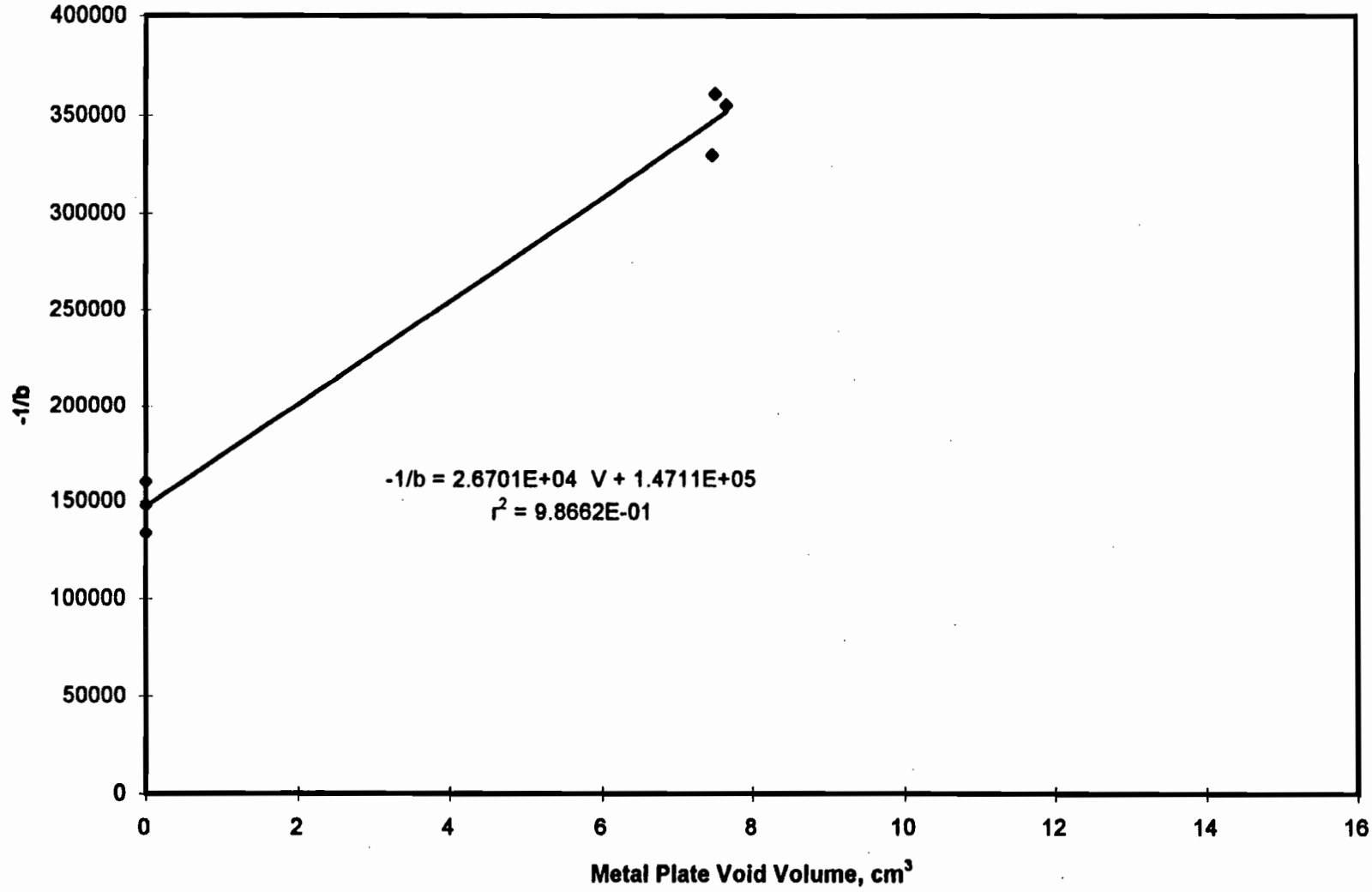

Figure 15. Analysis of Tyvek Void Volume for Panels in Air
The ordinate is the reciprocal of the negative of the slope of the logarithm of the pressure ratio v. time.

Table 12. Tyvek Void Volumes of Sets of Panels in Air and Helium

Panel Set	Void Volume (cm^3) for Air	Free Volume (cm^3) for Helium
1	6.00	6.36
2	4.61	6.84
3	6.07	5.18
Average	5.56	6.13

Table 13. Permeance of Vecat Film

Panel	Permeance for Air, cc (STP)/100 $in.^2$•atm•day	Permeance for Helium, cc (STP)/100 $in.^2$•atm•day
1-A	0.00054	2.31
1-B	0.00054	2.50
1-C	0.00020	2.38
2-A	0.00049	2.29
2-B	0.00049	2.44
2-C	0.00040	2.34
3-A	0.00059	2.19
3-B	0.00059	2.14
3-C	0.00028	2.17
Average	0.00046	2.31
Standard Deviation	0.00014	0.12

3.3.2 Measurement of Thermal Resistivity versus Pressure

GE Appliances furnished 21 PEPs for establishing the curve of thermal resistivity versus internal pressure. The panels were labeled with letters from A to U. Panels A through N had lateral dimensions of 10 in. by 10 in., and Panels O through U had lateral dimensions of 15.75 in. by 15.75 in. All panels were approximately 1/2 in. thick.

Thermal resistivity measurements were made in the Heat Flow Meter Apparatus, with the results given in Table 14. Internal pressures were measured using both the ORNL hand-held gauge and ORNL's vacuum chamber fitted with a sensor similar to that in the hand-held gauge. GE Appliances also measured the internal pressures. The three sets of internal pressure measurements are also given in Table 14.

Table 14 shows that the pressure measurements using the two vacuum chambers are in good agreement, but the hand-held gauge gives higher pressures. Using a panel with a solid metal filler and a feedthrough arrangement to control the internal pressure to known values, we have shown that pressures measured with the hand-held gauge are in good agreement with the known values, but the pressures measured in the vacuum chamber are much too low, as shown in Figure 16. This difference is thought to be due to a ballooning effect in the vacuum chamber, which greatly increases the internal volume of the metal-filled panels. These experiments give us confidence that the pressures measured in the aging experiments are accurate. Similar measurements using a panel with a filler consisting of two perforated metal plates separated by a 1/4 inch tube show much better agreement between the two methods, as shown in Figure 17. However, the pressures measured in the vacuum chamber are still lower than the known pressures. We have not yet been successful in performing this same type of experiment using a powder filled panel with a feedthrough arrangement to control the internal pressure to known values. Therefore, for the purposes of this report, we recognize this uncertainty in internal pressure and use the two ORNL measurements to develop two curves of thermal resistivity versus pressure, as shown in Figure 18. For purposes of this report, the thermal resistivity versus pressure data were fitted with a simple power law.

Table 14. Thermal Resistivities and Internal Pressures of PEPs for Phase III

Panel	Thermal Resistivity, h•ft²•°F/Btu•in.	Internal Pressure, torr		
		ORNL Hand-held Gauge	ORNL Vacuum Chamber	GE Vacuum Chamber
A	22.98	10.8	1.9	2
B	24.25	11.0	2.1	2
C	22.97	10.8	2.8	2
D	23.15	12.2	2.7	3
E	20.71	16.0	4.9	5
F	20.47	14.0	5.0	5
G	15.70	28.2	11.7	11
H	15.53	24.4	11.2	11
I	10.42	48.9	33.2	31
J	10.12	48.0	37.0	35
K	6.63	140.5	120.0	107.5
L	6.29	132.1	115.0	107.5
M	4.73	366.5	334.0	300
N	4.60	355.8	332.0	300
O	26.18	9.8		
P	25.23	10.0		
Q	21.97	12.5		
R	12.01	29.1		
S	11.13	40.3		
T	5.98	128.4		
U	5.17	342.8		

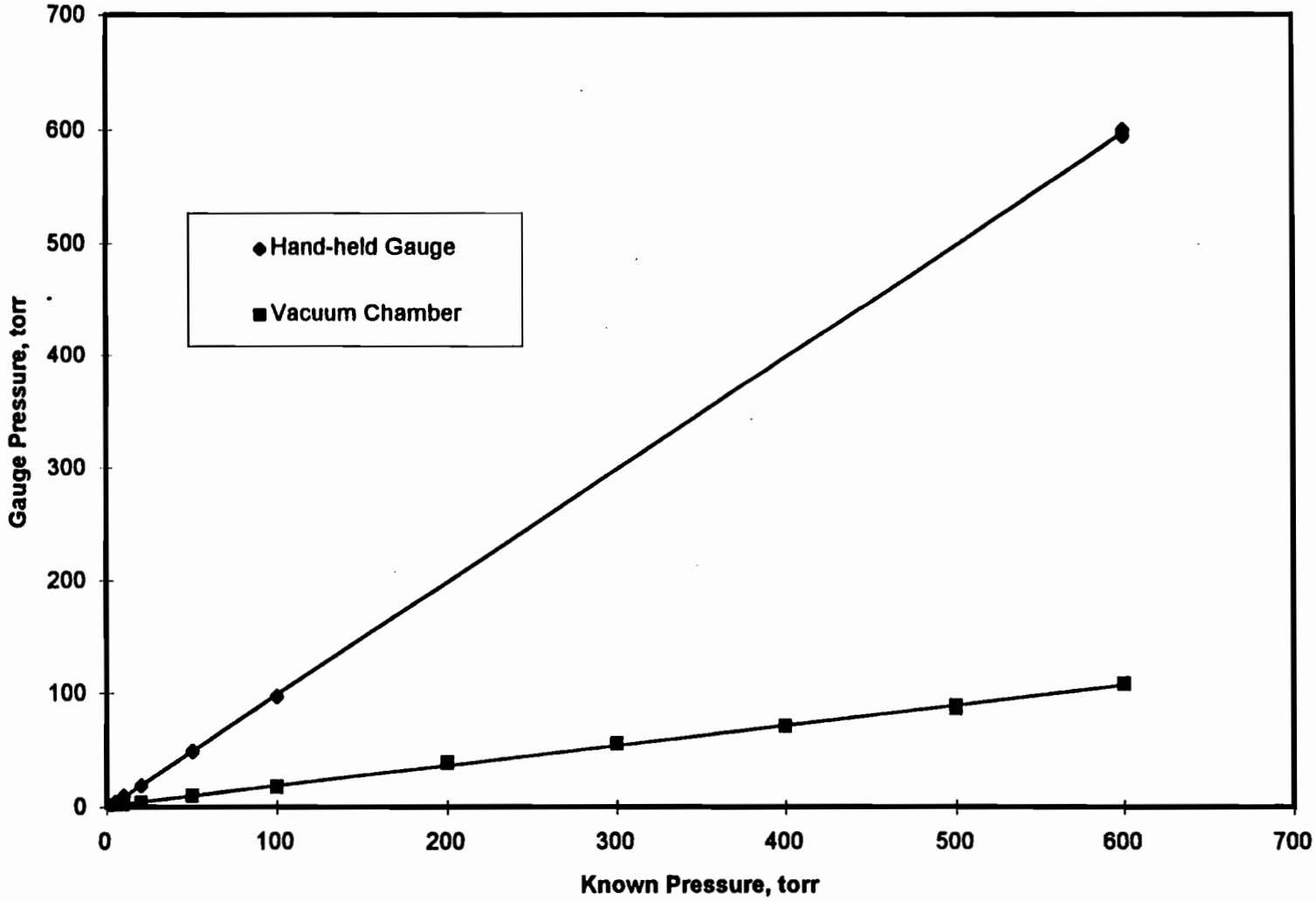

Figure 16. Probe Pressures Measured on Solid Metal-filled Panel with Known Internal Pressure

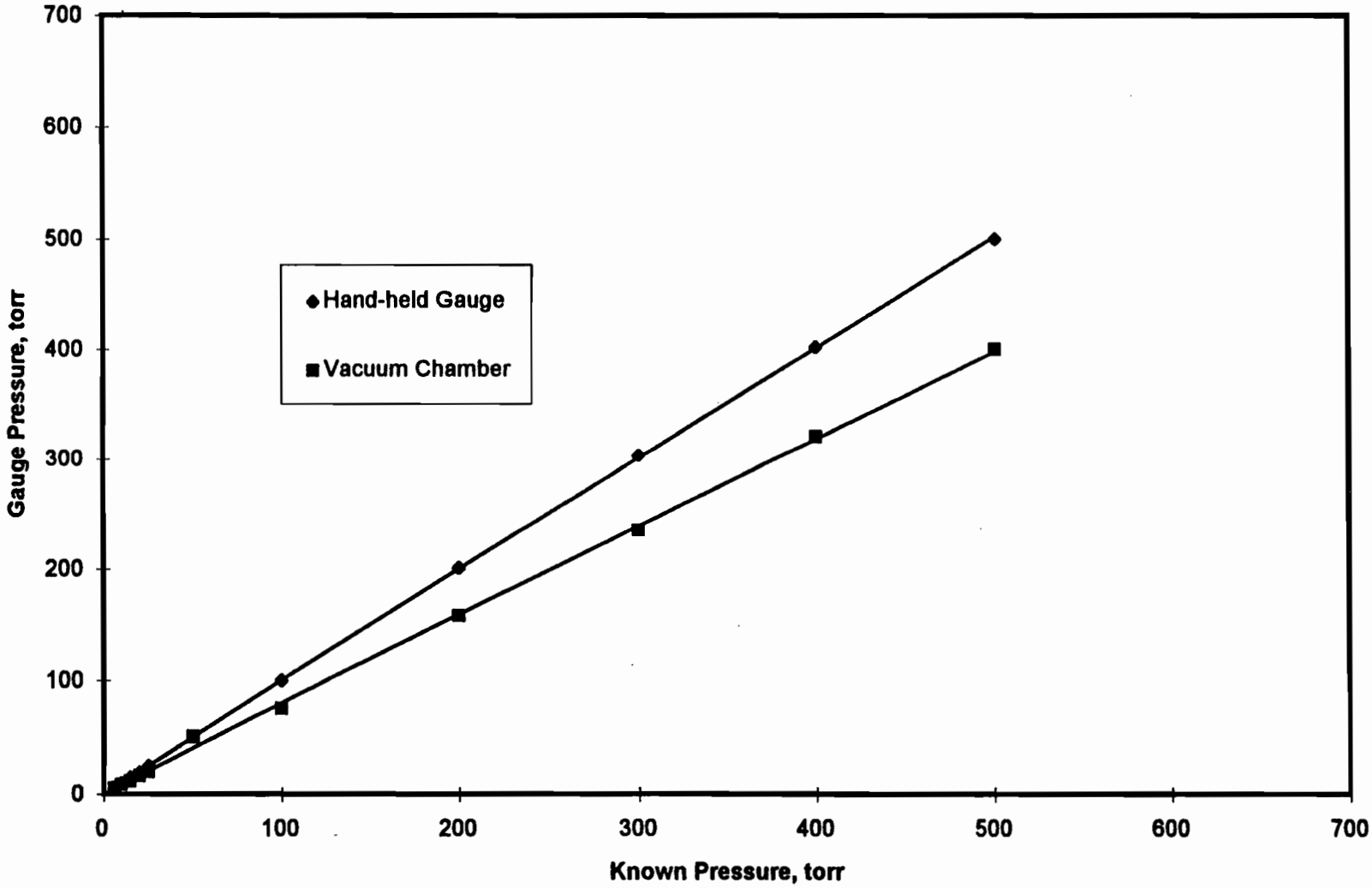

Figure 17. Probe Pressures Measured with Perforated Metal Panel with Known Internal Pressure

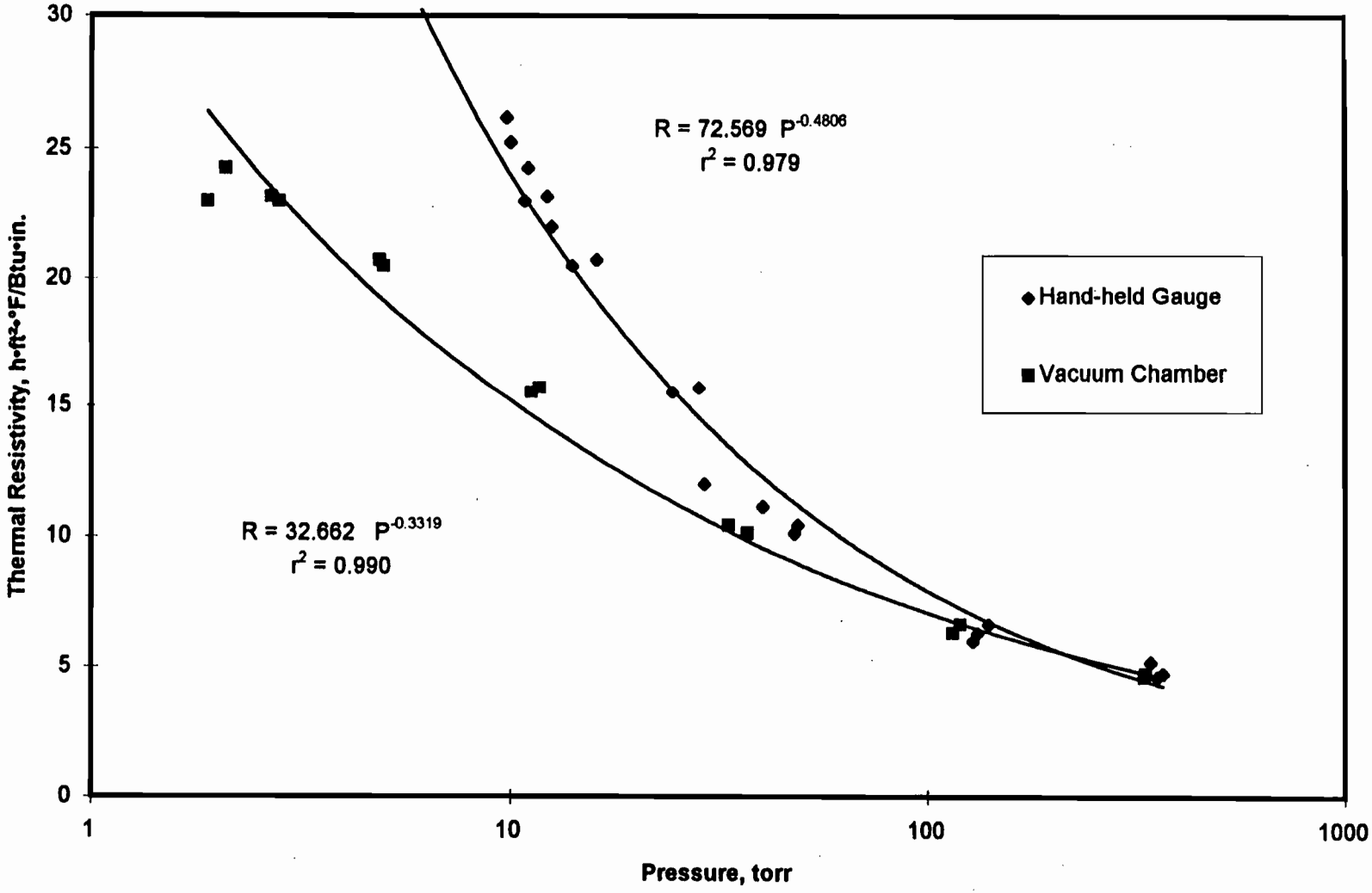

Figure 18. Thermal Resistivity of PEPs for Phase III

3.3.3 Predictions of Lifetime Aging of PEPs

The data developed in Sections 3.3.1 and 3.3.2 were used to predict the pressure rise and thermal resistivity decrease in typical PEPs. For these calculations, it was assumed that the PEP was two feet square and one-half inch thick, and contained 90 percent void volume. This gave a total surface area of 1152 in.^{2} and an internal void volume of 4248 cm^3. It was assumed that the initial thermal resistivity was 25 h•ft^2•°F/Btu•in. Initial internal pressures from the curves in Figure 18 were selected to match this resistivity, and were 2.24 torr for the vacuum chamber pressure measurements and 9.18 torr for the hand-held gauge pressure measurements. The ambient pressure was taken to be 760 torr.

Figure 19 shows the predictions for the pressure versus time within the PEP over a 20 year time period. The three curves for each type of pressure measurement correspond to the mean barrier permeance (0.00054 cc(STP)/100 in.^{2}•atm•day), and the mean plus or minus two standard deviations (i.e., permeances of 0.00063 and 0.00045, respectively). With the mean permeance, the pressure was predicted to rise by 8.8 torr over the 20 year life (for either type of pressure measurement).

Using the curves for pressure versus time from Figure 19, and the curves for resistivity versus pressure from Figure 18, the thermal resistivity versus time was predicted and plotted in Figure 20. Using the resistivity-pressure curve obtained from the hand-held gauge pressure measurements and the mean permeance value, the thermal resistivity is predicted to decrease to about 18 h•ft^2•°F/Btu•in. after 20 years. Using the resistivity-pressure curve obtained from the vacuum chamber pressure measurements and the mean permeance value, the resistivity is predicted to decrease to about 14.5 h•ft^2•°F/Btu•in. after 20 years.

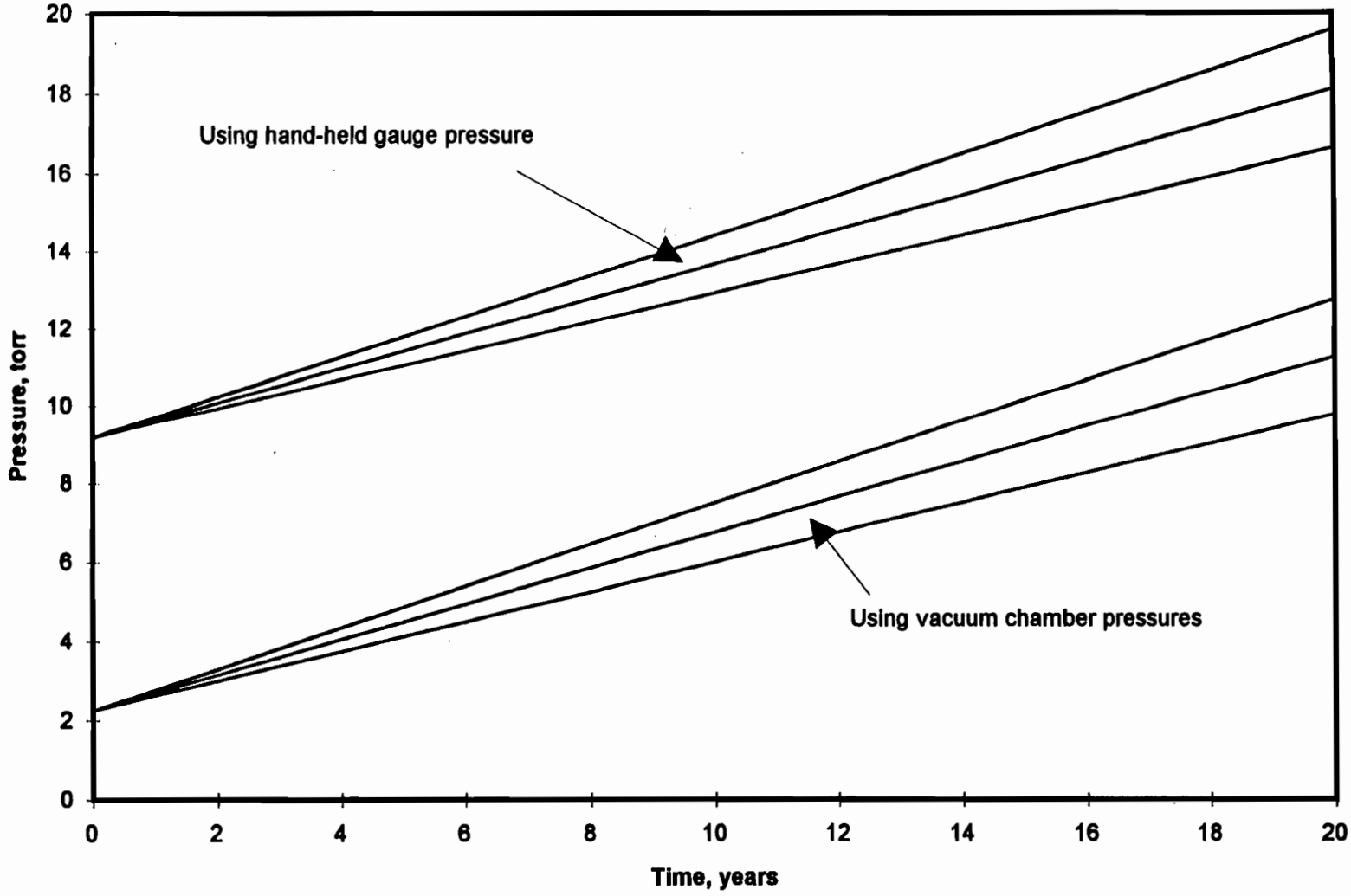

Figure 19. Lifetime Predictions for Internal Pressure for PEPs
The three curves correspond to the mean permeance and plus or minus two standard deviations.

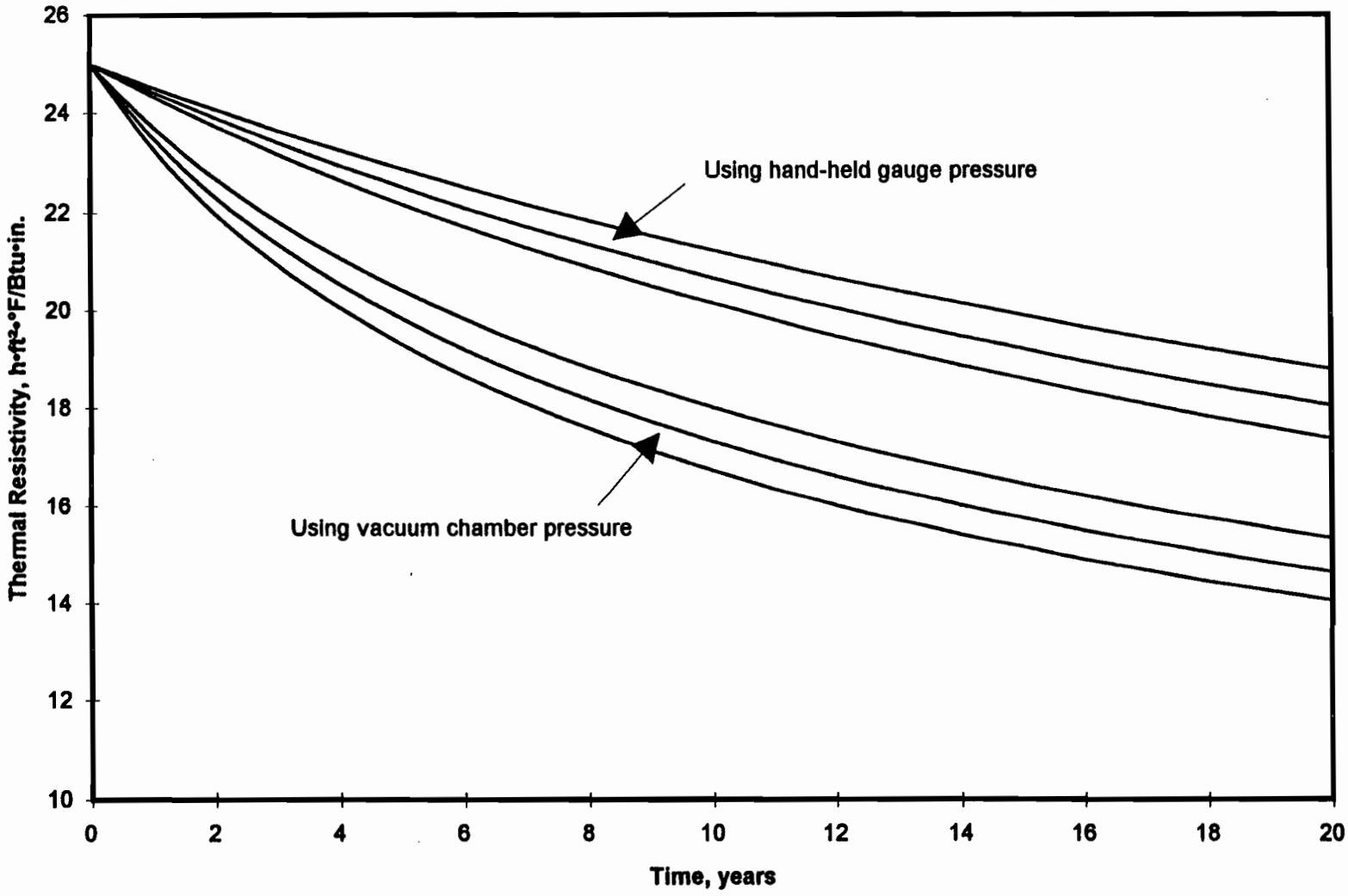

Figure 20. Lifetime Predictions for Thermal Resistivity of PEPs
The three curves correspond to the mean permeance and plus or minus two standards deviations.

3.4 Phase IV

The objective of Phase IV was to determine the lifetime of superinsulations when installed in simulated refrigerator doors.

3.4.1 Test Panels

Composite panels were fabricated to simulate the doors, as shown in Figure 21. One side of the panel was a sheet of 24 gauge (0.024 inch thick) mild steel that represents the outside of a refrigerator cabinet. The other side was an 0.12 inch thick sheet of acrylonitrile-butadiene-styrene (ABS) plastic that represents the inside lining. The total thickness of the panels was 2.0 inches, and the lateral dimensions were 24 by 24 inches. Normally, the space between these two sheets would be completely filled with a urethane foam insulation. For the superinsulation/foam composite panels, a superinsulation panel was attached to the center of the inside surface of the steel sheet using double-sided foam tape, and the remaining space was filled with urethane foam. The edges were sealed using aluminum tape.

Nine superinsulation panels were furnished by each of four organizations, each using a different construction, as follows: silica powder filler encapsulated in a polymer barrier film (denoted as Type A); fibrous glass insulation filler encapsulated in a stainless steel barrier (denoted as Type B); an undisclosed insulation filler encapsulated in a stainless steel barrier (denoted as Type C); panels containing radiation baffles within a polymer barrier film, and filled with krypton gas at atmospheric pressure (denoted as Type D). All superinsulation panels were approximately 1/2 inch thick, and had lateral dimensions of 14 by 14 inches (Types A and C) or 12 by 12 inches (Types B and D).

Installation of the urethane foam into the composite panels was performed by three foam suppliers, each of which used a different foam blowing agent for these test specimens. The three types of foam blowing agents used were CFC-11, HCFC-141b, and HCFC-142b/22 blend. This procedure resulted in a matrix of specimens with each type of superinsulation and each type of blowing agent produced in triplicates.

In addition to the superinsulation/foam composite panels, similar foamed panels were fabricated without the superinsulation panels. The purpose of these foam-only panels was to

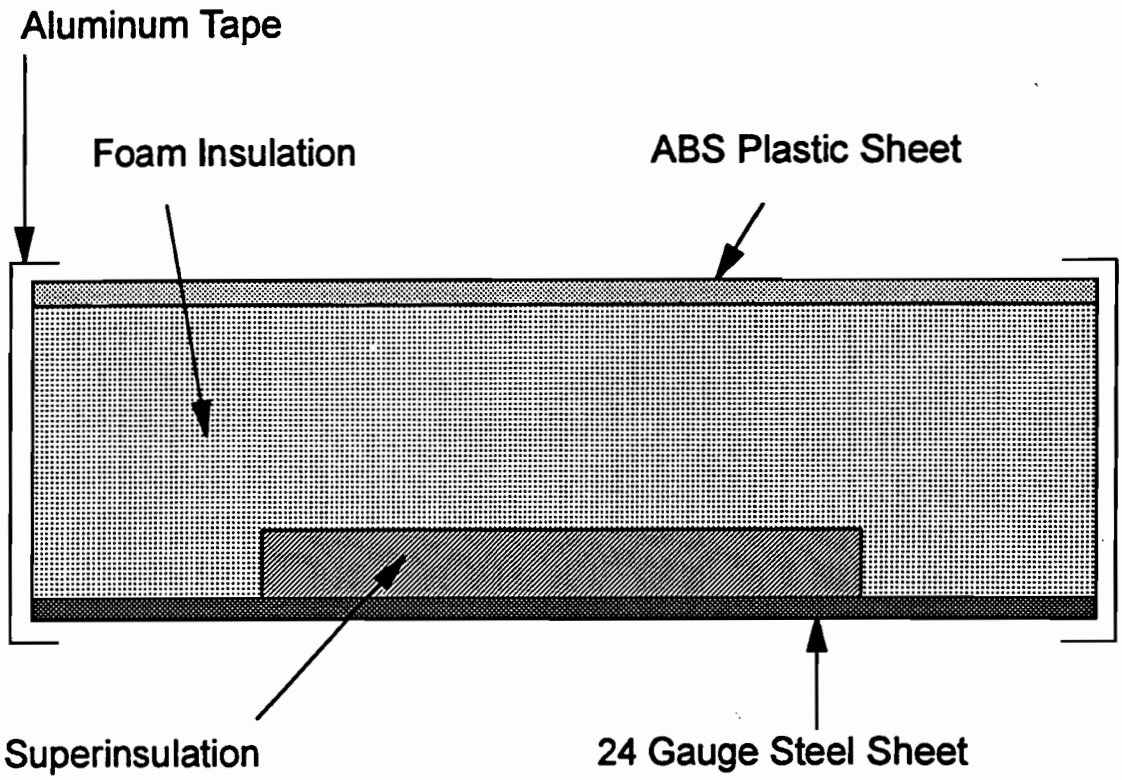

Figure 21. Construction of Composite Panels

provide a baseline for comparison with the panels containing superinsulations. All of the composite panels, with or without superinsulation, were stored in closed cabinets maintained at 90°F between the thermal measurements described below.

Several other test panels of the same construction as the foam-only panels were fabricated. The foam was removed from these panels and specimens were sliced from them. For each type of blowing agent, two specimens were sliced to approximately 1.5 inches thick and eight were sliced to slightly less than 0.35 inch thick. Half of these specimens were maintained at 75°F and the other half at 90°F between thermal measurements. Measurements on the stripped foam provided a baseline with which the results on the foamed panels could be compared.

3.4.2 Experimental Procedures

Thermal resistance measurements were made using two heat flow meter apparatuses (HFMAs), both of which conform to ASTM C 518. [3] In a HFMA, a flat rectangular specimen is sandwiched between hot and cold plates that are maintained at constant temperatures. The heat flux through the specimen is measured using a heat flux transducer (HFT), which is calibrated by making measurements on a standard specimen for which the thermal resistance is known. One HFMA accepted specimens with lateral dimensions of 12 in. by 12 in., and had a single 3 inch square HFT on each of the hot and cold plates. The other HFMA accepted specimens with lateral dimensions of 24 in. by 24 in. This HFMA had an array of 30 four-inch-square HFTs on the hot side. An average of the readings from the two HFTs nearest the center of the plate (giving an average heat flux over the central 4 inch by 8 inch area) was used in analysis of the data reported here. The smaller HFMA was used for measurements on the slices of foam insulation, while the larger HFMA was used for measurements on the superinsulation panels and on the composite panels.

The usual mode of operation of a HFMA requires the use of a homogeneous specimen. For measurements on the composite panels and on the superinsulation specimens, modifications were necessary in order to eliminate undesirable air gaps between the specimen and the plates and to protect the plates from the rigid specimens. The superinsulation specimens were sandwiched between two layers of fiberglass boards, and this package was placed between the plates of the HFMA. Likewise, the composite panels were sandwiched between two layers of foam rubber,

HFMA. Likewise, the composite panels were sandwiched between two layers of foam rubber, and the package was placed between the plates of the HFMA. In both cases, thermocouples were taped directly to the faces of the test specimen (either the superinsulation panel or the composite panel), so that the temperature difference across the specimen was measured directly.

3.4.3 Results of Tests

3.4.3.1 Superinsulation Panels

Upon receipt of the superinsulation panels, their thermal resistances were measured in the HFMA. The thickness of each panel was determined using a dial gauge and gauge block system at ORNL's Inspection Engineering Department. These measurements were made over the central 70% of the panel, also avoiding wrinkles and other undulations in the surface. Center-of-panel thermal resistivities (measured over the center 4 in. by 8 in. area) are given in Table 15. It must be strongly emphasized that these center-of-panel values do not account for any heat conduction around the edges of the panels due, for example, to high thermal conductivity stainless steel skins, and hence do not represent a thermal value for a complete panel. The values do, however, serve as an indicator of the condition of the vacuum within the evacuated insulations, or of the fill gas in the gas-filled panels. As Table 15 shows, the Type A panels had thermal resistivities that ranged from 26.72 to 29.44 $h \cdot ft^2 \cdot °F/Btu \cdot in$. The resistivities of Type B, C, and D panels had ranges of 54.64 to 71.58, 46.23 to 52.49, and 10.93 to 11.39 $h \cdot ft^2 \cdot °F/Btu \cdot in.$, respectively. Average resistivities were 28.03, 65.23, 48.18, and 11.13 $h \cdot ft^2 \cdot °F/Btu \cdot in.$ for Types A, B, C, and D, respectively.

3.4.3.2 Foam Insulation

It is well known that the thermal resistance of foam insulations blown with CFCs or HCFCs will change as the material ages. When freshly blown, the cells of the foam are filled primarily with the blowing agent gas, which has a relatively low thermal conductivity. During the first stage of aging, ambient air diffuses into the cells, raising the thermal conductivity of the internal gas mixture and hence lowering the thermal resistivity of the foam insulation. After this

Table 15. Center-of Panel Thermal Resistivities of Superinsulation Panels

Panel	Resis-tivity	Panel	Resis-tivity	Panel	Resis-tivity	Panel	Resis-tivity
A-1	26.72	B-1	68.29	C-1	51.12	D-1	10.95
A-2	27.93	B-2	71.33	C-2	47.33	D-2	11.06
A-3	29.33	B-3	57.60	C-3	46.45	D-3	11.38
A-4	26.78	B-4	54.64	C-4	52.49	D-4	11.37
A-5	27.93	B-5	64.83	C-5	46.23	D-5	10.96
A-6	29.44	B-6	71.58	C-6	47.15	D-6	11.00
A-7	28.08	B-7	69.05	C-7	48.52	D-7	10.93
A-8	29.00	B-8	71.09	C-8	47.76	D-8	11.16
A-9	27.03	B-9	58.66	C-9	46.60	D-9	11.39

Note: Thermal resistivities have units of $h \cdot ft^2 \cdot °F/Btu \cdot in$.

stage has saturated, the second stage of aging occurs by diffusion of the blowing gas out of the cells, again raising the thermal conductivity of the internal gas mixture. These aging processes occur over a period of many years for full thickness insulation. However, the aging can be greatly accelerated by cutting the insulation into thin slices. This allows the gases to diffuse in or out of the cells much more quickly. A test protocol has been developed for performing such accelerated aging tests [4], and the method has been developed into an ASTM Standard.[5]

The 1.5-inch-thick foam specimens were tested singly, while four of the 0.35-inch-thick specimens were stacked and their average thermal resistance was measured. Tests on the specimens were conducted over a period of 180 days. Results are shown in Figures 22-24, where the logarithm of the thermal conductivity [ℓn (100 k)] is plotted versus the square root of the aging time divided by the slice thickness ($\sqrt{t}/L$). This type of plot is convenient for analysis since the data separate into two linear regions which are interpreted as corresponding to the two stages of aging. Regression constants for the two linear regions and the coefficients of determination (r^2) are given in Table 16.

A comparison of the results of tests on specimens aged at 75°F and at 90°F shows that the aging temperature has a relatively minor effect on the thermal conductivity. Differences between the data for the two aging temperatures are only about 2 to 3.5 percent. The type of blowing agent does have an influence on the thermal conductivity, especially at short times. At short aging times, the conductivity of foam blown with HCFC-141b is about 5 to 6 percent higher than that of foam blown with CFC-11, and the values for HCFC-142b/22 are about 15 to 16 percent higher than those for CFC-11. At long times, the differences among the blowing agents are diminished. The long term conductivity for HCFC-141b-blown foam is about 3 to 4 percent higher than that for CFC-11-blown foam, and the values for HCFC-142b/22-blown foam are about 3 to 7 percent higher than for CFC-11-blown foam.

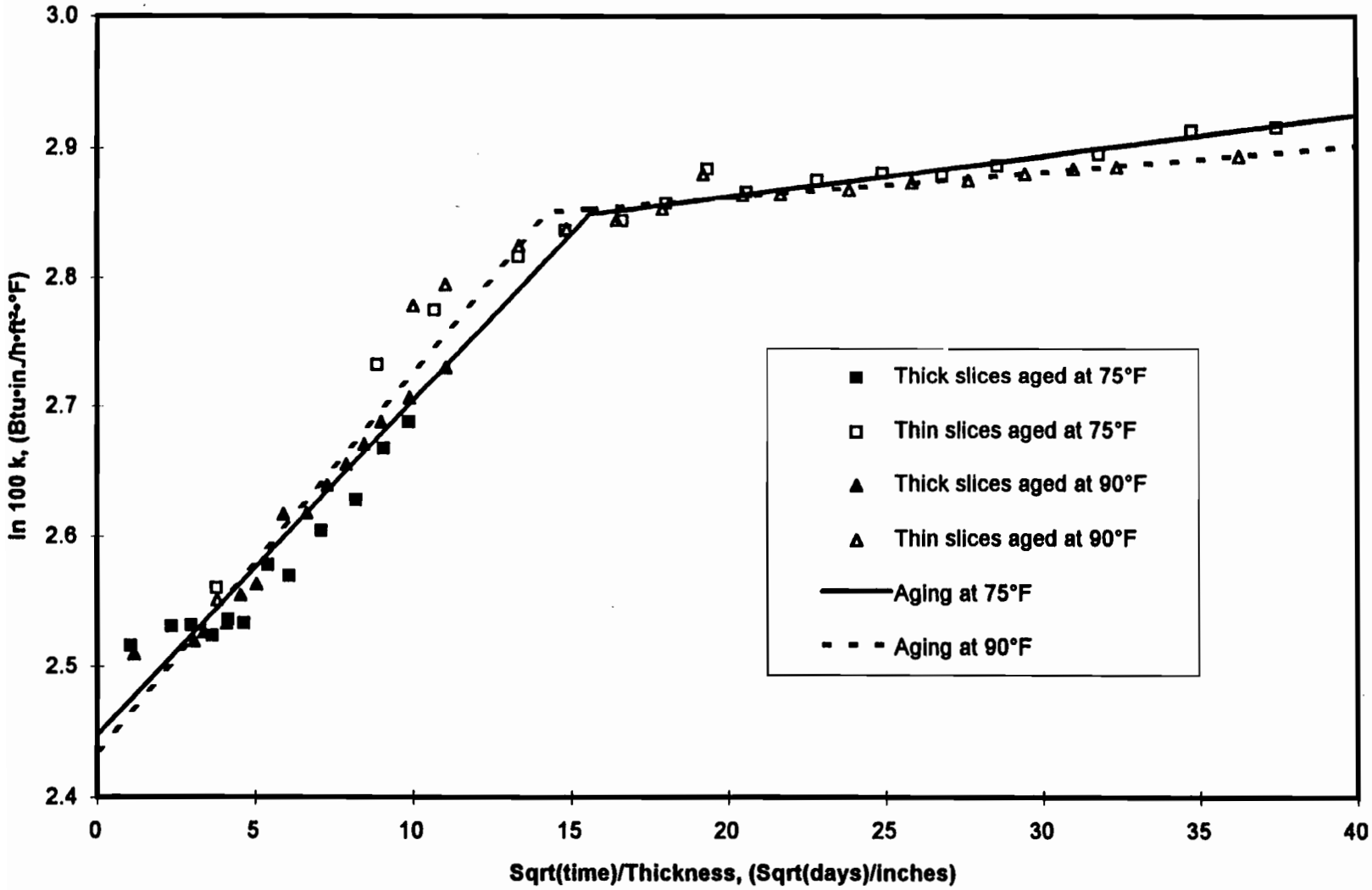

Figure 22. Thermal Conductivity of CFC-11 Foam from Thin-Slicing Studies

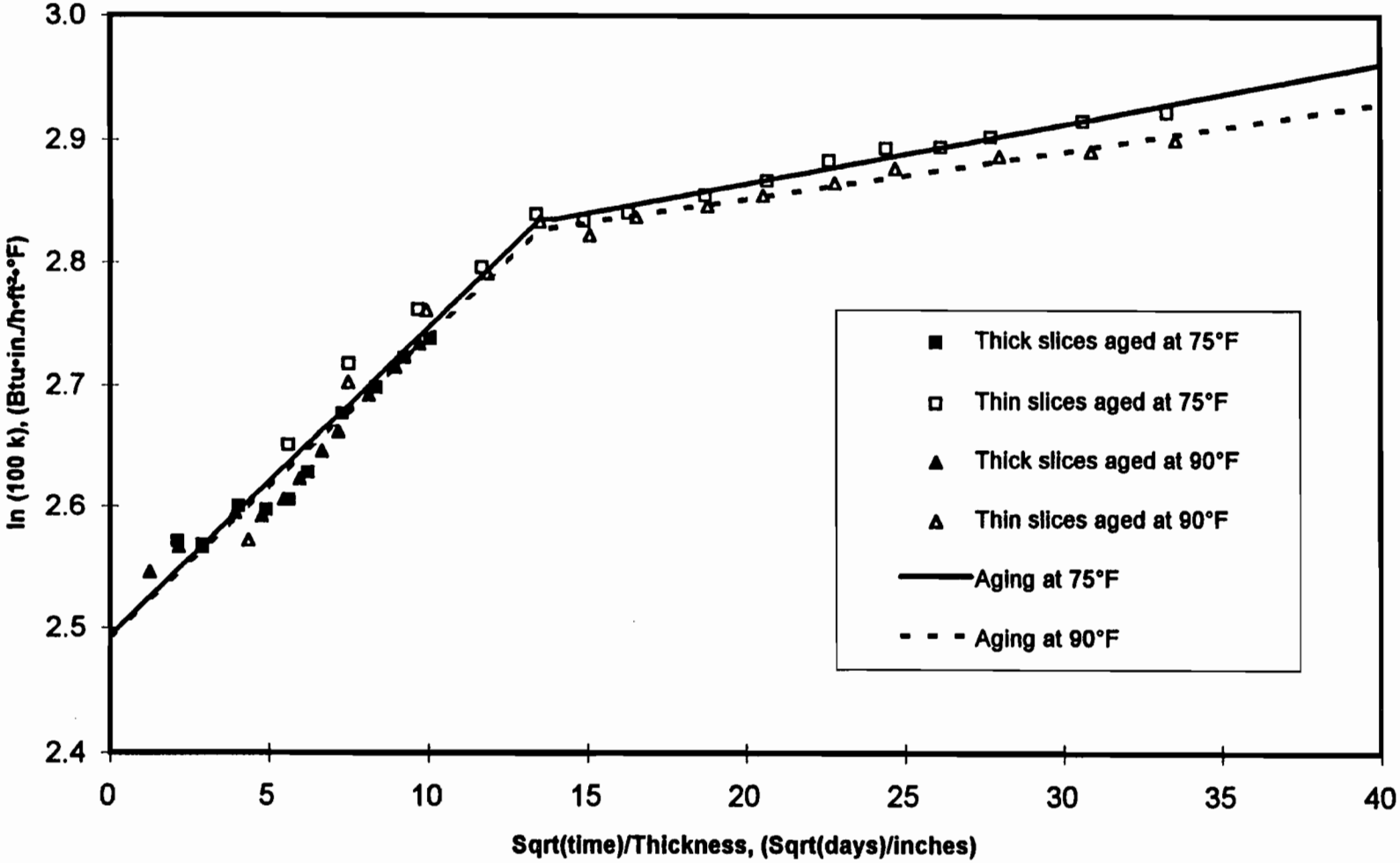

Figure 23. Thermal Conductivity of HCFC-141b Foam from Thin-Slicing Studies

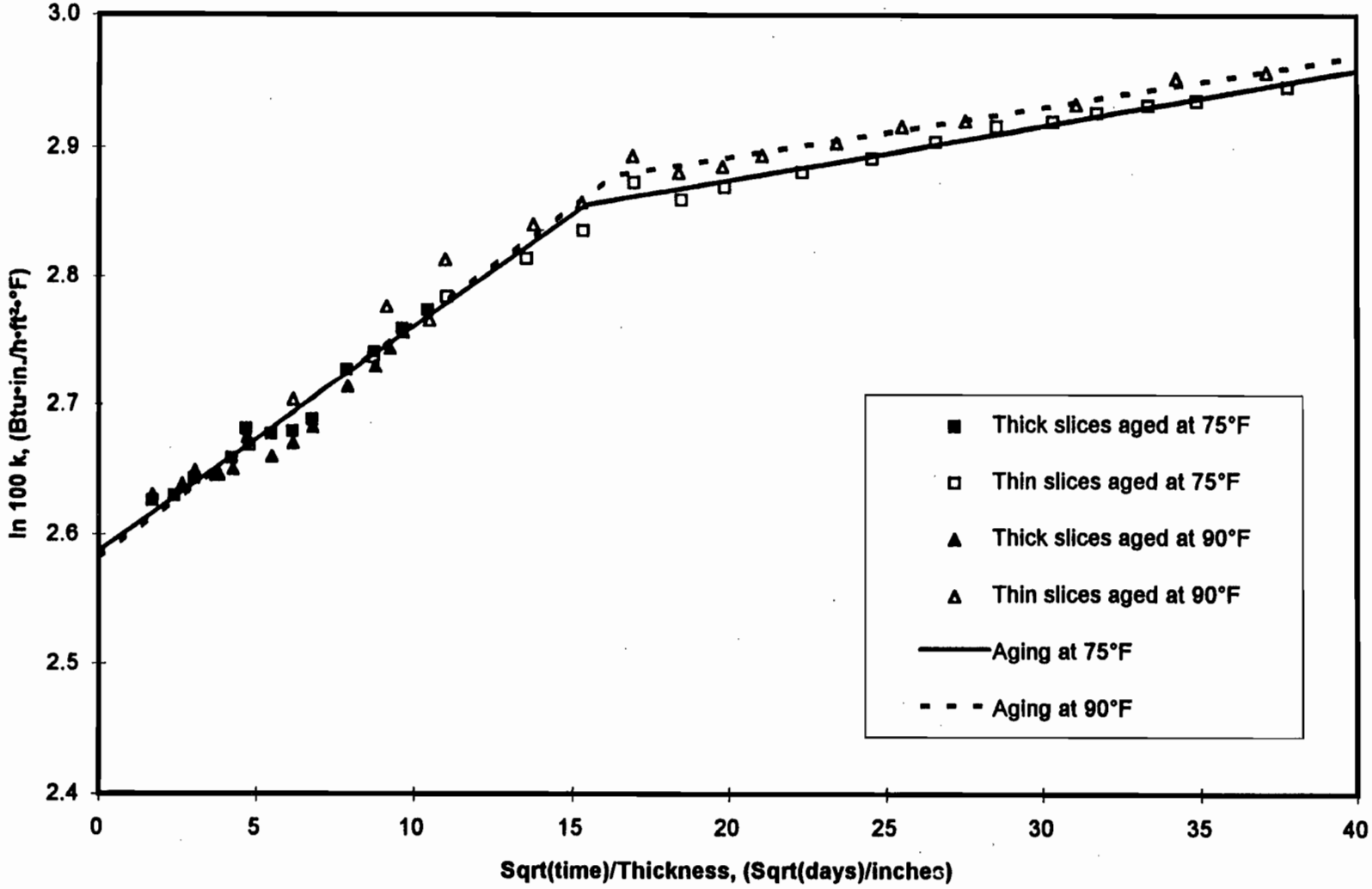

Figure 24. Thermal Conductivity of HCFC-142b/22 Foam from Thin-Slicing Studies

Table 16. Regression Analyses of Foam Thermal Conductivity from Thin-Slicing Studies

Blowing Agent	Aging Temperature, °F	Aging Region	a	b	r^2
CFC-11	75	1	2.4474	0.02576	0.86
	75	2	2.8005	0.00312	0.87
	90	1	2.4337	0.02927	0.94
	90	2	2.8221	0.00199	0.77
HCFC-141b	75	1	2.4935	0.02532	0.93
	75	2	2.7676	0.00484	0.97
	90	1	2.4914	0.02484	0.95
	90	2	2.7743	0.00388	0.96
HCFC-142b/22	75	1	2.5868	0.01742	0.98
	75	2	2.7912	0.00417	0.97
	90	1	2.5817	0.01816	0.91
	90	2	2.8161	0.00381	0.96

Note: a and b are regression constants from $\ell n\,(100\,k) = a + b\,\sqrt{t}/L$, where k is thermal conductivity (Btu•in./h•ft²•°F), t is aging time (days), and L is thickness (inches); r^2 is the coefficient of determination.

3.4.3.3 Composite Panels with Only Foam Insulation

Thermal measurements were performed on nine foam-only composite panels that contained slightly less than 2 inches of foam insulation. Three specimens of insulation foamed with each of the three blowing agents were tested over a one-year period. Additionally, one specimen foamed with each blowing agent was tested at the end of two years. The thermal measurements yielded the overall thermal resistance of the composite panel, including the contributions of the foam, steel sheet, and plastic sheet. The thermal resistances of the steel and plastics sheets were subtracted from the overall thermal resistance to obtain the resistance of the foam insulation itself. For these calculations, the thermal conductivities of steel and plastic were taken to be 480 and 1.8 Btu•in./h•ft²•°F. These two layers contributed less than 0.5 percent of the total resistance of the panel.

Foam insulation thermal conductivities obtained from these measurements are given in Table 17. For an individual specimen, there is no clear trend for thermal conductivity with time. The variations are within the estimated experimental uncertainty of ±10 percent for these high-resistance panels. Coefficients of determination (r^2) for linear regressions of the thermal conductivity versus time were 0.02, 0.11, and 0.02 for CFC-11, HCFC-141b, and HCFC-142b/22 blowing agents, respectively, confirming the lack of any clear trends for thermal conductivity versus time.

Foam thermal conductivities from the tests on composite panels are compared with thermal conductivities predicted from the thin-slice aging studies in Figure 25. Here the regressions corresponding to an aging temperature of 90°F from Table 16 were evaluated assuming a 2 inch thickness of foam. The thin-slice aging studies predict that the thermal conductivity of a two- inch layer of foam will increase over a one-year period by 32, 27, and 19 percent for CFC-11, HCFC-141b, and HCFC-142b/22 blowing agents, respectively. However, average values for the panels for each type of blowing agent varied by only 2 to 3 percent over the one-year period. Since the predicted increases based on thin-slicing are much larger than the changes observed in the composite panels, it must be concluded that the encapsulation of the foam with steel and plastic face sheets and aluminum edge tape greatly reduces the ability of air to

Table 17. Thermal Conductivity of Foam Insulation in Composite Panels

Blowing Agent	Aging Time			
	0 Months	6 Months	12 Months	24 Months
CFC-11	0.1158	0.1286	0.1192	
	0.1270	0.1129	0.1192	
	0.1087	0.1167	0.1217	0.1194
	(0.1172)	(0.1194)	(0.1200)	
HCFC-141b	0.1369	0.1462	0.1409	
	0.1353	0.1473	0.1364	
	0.1362	0.1283	0.1368	0.1443
	(0.1361)	(0.1406)	(0.1381)	
HCFC-142b/22	0.1311	0.1353	0.1372	
	0.1291	0.1326	0.1352	0.1298
	0.1305	0.1317	0.1301	
	(0.1302)	(0.1332)	(0.1342)	

Note: Values in parentheses are averages of three numbers directly above. Thermal conductivity values have units of Btu•in./h•ft²•°F.

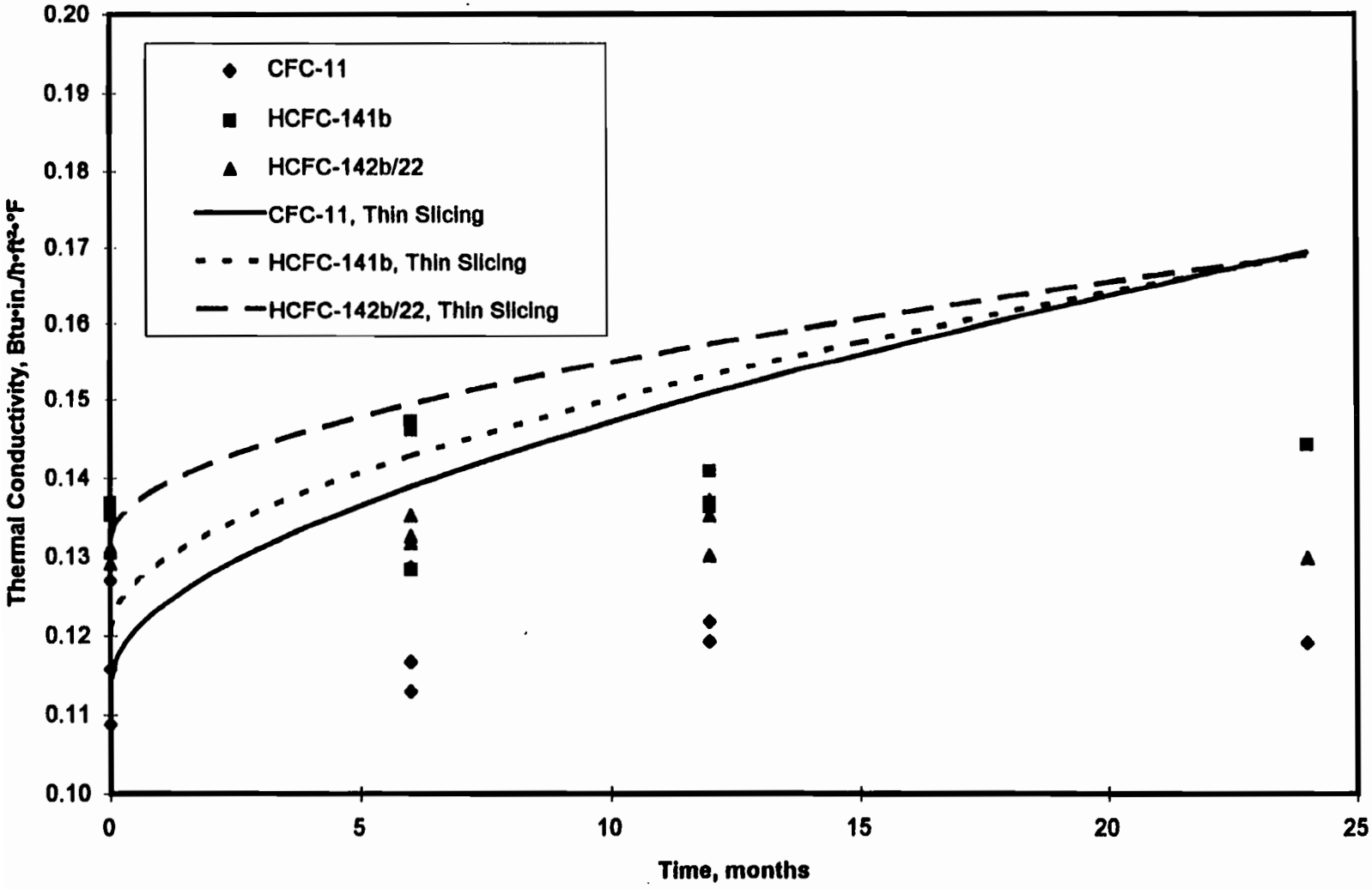

Figure 25. Thermal Conductivity of Foam Insulation from Composite Panels

enter the cells and of the blowing gas to escape.

3.4.3.4 Composite Panels Containing Superinsulations

Thermal measurements were performed on 36 composite panels that contained superinsulations. Measurements were made on all 36 panels at 0, 6, and 12 months of aging, and on 12 panels at 24 months. Raw data on the actual test panels were analyzed using a computer model to normalize them for differences in the sizes of the superinsulation panels and to estimate the total effective thermal resistance of panels that would likely be used in refrigerators. The computer model was a three-dimensional finite-difference heat conduction model based on the HEATING code. [6] Analysis of the data consisted of two steps.

For the first step of analysis, a model was set up that included the composite panel as well as the foam rubber sheets that were laid between the panel and the plates of the HFMA, as shown in Figure 26. The stainless steel claddings on some of the superinsulation panels were also included in the model, but because their thickness is much smaller than the grid spacing in the overall model, they are not shown explicitly in Figure 26. Using symmetry, the computer model only needed to consider a quadrant of the actual panel. The model for this quadrant consisted of about 7000 nodes at which temperatures and heat flows were calculated. Boundary conditions for the model consisted of the temperatures measured on the plates. This boundary condition was chosen instead of the temperatures measured at the centers of the faces of the composite panels because the plates are more isothermal. This way, the model allows for variations of temperature over the faces of the composite panels. Handbook values for thermal conductivities of several of the materials were used, viz., 480, 1.8, and 96 Btu•in./h•ft²•°F for the steel sheet, the ABS plastic sheet, and the stainless steel superinsulation cladding, respectively. A measured value of 0.7 Btu•in./h•ft²•°F was used for the foam rubber sheets. The value used for the urethane foam insulation was the average value measured on the foam-only composite panels at each time period for each blowing agent. The thermal conductivity of the superinsulation was treated as the only unknown quantity. The thermal conductivity of the superinsulation was systemically varied in the calculations until the calculated heat flux over the central 4 inch by 8 inch area matched the value measured by the heat flux transducers.

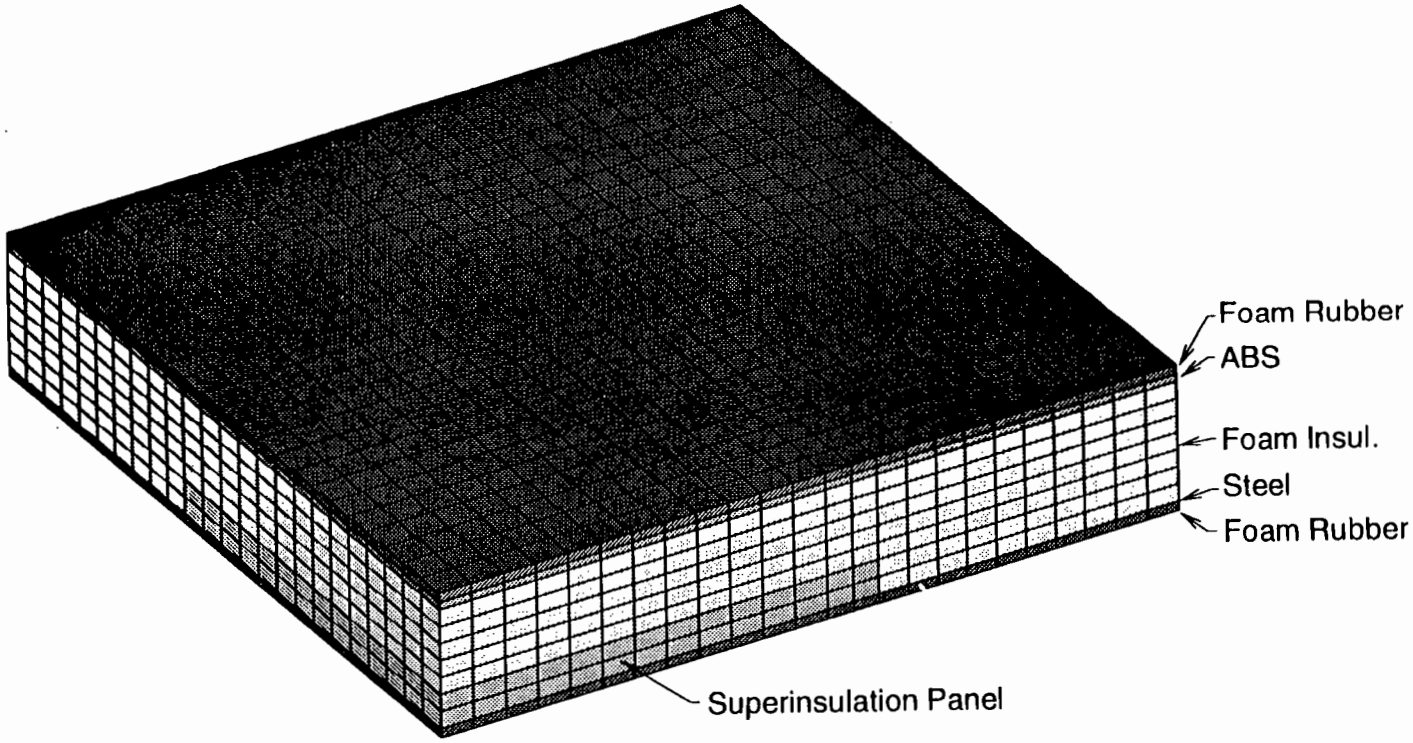

Figure 26. Computer Model of Composite Panels Containing Superinsulations

With values for the thermal conductivity of each of the materials, another computer model was used to estimate the overall thermal resistance of composite panels of various sizes in which the superinsulation covered 60 percent of the total area. For this model, the steel and plastic boundary sheets were taken to be exposed to air with a heat transfer coefficient of 1.0 Btu/h•ft²•°F. Overall thermal resistances obtained by this procedure are given in Table 18.

The overall thermal resistance depends upon four factors in this study: the type of superinsulation, the blowing agent for the foam insulation, the aging time, and the size of the simulated panels. Inspection of the data in Table 18 shows that the effect of panel size depends upon the type of superinsulation, but is essentially independent of the blowing agent or the aging time. For Type A panels, increasing the size from 18 to 24 inches increases the resistance by 0.5 percent, and increasing from 18 to 30 inches causes a 1 percent increase in resistance. For Type B panels, the resistance increases for these two size changes are 4 and 6-7 percent, while for Type C panels, the resistance increases are 4-5 percent and 7-8 percent. For Type D panels, the resistance increases are 0.1 percent or less. Thus, the effect of panel size is only significant for those superinsulations that have stainless steel claddings. Since the thickness of the stainless steel is constant, the heat conduction around the edges of the superinsulations becomes less important as the overall panel size increases while maintaining the same percentage of area covered by the superinsulation.

As was found for the foam-only composite panels, the overall resistances with superinsulation show no clearly evident trends for any decrease of resistance with time. Considering the averages of the triplicate sets of data at 24 inch panel size, the resistance changes over the two-year period range from an increase of 4.5 percent to a decrease of 6.0 percent. These variations are generally within the estimated experimental uncertainty of ±10 percent for these high-resistance panels. No obvious trends with type of superinsulation or blowing agent are seen in the results for thermal resistance versus time.

The type of blowing agent has a clear effect on the thermal resistances. The resistances with CFC-11 are greater than those for HCFC-141b by 2.2 to 12.0 percent, with an average of 8.5 percent. Likewise, the resistances with CFC-11 are greater than those for HCFC-142b/22 by 0.6 to 12.8 percent, with an average of 6.4 percent. These are to be compared with the results on

Table 18. Thermal Resistance of Composite Panels Containing Superinsulations

Panel	Blowing Agent	0 Months**		6 Months		12 Months			24 Months		
		18 in.*	24 in.	18 in.	24 in.	18 in.	24 in.	30 in.	18 in.	24 in.	30 in.
A-1	CFC-11	20.15	20.19	22.82	22.95	22.41	22.52	22.61			
A-2	CFC-11	23.02	23.14	22.92	23.05	22.89	23.02	23.13			
A-3	CFC-11	22.85	22.97	22.42	22.54	22.15	22.25	22.34	22.19	22.29	22.37
A-4	HCFC-141b	20.96	21.09	20.42	20.54	20.93	21.07	21.18			
A-5	HCFC-141b	20.68	20.80	20.56	20.69	20.28	20.39	20.48			
A-6	HCFC-141b	20.93	21.06	20.44	20.57	20.62	20.75	20.85	19.82	19.94	20.04
A-7	HCFC-142b/22	21.00	21.11	20.21	20.30	19.91	19.99	20.06	20.92	21.03	21.11
A-8	HCFC-142b/22	22.09	22.24	19.71	19.78	20.64	20.74	20.83			
A-9	HCFC-142b/22	20.68	20.78	20.57	20.67	20.28	20.37	20.45			
B-1	CFC-11	20.62	21.28	21.08	21.93	20.80	21.60	22.15			
B-2	CFC-11	21.09	21.88	20.36	21.02	20.37	21.06	21.53	20.23	20.86	21.29
B-3	CFC-11	19.49	19.91	19.93	20.49	19.14	19.55	19.83			
B-4	HCFC-141b	18.78	19.45	18.31	18.95	18.72	19.41	19.90			
B-5	HCFC-141b	19.85	20.82	18.93	19.74	19.67	20.64	21.34			
B-6	HCFC-141b	19.88	20.86	18.73	19.49	19.38	20.26	20.89	18.76	19.61	20.22
B-7	HCFC-142b/22	19.80	20.60	19.47	20.26	19.45	20.26	20.83	19.58	20.32	20.83
B-8	HCFC-142b/22	20.19	21.10	20.07	21.03	19.91	20.85	21.53			
B-9	HCFC-142b/22	19.37	20.06	18.67	19.25	19.40	20.19	20.75			

Note: Thermal resistance of composite panel has units of $h \cdot ft^2 \cdot °F/Btu$.

* Size of simulated square composite panel, assumes superinsulation covers 60 percent of area.

** Aging time

Table 18. Thermal Resistance of Composite Panels Containing Superinsulations (cont.)

Panel	Blowing Agent	0 Months**		6 Months		12 Months			24 Months		
		18 in.*	24 in.	18 in.	24 in.	18 in.	24 in.	30 in.	18 in.	24 in.	30 in.
C-1	CFC-11	21.55	22.52	20.64	21.42	21.21	22.17	22.85			
C-2	CFC-11	20.76	21.51	21.31	22.28	21.34	22.34	23.05			
C-3	CFC-11	21.37	22.29	20.04	20.67	20.48	21.24	21.76	20.86	21.70	22.29
C-4	HCFC-141b	19.63	20.57	19.05	19.93	19.36	20.27	20.92	18.79	19.68	20.31
C-5	HCFC-141b	19.56	20.48	18.66	19. 43	19.59	20.57	21.27			
C-6	HCFC-141b	19.32	20.17	18.86	19.68	19.15	19.99	20.60			
C-7	HCFC-142b/22	19.74	20.57	19.46	20.28	19.84	20.80	21.48			
C-8	HCFC-142b/22	19.18	19.86	18.88	19.56	19.45	20.29	20.89	19.89	20.75	21.36
C-9	HCFC-142b/22	19.07	19.72	19.73	20.62	19.63	20.52	21.16			
D-1	CFC -11	19.25	19.27	18.68	18.69	18.80	18.81	18.82			
D-2	CFC-11	19.15	19.16	18.25	18.25	18.88	18.89	18.90			
D-3	CFC-11	19.04	19.05	18.86	18.87	18.75	18.76	18.77	18.80	18.81	18.82
D-4	HCFC-141b	18.30	18.33	17.43	17.45	17.73	17.75	17.77			
D-5	HCFC-141b	17.21	17.22	16.79	16.80	16.26	16.26	16.27	16.95	16.96	16.98
D-6	HCFC-141b	17.47	17.49	17.11	17.12	17.14	17.15	17.16			
D-7	HCFC-142b/22	17.37	17.38	17.01	17.02	17.12	17.13	17.13			
D-8	HCFC-142b/22	17.67	17.68	17.11	17.11	17.31	17.32	17.33			
D-9	HCFC-142b/22	18.07	18.09	17.26	17.27	17.08	17.09	17.10	17.94	17.95	17.96

Note: Thermal resistance of composite panel has units of $h \cdot ft^2 \cdot °F/Btu$.

* Size of simulated square composite panel, assumes superinsulation covers 60 percent of area.

** Aging time.

the foam insulation from the composite panels, where the average thermal conductivity for CFC-11 was 17.5 percent less than for HCFC-141b, and 10.8 percent less than for HCFC-142b/22. These comparisons are in good agreement, since the foam contributes about one-half of the center-of-panel resistance of the composites with superinsulation.

Averaging all the results for each type of superinsulation gives average composite panel thermal resistances of 21.2, 20.2, 20.5, and 17.8 for panels with Types A, B, C, and D superinsulation. Thus panels with Types A, B, and C superinsulations are relatively similar, while the panels with Type D superinsulation have resistances that are about 12 to 16 percent lower. This is in agreement with the center-of-panel results on the superinsulation panels, where the average thermal resistivity of Type D panels was 40 percent less than those of Type A panels. The thermal resistance of composite panels with Types A, B, and C superinsulations are remarkably similar, even though the center-of-panel thermal resistivities were greatly different. The higher center-of-panel thermal resistivities for Type B and C superinsulations were offset by heat conduction through the stainless steel encapsulation material.

4. INVENTIONS

Three inventions were made by ORNL during this CRADA. They are covered under ESIDs 1458X, 1465X, and 1469X.

5. COMMERCIALIZATION POSSIBILITIES

Superinsulations based on PEPs and superinsulations with other filler materials are presently being commercialized. Some refrigerator manufacturers are utilizing superinsulations in certain models of refrigerators.

6. PLANS FOR FUTURE COLLABORATIONS

While there are no definite plans for future collaborations, ORNL and the Appliance

Research Consortium will continue to explore possibilities related to both PEP superinsulation and urethane foam insulation, including studies of replacements for HCFC-141b blowing agent.

7. CONCLUSIONS

In Phase I, equipment and procedures were developed for performing an accelerated lifetime aging procedure for PEPs. The procedure involved the fabrication of test panels that replaced the usual powder filler with metal plates with either zero void volume or with small known amounts of voids. The small internal volume in these panels as compared with that in PEPs provides the acceleration of the aging process. Proof-of-principle tests were conducted that showed the pressure rise curves in the test panels followed the expected trends. The accelerated aging test results are used to predict the pressure versus time within a PEP. The second step involves determination of the curve of thermal resistivity versus internal pressure. These two pieces of information are then combined to develop a curve of thermal resistivity versus time. This curve predicts the thermal performance of the PEPs over their lifetimes.

In Phase II, an interlaboratory comparison was made of the ability of nine laboratories to measure the thermal resistivity of PEPs. Heat Flow Meter Apparatus measurements were made on three sizes of PEPs (6 × 6 in., 9.5 × 9.5 in., and 21.5 × 21.5 in.). All PEPs were about 0.75 in. thick, and were made with the same materials and with about the same density of powder. Measurements on the five specimens of the two larger sized PEPs by six laboratories demonstrate a 2σ of 7.4% about the mean. When the measurements of four laboratories on the five smallest sized PEPs are included, the 2σ increases to 12.9% about the mean because the thermal conductivities of the smallest PEPs are higher than the other two sizes. The reason that the thermal conductivity of the smallest PEPs was higher than that of the other two sizes is not known. The measured R-value for the nominally 0.75-inch-thick PEPs is 17.4 $h \cdot ft^2 \cdot °F/Btu$ if the small specimen measurements are not included. The average thermal resistivity for the large test specimens was 23.2 $h \cdot ft^2 \cdot °F/Btu \cdot in$. To within experimental error, the internal pressures in the PEPs did not change during the course of this work. These results demonstrated the ability of the nine laboratories to obtain consistent thermal resistances on PEPs.

In Phase III, the lifetime aging procedure developed in Phase I was applied to a set of nine panels that were encapsulated in Vecat barrier film with a Tyvek intervening layer. The panels had three levels of known internal volume within the metal plates (0, 2.5%, and 5% void fraction). The panels were aged in air for about five months and then in helium for about a week. Plots of pressure versus time in the panels followed the expected trends. The pressure rose much faster in the panels with very small void volume and slowest in the panels with the largest void volume. The pressure rise in helium was several orders of magnitude faster than in air. Analyses of the data showed that the shape of the pressure-time curves corresponded to the theoretical equations for permeation of gases through films. Analysis of the data showed that the internal volume within the Tyvek layer was close to the internal volume of the metal plates that contained 2.5 percent void volume. An experimental determination of this extra volume is necessary for a correct estimation of the permeance of the barrier film. Analysis of the data on two sizes of Vecat pouches showed that the effective permeating area of the Vecat film is not the total area within the heat seal lines, but rather is closer to the area just over the metal plate itself. While gases permeate through the film in regions removed from the metal plate, they do not appear to be able to travel laterally between the two layers of Vecat which are compressed together by atmospheric pressure. During aging in helium, blisters were observed in the Vecat film away from the plates, further confirming this conclusion. The average permeance of the Vecat film was determined to be 0.00054 and 2.31 cc(STP)/100 $in.^2$•atm•day for air and helium, respectively. Standard deviations of the permeance with air and helium were 8 percent and 5 percent of the mean values.

Thermal resistance measurements were made on 21 PEPs that had been fabricated by GE Appliances at internal pressure levels up to about 300 torr. The purpose of these data was to develop the curve of thermal resistivity versus pressure that is needed for the lifetime procedure. Measurements of PEP internal pressure were performed using two techniques: the ORNL hand-held gauge and a vacuum chamber fitted with a sensor similar to the one used in the hand-held gauge. The vacuum chamber measurements always yielded lower pressures than the hand-held gauge. It was demonstrated that when applied to panels with solid metal fillers and with known internal pressures, the vacuum chamber gives pressures that are much lower than the known values, while the hand-held gauge results are in good agreement with the known values. This

difference is thought to be due to a ballooning effect in the vacuum chamber, which greatly increases the internal volume of the metal-filled panels. Similar demonstrations have not yet been successful with powder-filled panels, which have a much larger internal volume. Since the internal pressures of the thermal specimens are not accurately known, two curves of thermal resistivity versus pressure were developed from the two sets of pressure data.

Using the mean measured permeance value for the Vecat film and the resistivity-pressure curves, the thermal resistivity versus time was predicted for PEPs of the size that might be used in refrigerators. These analyses predicted that the thermal resistivity of a PEP with an initial thermal resistivity of 25 h•ft²•°F/Btu•in. would be 14.5 to 18 h•ft²•°F/Btu•in. at the end of 20 years.

In Phase IV, thermal resistances were measured on composite panels that simulate walls or doors of refrigerators that contain superinsulations along with urethane foam. It was demonstrated that both gas-filled and vacuum superinsulations can withstand the processes necessary to fabricate refrigerator/freezer walls and doors, including the foaming of urethane insulation around the superinsulations. The overall range of resistance for the composite panels was from 16 to 23 h•ft²•°F/Btu. Composite panels measured over a two-year time period showed less than a 6 percent change in overall thermal resistance. Similar results on composite panels without superinsulation showed resistances changes of less than 3 percent. These small changes with time indicate that the bounding surfaces of the simulated refrigerator walls or doors hinder the movement of air into and the blowing agent out of the cells of the foam. With 60 percent of the panel area covered with superinsulation, increasing the panel size from 18 to 30 inches square results in about an 8 percent increase in overall resistance when the superinsulation is encapsulated in stainless steel foil, and very small increases for other superinsulations.

8. ACKNOWLEDGEMENTS

The authors would like to acknowledge the contributions of a number of organizations. Funding for this project was provided by the Appliance Research Consortium, and the U.S. Department of Energy, Office of Buildings Energy Research, under contract number DE-AC05-96ORR22464 with the Oak Ridge National Laboratory, managed by Lockheed Martin Energy

Research Corp. Superinsulation panels were provided by Aladdin Industries, Inc., GE Appliances, Lawrence Berkeley National Laboratory, and Owens-Corning. Composite panels were foamed by Dow Chemical Corp., ICI Chemicals, Inc., and Miles Laboratories (Bayer). Fred Weaver of ORNL performed the heat flow meter measurements.

9. REFERENCES

1. T. G. Kollie and L. H. Thacker, Review of Scientific Instruments 63 (12), 5774-5779 (1992).

2. R. S. Graves and T. G. Kollie, "Interlaboratory Comparison Measurements of the Thermal Conductivity of Powder-Filled Evacuated Panel Superinsulation," Thermal Conductivity 22, T. W. Tong (ed.), pp. 435-446, Technomic Publishing Co. (1993).

3. C 518, "Standard Test Method for Steady-State Heat Flux Measurements and Thermal Transmission Properties by Means of the Heat Flow Meter Apparatus," in 1995 Annual Book of ASTM Standards, Vol. 04.06, pp. 151-162, American Society for Testing and Materials, Philadelphia (1995).

4. R. S. Graves, D. L. McElroy, F. J. Weaver, and D. W. Yarbrough, "Interlaboratory Comparison on Estimating the Long-Term Thermal Resistance of Unfaced, Rigid, Closed-Cell Polyisocyanurate (PIR) Foam Insulation - A Cooperative Industry/Government Project," ORNL/M-3976 (January 1995).

5. C 1303, "Standard Test Method for Estimating the Long-Term Change in the Thermal Resistance of Unfaced Rigid Closed Cell Plastic Foams by Slicing and Scaling Under Controlled Laboratory Conditions," to be published in 1996 Annual Book of ASTM Standards, Vol. 04.06, American Society for Testing and Materials, Philadelphia (1996).

6. K. W. Childs, HEATING 7.2 User's Manual, ORNL/TM-12262, Oak Ridge National Laboratory, Oak Ridge, Tennessee, February 1993.

APPENDIX A

PHASE III PROCEDURE FOR ARC CRADA (ORNL 91-0042)

ORNL/M-3335R/1

~~CRADA PROTECTED INFORMATION (EGID 1469-X)~~

Expired 3/22/1999 per KEW

PHASE III PROCEDURE FOR ARC CRADA (ORNL 91-0042)*

T. G. Kollie, K. E. Wilkes, and G. M. Ludtka

July 1994

---

*Research sponsored by the U.S. Department of Energy, Assistant Secretary for Energy Efficiency and Renewable Energy, Office of Buildings Energy Research, Building Systems and Materials Division, under contract DE-AC05-84OR21400 with Martin Marietta Energy Systems, Inc.

CRADA PROTECTED INFORMATION (ESID 1469-X)
Expired 3/22/1999 per KEW

PHASE III PROCEDURE FOR ARC CRADA (ORNL 91-0042)

T. G. Kollie, K. E. Wilkes, and G. M. Ludtka

SUMMARY

This method enables the determination of the permeance of different candidate powder-filled evacuated (PEP) barrier materials at an accelerated rate, i.e., within six months or less in contrast to several years if conventional PEPs and techniques were used. This acceleration is accomplished through the minimization of the internal "free volume" of the PEP by using a solid aluminum filler inside the barrier material rather than conventional filler powder, which is of very large free volume (on the order of 90% of the internal volume of the PEP) and which can absorb water vapor, nitrogen, or oxygen onto its very large surface area (>175 m^2/g for typical ceramic filler powders) and result in a very sluggish rate of pressure rise which would hinder rapid permeance testing/determination.

In addition, this method relies on the ratioing of the slopes of the logarithmic pressure versus exposure time curves for different gas environments (dry nitrogen, dry air, or dry oxygen) with that of helium gas to facilitate extrapolation of long term (20 and 100 years) performance of the candidate barrier materials.

INTRODUCTION

The successful implementation of a super-insulating, powder-filled evacuated panel (PEP) requires long term stability of the insulating capability of the PEP. These panels maintain their excellent thermal resistances as long as the internal pressure of the PEP is very low, i.e., absolute pressure of 0.1 to 10 mm Hg. The usual construction of a PEP requires an outer barrier material which contains the super-insulating powder under these vacuum conditions. The outer barrier material can be a polymer laminate film, a metallized polymer laminate film, metal film, or metal foil. The polymer laminate materials (metallized or not) provide the optimum barrier material from a thermal performance viewpoint because they will not conduct heat around the perimeter (outer surface) of a PEP to the degree that a very highly conducting metal envelope would. In addition, relatively simple heat sealing equipment can be used to join the polymer laminates in contrast to more complicated seam welding techniques for metallic containments. The performance of the polymer laminate films is limited, however, by the permeance (or permeability) of the film to typical gaseous environments of nitrogen, oxygen, carbon dioxide, and water vapor which will be seen in actual use of the PEP. As these gases diffuse through the polymer laminate, the internal pressure of the PEP will rise, resulting in degradation of the super-insulating capabilities

of the PEP. It is important, therefore, to select the best candidate materials for the outer barrier material of the PEP from the many laminate combinations made by the polymer industry. Unfortunately, the permeability of the available films is generally not well characterized and so a potential manufacturer or user of a PEP must do a permeability study in support of a PEP development program.

The powders (or fillers) inside a PEP are typically at a fraction of theoretical density (usually 7 to 15%), which means that there is a tremendous free volume (about 90%) within the PEP. Defining equations for the pressure rise in a PEP show that the ratio of the surface area of the PEP to the internal free volume must be maximized to achieve a rapid pressure rise in a PEP. Unfortunately, years (about five years for 0.1 mm thick VECAT film laminate) would be required to observe an increase in internal pressure from 1 mm Hg to 5 mm Hg inside a conventional PEP made with existing barrier materials. Permeability testing of this duration is impractical, expensive, and equipment intensive, especially when product lifetimes of 20 years are required for refrigerator/freezer PEPs and 100 years for home insulation PEPs. An inexpensive, rapid (less than six months) method of characterizing the permeance of different candidate materials is accomplished by the procedure presented in this report. The need and acceptance of such a technique is highlighted by the fact that the Appliance Research Consortium (ARC) established a CRADA (ORNL 91-0042) with ORNL to develop a procedure to predict the lifetime of a PEP.

The lifetime of a PEP must be judged by the user. First, the apparent thermal conductivity (k) of the powder (filler) must be determined as a function of pressure. Second, the permeability of the barrier material must be measured for the environment to which the PEP is exposed. (This procedure is developed for dry air.) Third, the pressure versus time inside the PEP is computed from the measured permeability and the known physical dimensions of the PEP. Fourth, the k of the PEP is computed as a function of time from the measured k versus pressure and the computed pressure versus time. The user must determine the maximum k allowable for the application; the lifetime of the PEP is the time at which the k of the PEP reaches the selected maximum k.

CRADA PROTECTED INFORMATION (ESID 1469-X)

Expired 3/22/1999 per KEW

MEASUREMENT OF k VERSUS PRESSURE

The k of the PEP versus its internal pressure can be measured in a number of ways. For the purpose of Phase III of this CRADA, up to seven PEPs with different levels of pressure will be supplied to each participant. The procedure used in Phase II of the CRADA will be used to measure the k of these panels. The pressure inside the PEPs must be measured by the participant. Arrangements can be made with ORNL to use one of its pressure gauges for this measurement. Written details of the procedure for the pressure measurements will be supplied with the gauge, if the ORNL gauge is used. Presently, ORNL has three methods of measurement of the pressure inside a PEP, all based on a technique developed at ORNL (T. G. Kollie and L. H. Thacker, *Rev. Sci. Instrum. 63 (12),* December 1992, pp. 5774-5779, and U.S. Patent 5,249,454). At present, ORNL has not yet established which of these is the most accurate and repeatable method to use. Experimentation necessary to select this technique will have been completed before the seven PEPs for Phase III are distributed to the ARC members who participate in conducting the procedure.

An alternate procedure is to use a variable-pressure barrier material feedthrough device (invention disclosure ESID 1465-X submitted to DOE and considered to be CRADA generated information) with pressure monitoring equipment. With this device, only one PEP is used because the pressure in the PEP can be varied and measured directly, i.e., the ORNL pressure gauge is not needed for this technique. This method was discussed at the ARC meeting held at ORNL in 1993. Special arrangements must be made with GE Appliances to fabricate the type of PEP required for this technique.

Figure 1 is a plot of the thermal resistivity (R/in.) of a typical powder versus pressure. The R/in. is the reciprocal of the apparent thermal conductivity, k, of the powder.

Expired 3/22/1999 per KEW

MEASUREMENT OF PERMEABILITY OF BARRIER MATERIAL

The method for accelerated permeability measurements on PEP barrier materials includes the following equipment and test specimens:

One or more chambers (ORNL example is three: one each for dry nitrogen, dry air, and helium environments) with pressure/vacuum control capability (mechanical pump system) and gas supply equipment (e.g., bottled gas cylinders with regulator valves). Line drawings for these chambers have been supplied to ARC members. These drawings include the above mentioned equipment.

Chamber pressure measurement equipment, which for ORNL includes capacitance manometers ("Baratron" gauges) and Hastings gauges.

PEP internal pressure measurement equipment, which at ORNL includes two versions of a hand-held gauge (U.S. Patent 5,249,454 and a Continuation In Part patent application pending).

Minimized internal (PEP) "free volume" test piece assemblies, which for this procedure are solid aluminum plates and aluminum plates with known volumes of small holes, encapsulated with the candidate barrier material and an intermediate layer of semipermeable material such as TYVEK.

Temperature control and measurement equipment for the chambers to maintain temperatures at 90°F .

The following is a description of how the method for accelerated permeability measurements is performed using the components described above.

A solid aluminum (other non-outgassing materials would work also) plate is covered with an inner bag of TYVEK or other similar semi-porous material and heat sealed into the barrier material by GE Appliances. Upon receipt of the aluminum-filled evacuated panel, the internal pressure is measured and recorded by the participant.

The aluminum-filled evacuated panel is placed onto an open mesh (to allow gas exposure on all surfaces of the panel) shelf in one of the chambers selected for the gas system (dry air) that is hooked up to it and will be the first gaseous environment that will permeate into the panel. The chamber, which is operating at the specified temperature (typically using a recirculating controlled temperature bath and copper coils around the exterior of the chamber) for the permeability study is closed and evacuated. Care is taken to keep the vacuum level about 20 mm Hg above the internal pressure of the panel which generally is in the range of 0.1 to 100 mm Hg. The system is backfilled to atmospheric pressure or slightly higher (generally not above 780 mm Hg total chamber pressure) with the gas to be used in the permeability study. This process of evacuating and backfilling is repeated several times to insure that minimal residual, unwanted gas species (like water vapor) are not present inside the chamber {Instead of the evacuation/backfill procedure, the chamber can be flushed with the fill gas. The authors do not recommend this procedure because purity levels of the fill gas can not be easily estimated}.

The specimens are left in the chamber for varying amounts of time, depending on the gas environment and its estimated permeation rate through the barrier material. Typically, the chambers should be opened and the aluminum-filled evacuated panel internal pressures measured at two week time intervals when exposure would be in dry air. Only a few hours to one or two days between measurements are needed if the environment is dry helium because this gas species permeates approximately a thousand times faster in polymeric film laminate barrier materials than nitrogen or oxygen. Care should be taken to make sure that all of the internal pressure measurements are performed on the aluminum-filled evacuated panels at the same temperature (within each sampling period and between each sampling period) since different sample temperatures will change the volume of the internal gas (ideal gas law) and, therefore, the pressure reading could vary. Also, the aluminum panel will change volume due to thermal expansion or contraction and affect the pressure inside the panel.

An example of the aluminum-filled evacuated panel internal pressure rise monitored with time for a 0.1 mm thick VECAT barrier material for a dry nitrogen environment is shown as a plot of pressure versus time in Fig. 2. This relationship is contrasted to the internal pressure rise measured in a PEP filled with a PPG Industries T600 powder which was exposed to a dry air environment, see Fig. 3. These figures clearly show that the unique idea of using a minimized internal free volume panel (i.e., the solid aluminum-filled evacuated panel) definitely accelerates the internal pressure rise measured over an extended time period whereas the pressure versus time history in the powder-filled evacuated panels using the same 0.1 mm thick VECAT barrier material show no real measurable pressure rise for the same time period after the initial pressure rise caused by powder outgassing at the very early stage of exposure. This outgassing is attributable to the very large surface area of the powders used in PEPs (typically 175 m^2/g) and is possibly due to absorbed water, oxygen, or nitrogen. The lack of any significant internal pressure rise is directly attributable to the very large internal free volume of this type of PEP.

The powders typically are at very low theoretical densities (7% to 20%) and so the internal free volume for a 0.23m x 0.23m x0.01m ceramic powder filled PEP is on the order of 468 cm^3. This is in contrast to the minimized free volume (in reality, maximization of the PEP barrier material permeating surface area, A, divided by the internal free volume, V) solid aluminum-filled evacuated panels which have an internal free volume on the order of about 5 cm^3. Only small amounts of gas have to permeate through the barrier material in the aluminum-filled evacuated panel to cause a pressure rise in the very small free volume whereas significant gas would have to permeate through the barrier material in the powder-filled evacuated panels to cause a pressure rise in the very large (468 cm^3) internal free volume of the powder. Using literature data for the permeance of oxygen through VECAT and a powder-filled evacuated panel of the above dimensions, an exposure time of 10.6 years is calculated for PEP internal pressure rise to occur from 0.3 mm Hg to 5.0 mm Hg. The accelerated rate, aluminum panel tests in dry nitrogen, which permeates at only approximately one-fourth the rate of oxygen, clearly show that a very significant internal pressure rise of about 15 mm Hg occurs in a little over 100 days. These data verified the concept of an accelerated permeation rate procedure/system for barrier material permeation rate studies.

After sufficient exposure time, which is dependent on the permeating gas species, a steady state condition develops which will yield a straight line slope on a plot of the quantity *ln* $((P-P_a)/(P_i-P_a))$ versus time, where P_a is the ambient pressure and P_i is the initial pressure inside the panel, and *ln* denotes the Naperian or natural logarithm (see Fig. 4 for a plot of this logarithmic function of pressure versus time). This slope is relatable to the permeance of the gas, p, through the barrier material and the internal free volume, V, of the PEP as follows:

$$\text{SLOPE} = (-pATRd_o)/(VM) \quad ,$$

where "p" is the gas permeance, "A" is the permeating surface area of the PEP barrier material, "T" is the test temperature, "R" is the ideal gas constant, "d_o" is the density of the gas at STP (Standard Temperature and Pressure), "V" is the PEP internal free volume, and "M" is the molecular weight of the permeating gas. Once the internal free volume of the PEP is known, the "steady state" permeance can be calculated from the linear slope since all of the other parameters are known.

After the first gas environment has been studied, which for this procedure would generally be dry air, the specimens are moved to another chamber (or the same chamber could be used with a new gas hook-up that is plumbed for a different gaseous species), which for this procedure would contain helium. Similar procedures are employed as described above for the air exposure to obtain the slope of the pressure versus time relationship as the panel "ages." Plots of pressure versus time and logarithmic function of pressure versus time for aluminum-filled evacuated panels in dry helium are shown in Figures 5 and 6. Note how much more rapidly the pressure rises in helium than in nitrogen.

The ratio of the two slopes (i.e., the slope of the logarithmic pressure versus time plot in helium to that in dry air) is directly proportional to the ratio of the permeabilities of the barrier for the two gases, helium and dry air. The only unknown is the "free volume," V. Several methods are available for estimating this free volume directly. The authors suggest, however, that other measurements or tests be performed simultaneously with that already described. For these measurements, very small holes are drilled through the aluminum panels before they are encapsulated in the barrier material and TYVEK. The

authors suggest that the volume of these holes be 1 to 5% of the volume of the aluminum plate (ORNL has used 9 in. x 9 in. x 0.25 in. panels.). The volume of the holes must be measured as accurately as possible, either mechanically or by liquid or gas displacement methods. After encapsulation in TYVEK and the barrier film, this panel is placed directly in the helium chamber. The pressure rise will be slowed considerably by the holes, probably a factor of two to four, depending on the volume percent of the total volume represented by the holes.

Obviously, the volume of the holes should be as small as possible to accelerate the pressure change, but not much smaller than the free volume without holes, which was found to be about 5 cm^3 for the VECAT barrier, TYVEK intermediate layer, and aluminum panel of the size used at ORNL. From the measurements of the slopes of the pressure versus time plots for these panels, the permeability for helium can be calculated directly. Since the free volume without holes (which is due mainly to the porosity of the TYVEK intermediate layer) is not negligible compared to the known volume of the holes, the total volume used to calculate permeability must include the free volume without holes. In general this volume will not be known accurately beforehand, but may be estimated from the experimental data. This may be done by plotting the diffusing area (A) divided by the slope of the log pressure versus time plot (SLOPE) against the known volume of holes for the three panels with 0, 1, and 5% holes. As shown in Figure 7, a straight line fitted to these data points will give the free volume without holes as the intercept on the negative x-axis. This free volume should then be added to the known volume of the holes to obtain a total volume for use in calculating the permeability to helium.

Then the permeability, p, of the barrier for dry air is calculated by multiplying the measured ratio of the air/helium permeabilities by the measured permeability in helium.

COMPUTE PRESSURE VERSUS TIME IN PEP

The pressure, P, versus time in the PEP is computed using the equation

$$P = P_a - (P_a - P_i) \exp\left(-p \frac{A}{V} \frac{RTd_o}{M} t\right)$$

where P_a is the ambient pressure of dry air, P_i is the initial pressure in the PEP, and t is time. Figure 8 gives two examples of pressure (right hand axis) versus times computed for two barriers having permeabilities that differ by a factor of four in value.

COMPUTE k VERSUS TIME OF PEP

The 1/k or R/in. for the PEP as a function of time is computed from the pressure versus time in the PEP (Fig. 8) and the k or R/in. versus pressure of the powder (Fig. 1). Such a computation is also shown in Fig. 8, left hand axis. The user must determine the maximum k allowable for the application; the lifetime of the PEP is the time at which the R/in (1/k) of the PEP in Fig. 8 reaches the selected maximum k.

RESISTIVITY OF MOST POWDERS IS A STRONG FUNCTION OF THE INTERNAL PRESSURE OF A PEP

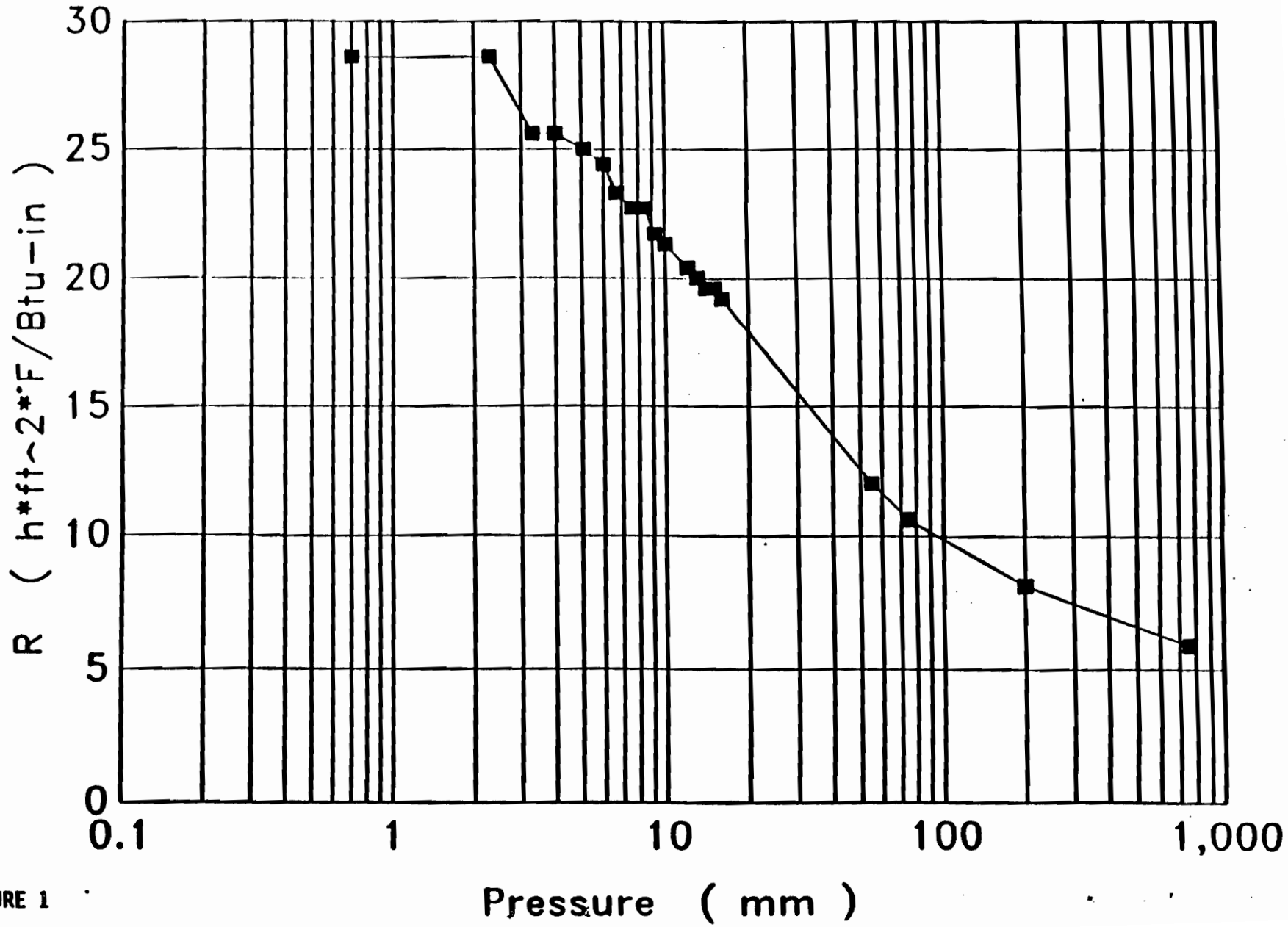

FIGURE 1

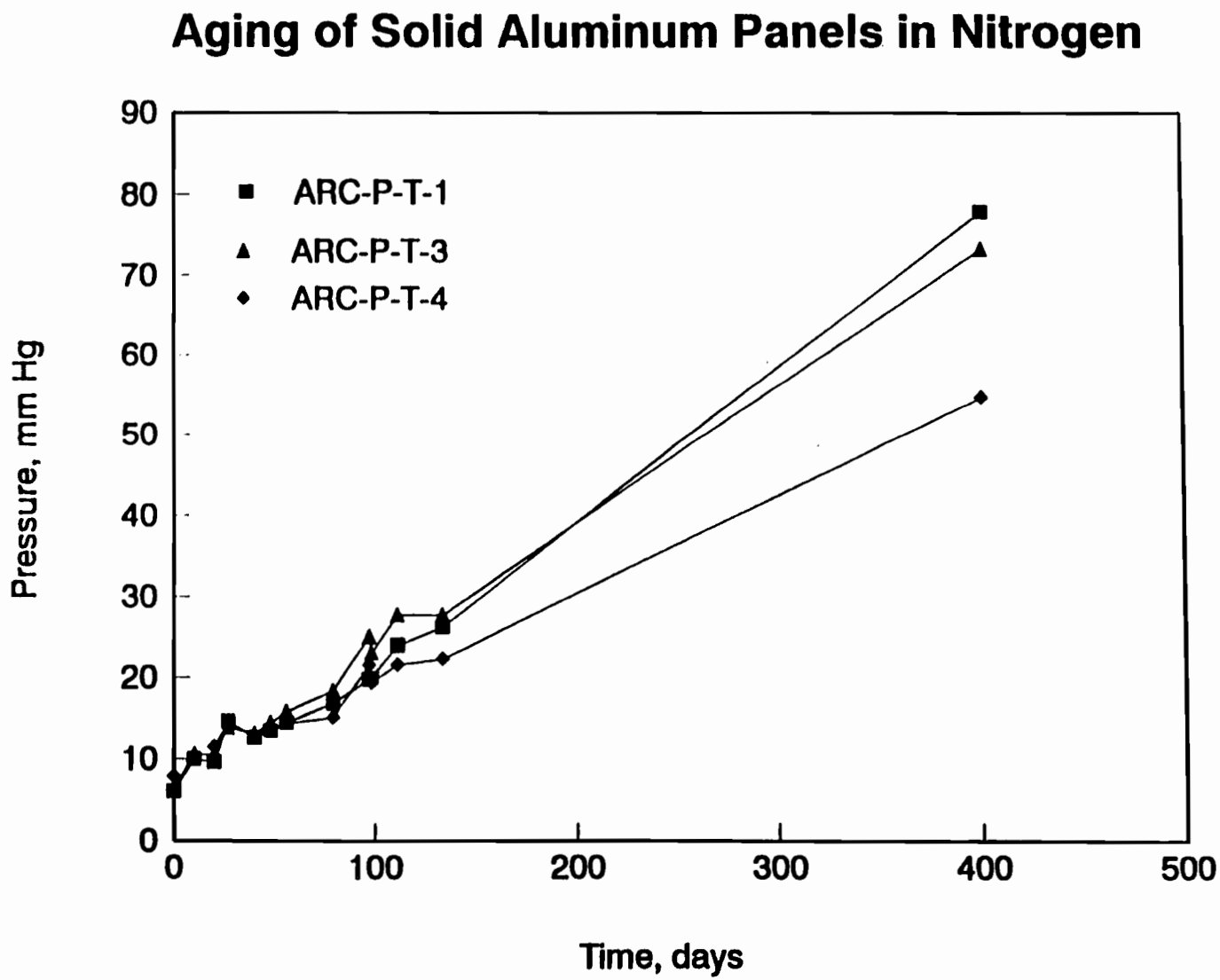
Aging of Solid Aluminum Panels in Nitrogen
ARC-P-T-1
ARC-P-T-3
ARC-P-T-4
Pressure, mm Hg
Time, days
0
10
20
30
40
50
60
70
80
90
0
100
200
300
400
500

FIGURE 2

Powder-filled Evacuated Panel (PEP) Powder Outgassing Study

Dry Air at 32.2 °C (90 °F)

Powder: T600 (prebaked overnight @120 °C)

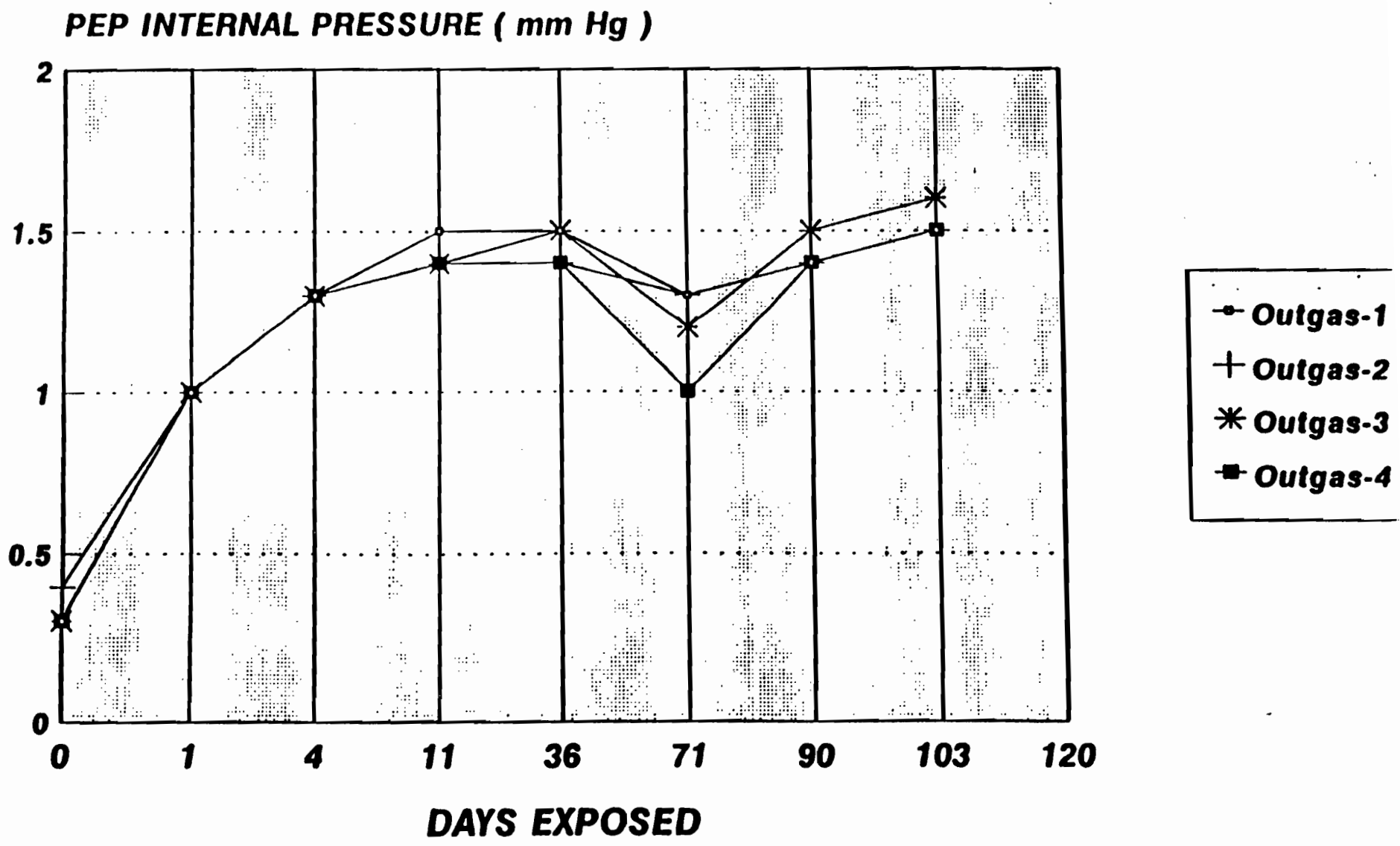

Powder Bag Material: TYVEK

FIGURE 3

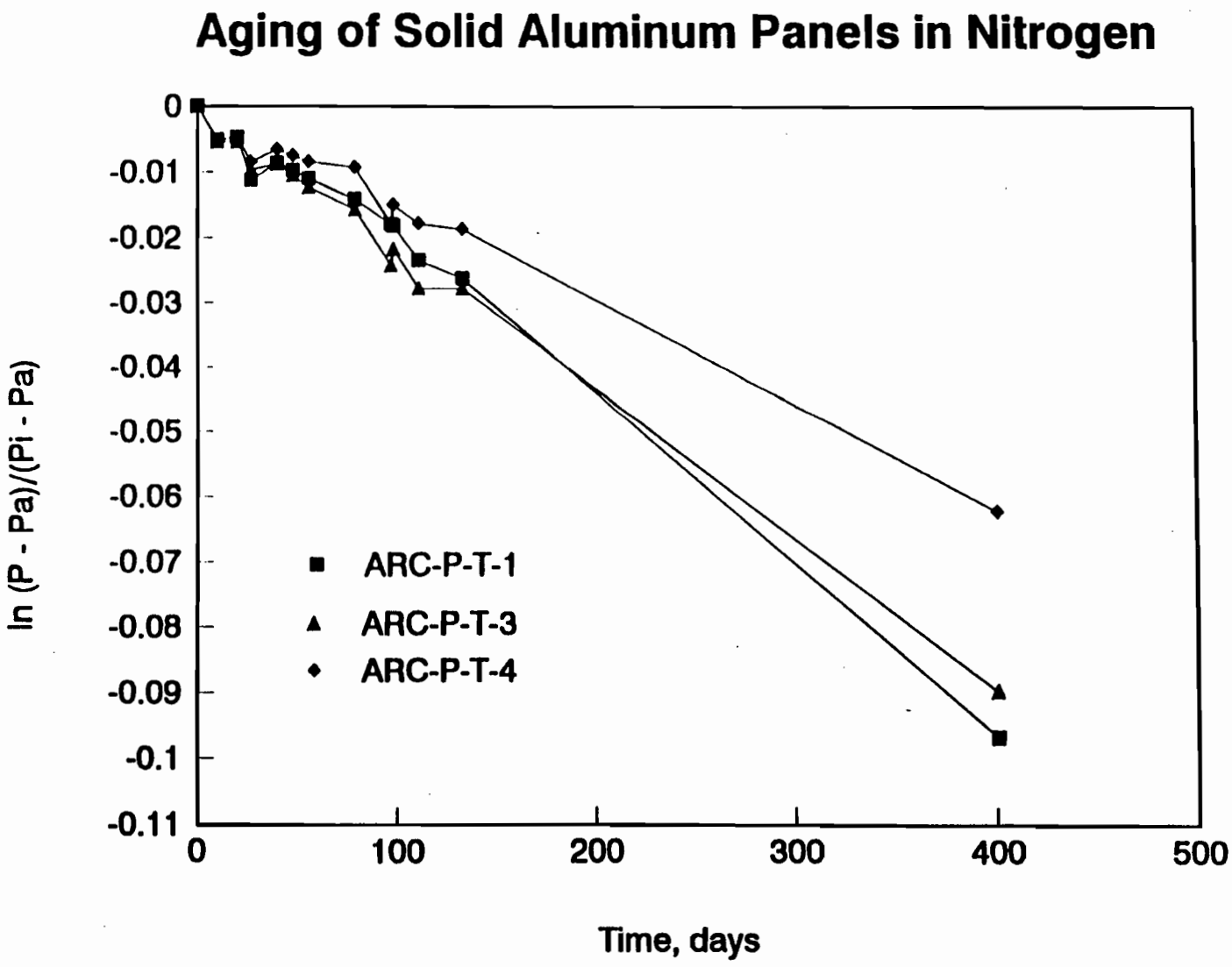
Aging of Solid Aluminum Panels in Nitrogen
ln (P - Pa)/(Pi - Pa)
0
-0.01
-0.02
-0.03
-0.04
-0.05
-0.06
-0.07
-0.08
-0.09
-0.1
-0.11
0
100
200
300
400
500
Time, days
ARC-P-T-1
ARC-P-T-3
ARC-P-T-4

FIGURE 4

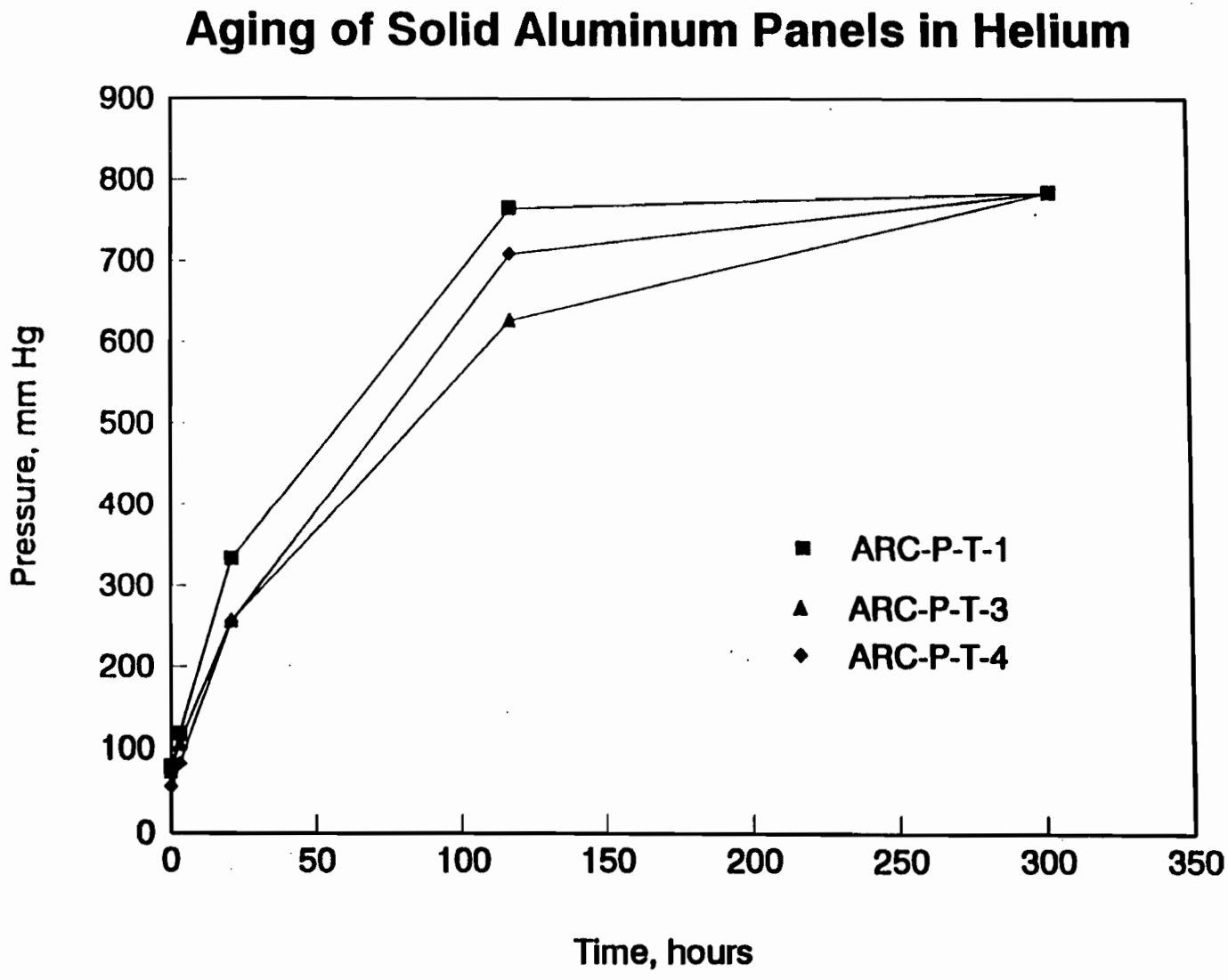
Aging of Solid Aluminum Panels in Helium
900
800
700
600
500
400
300
200
100
0
Pressure, mm Hg
0
50
100
150
200
250
300
350
Time, hours
ARC-P-T-1
ARC-P-T-3
ARC-P-T-4

FIGURE 5

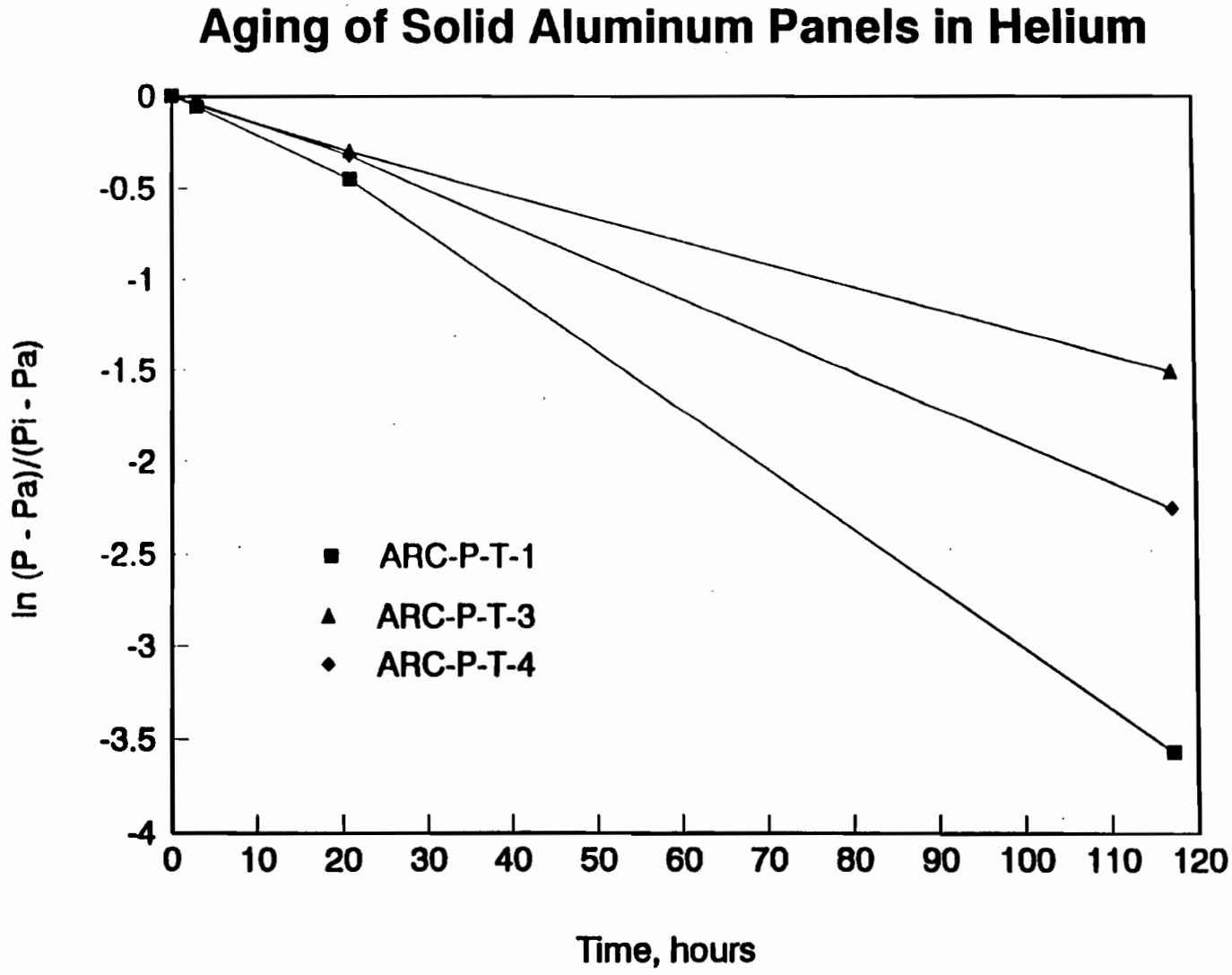
Aging of Solid Aluminum Panels in Helium
ln (P - Pa)/(Pi - Pa)
0
-0.5
-1
-1.5
-2
-2.5
-3
-3.5
-4
0
10
20
30
40
50
60
70
80
90
100
110
120
Time, hours
ARC-P-T-1
ARC-P-T-3
ARC-P-T-4

FIGURE 6

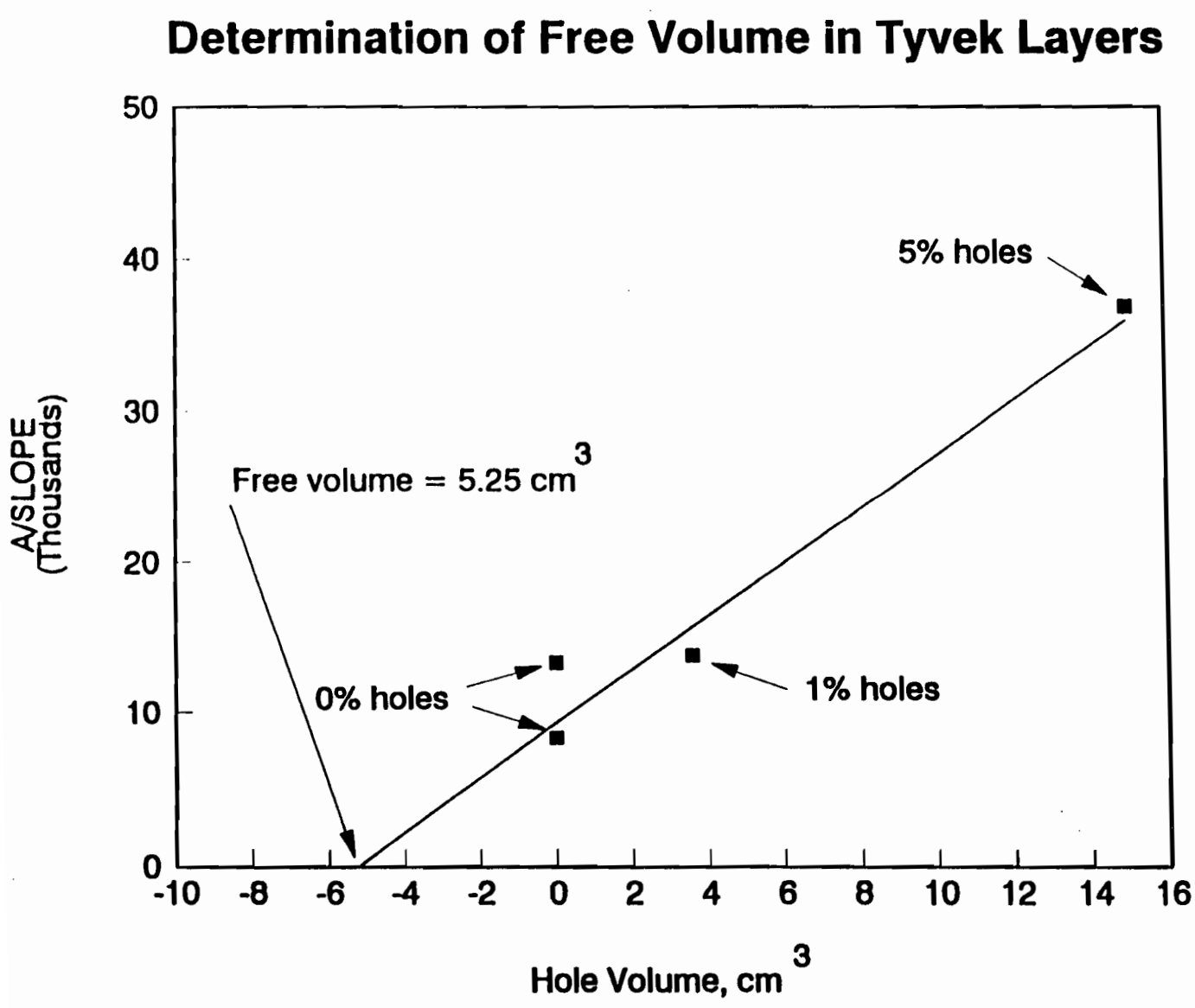
Determination of Free Volume in Tyvek Layers
A/SLOPE (Thousands)
50
40
30
20
10
0
-10
-8
-6
-4
-2
0
2
4
6
8
10
12
14
16
Hole Volume, cm 3
5% holes
Free volume = 5.25 cm 3
0% holes
1% holes

FIGURE 7

RESISTANCE, PRESSURE AND PERMEABILITY MEASUREMENTS ARE USED TO PREDICT THE LIFETIME OF VACUUM INSULATION.

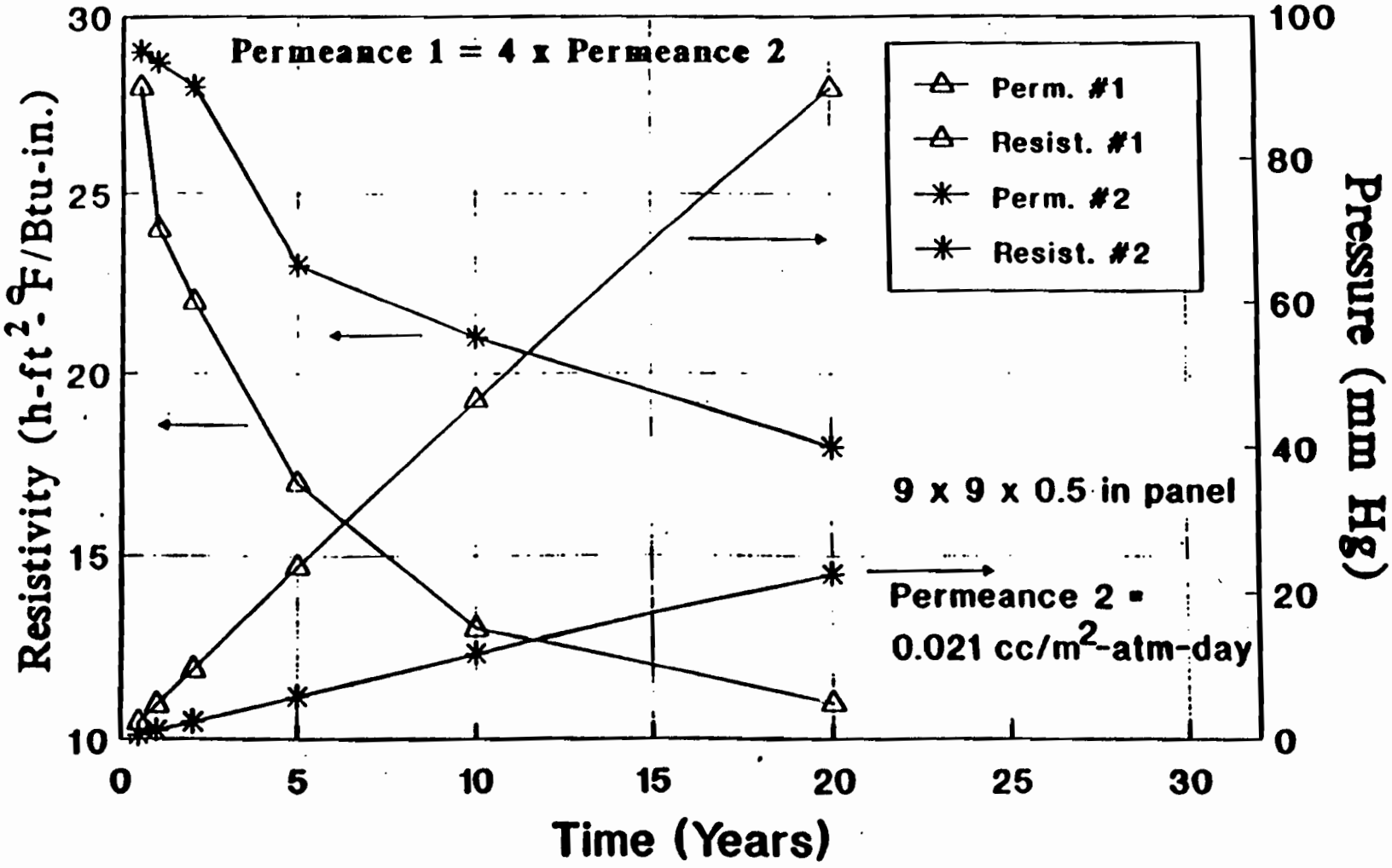

FIGURE 8

APPENDIX B

DETAILED PHASE III PROCEDURE FOR ARC CRADA (ORNL 91-0042)

Modifications to Phase III Procedure

Based upon work performed during Phase III of this project, the following changes to the procedure are recommended:

1) Triplicate sets of panels with 0, 2.5%, and 5% void volumes in the metal plates should be used (i.e., nine panels).

2) Task 3, No. 4. The appropriate area to use is the area of the metal plates (both sides), instead of the area of the Vecat bag measured between the heat seal lines.

3) Task III, No. 20. For aging in helium, the quantity X should be calculated from

$$X = \ln\left[\frac{(P - Po - Pg)}{-Pg}\right]$$

4) Task III, No. 24. Use the area of the metal plates instead of the area of the Vecat bag between the heat seal lines.

5) Task III, No. 26. Same as Item 3.

6) The free volume in the Tyvek layer should be obtained from a regression of -A/b versus V for the data in air obtained on the panels with 0 and 2.5% void volume in the metal plates. The free volume obtained in helium should be used as a check.

7) The permeance to air should be calculated from an equation analogous to that in No. 26, but with b_{air} instead of b_{He}.

DRAFT

PHASE III PROCEDURE FOR ARC CRADA (ORNL 91-0042

Task I. Setup of Required Equipment

1. ORNL will loan hand-held pressure gauges to three participants. The following equipment will be loaned:

   - hand-held vacuum gauge head
   - electronic circuitry to run the hand-held gauge

   Note: ORNL currently has two gauges and sets of electronics to loan out. A third gauge and set of electronics is being built by ORNL's Instrumentation and Controls Division.

2. Each participant will be required to furnish the following equipment:

   - vacuum pump to evacuate the gauge head
   - valving to allow controlled evacuation of the gauge head
   - a vacuum pressure gauge to calibrate the hand-held gauge
   - an X-Y recorder to plot the output of the hand-held gauge
   - one or more vacuum/purge chambers for aging of test panels, with vacuum pumps, valves, pressure gauges, and cylinders of compressed air and helium.

Task II. Measure Thermal Resistivity versus Pressure of Powder-Evacuated Panels

1. GE Appliances will prepare specimens of powder-evacuated panels with seven different internal pressures. GE will prepare a set of seven specimens for each of the participants in the Phase III Lifetime Procedure Verification.

2. GE Appliances will measure the pressure of each of 21 panels (3 participants × 7 pressures).

3. GE Appliances will send the 21 panels to ORNL. ORNL will measure the thermal conductivity and pressure of each of the panels.

4. ORNL will send a set of seven panels to each of the three participants.

5. Each participant will measure the thermal resistivity of each of seven panels at a mean temperature of 75°F.

6. Each participant will measure the internal pressure of each of seven panels.

7. Each participant will draw a graph of thermal resistivity versus internal pressure, and will fit a smooth curve through the data points (either through a least-squares procedure or visually). An example is given in Figure 1.

> Note: Data presented in the attached figures and tables are a combination of real and made up numbers. They were selected only to illustrate the procedures.

8. Each participant will tabulate the thermal resistivity and pressure measurements and report these back to ORNL for analysis and summarization.

Task III. Measure Rate of Aging of Evacuated Panels

1. ORNL will prepare test panels. The test panels will be made of aluminum, about 1/4 inch thick, and approximately 9 inches square with rounded corners. One set of panels will be solid aluminum, a second set will be drilled with over 1000 small holes to give a void volume of about 2.5% of the total volume of aluminum, and a third set will be drilled similarly with a void volume of about 5%. ORNL will weigh each panel before and after drilling, and will determine the volume of holes in each panel. Each panel will be encapsulated in a single layer of Tyvek, heat sealed around the edges, and then vacuum encapsulated in a heat sealed Vecat bag. ORNL will measure the initial pressure of each panel.

2. ORNL will send a set of three panels to each of the three participants. ORNL will provide each participant with values for the volume (in cm^3) of holes in the panels. Each participant will receive the following panels:

- Panel No. 1, with no holes
- Panel No. 2, with 2.5% holes
- Panel No. 3, with 5% holes

The following steps should be performed by each participant:

3. Upon receipt of the panels, measure (and record) the internal pressure of each of the three panels. If any panels have been damaged in shipment, and have leaked, report this immediately to ORNL. If any panel has leaked, it should be sent back to ORNL for repackaging.

4. Measure the area of the Vecat bag. This should correspond to the area defined by the insides of the heat seals. Be sure to multiply by two to account for both sides of the panel. Express the area in square inches.

5. After the initial pressure measurements, place the three panels in a dry air atmosphere at a temperature of 90°F and a (constant) pressure in the range of 760 to 780 torr. Note, it is not critical that any specific pressure within this range be maintained. However, it is critical that, whatever pressure is selected, the same pressure must be maintained throughout the course of the aging of these panels. The time that the panels are placed in the atmosphere and the actual pressure should be recorded. Data should be recorded on a form such as that shown in Figure 2.

6. After about two weeks have passed, remove the three panels from the dry air environment. Note the time that they were removed from the dry air.

7. Allow the panels to sit in the room air for a few minutes, until they have cooled to near room temperature. Measure the pressure of each panel using the hand-held gauge.

8. Replace the panels back into the dry air atmosphere at the same temperature and pressure that was used for Step 5. Note the time that the panels were replaced in the dry air. The objective of recording the time that the panels are removed from and replaced in the dry air environment is to keep track of the total accumulated time that the panels have been aging at the selected temperature and pressure.

9. Repeat Steps 6 through 8 at about two week intervals. This process should be continued for about five months, or until the pressure in any panel has risen to about 50 torr, whichever comes first. Raw data should be sent back to ORNL on a monthly basis to help spot any problems that may be occurring.

10. After taking each set of pressure readings, make a plot of the measured pressure versus time, as shown in Figure 3.

11. After taking each set of pressure readings, calculate the following quantity:

$$X = \ln\left[\frac{(P - Pg)}{(Po - Pg)}\right]$$

where P = measured internal pressure of panel
Pg = pressure of gas in environmental chamber
Po = initial measured internal pressure of panel
ln = natural logarithm

Make a plot of the quantity X versus time, as shown in Figure 4. If the aging is controlled by permeation through the Vecat bag, the plot in Figure 4 should be linear.

12. After taking each set of pressure readings, perform a linear regression on X versus time (t) to obtain the constants in

$$X = a + bt$$

The constant "a" should be close to zero, "b" should be a negative number, and the coefficient of determination (r^2) should be close to one. The absolute value of "b" should be largest for the panels with no holes, and smallest for the panel with the most hole volume.

Note: I've found that the easiest way to tabulate the data, make plots, and perform regressions is to use a spreadsheet such as Lotus 1-2-3 (or Excel or Quattro Pro). I make the plots and look at them on the computer, but don't actually print out hard copies each

time.

13. After aging in dry air for about five months (or until the pressure of any panel has reached about 50 torr, whichever is sooner), make the last pressure measurement for aging in dry air. Try to do this last pressure measurement early in the day.

14. Place the panels in a helium environment. Start a new data sheet, as shown in Figure 5, with the first entries corresponding to the last measurements after aging in dry air. Start the counting of accumulated time in helium at zero. (Note, the last pressure reading after aging in dry air goes on both data sheets: it is the final entry on the sheet for dry air, and the initial entry on the sheet for helium.)

15. After about six hours, remove the panels from helium, allow a few minutes to cool to room temperature, measure the internal pressure, and quickly replace the panels back in the helium. Note, very carefully (to within a few minutes) the times at which the panels are removed and replaced in helium.

16. After an accumulated time in helium of about 24 hours, repeat the pressure measurements.

17. Measure the pressure of the panels on a daily basis until about nine days exposure to helium has been accumulated.

18. After taking each set of pressure readings for aging in helium, record the appropriate data on the data sheet as shown in Figure 5.

19. After taking each set of pressure readings for aging in helium, make a plot of the measured pressure versus time, as shown in Figure 6.

20 After taking each set of pressure readings, calculate the following quantity:

$$X = \ln\left[\frac{(P - Pg)}{(Po - Pg)}\right]$$

where P = measured internal pressure of panel
Pg = pressure of gas in environmental chamber
Po = measured internal pressure of panel at start of aging in helium
ln = natural logarithm

Make a plot of the quantity X versus time, as shown in Figure 7. If the aging is controlled by

permeation through the Vecat bag, the plot in Figure 7 should be linear.

21. After taking each set of pressure readings for aging in helium, perform a linear regression on X versus time (t) to obtain the constants in

$$X = a + bt$$

The constant "a" should be close to zero, "b" should be a negative number, and the coefficient of determination (r^2) should be close to one. The absolute value of "b" should be largest for the panel with no holes, and smallest for the panel with the most hole volume.

22. After aging in helium for about nine days (or until the pressures of all the panels have reached about 500 torr, whichever is later), make the last pressure measurement for aging in helium.

23. For each panel separately, calculate the following ratio:

$$\gamma = \frac{b_{He}}{b_{air}}$$

where b_{He} is the slope of the least-squares regression for the aging in helium
b_{air} is the slope of the least-squares regression for the aging in dry air.

γ is equal to the ratio of the Vecat's permeances to helium and dry air. This ratio should be in the neighborhood of 2500 or so.

24. For the data obtained by aging in helium, calculate the following quantity for each of the three panels:

$$Z = \frac{A}{-b_{He}}$$

where A is the area of the Vecat bag within the lines of the heat seal, in^2
b_{He} is the slope of the least-squares regression for the aging in helium

Since "b_{He}" is a negative number, Z will be a positive number.

Plot "Z" versus the volume of holes, V (in cm^3), as shown in Figure 8. The points should be nearly on a straight line.

25. Perform a linear regression of Z versus V from Step 24 as:

$$Z = \alpha + \beta V$$

From the constants in this equation, calculate the quantity V_o from

$$V_o = \frac{\alpha}{\beta}$$

The quantity V_o is an estimate of the free volume within the Tyvek layer, in cm^3.

26. For each panel, calculate the permeability of the Vecat to helium, K_{He}, from

$$K_{He} = \frac{(-b_{He}) \times (V_o + V) \times 100 \times 24}{A \times 1.11866}$$

where b_{He} is the slope of the least-squares regression for the aging in helium
V_o is the free volume within the Tyvek layer, cm^3
V is the volume of holes in the aluminum plate, cm^3
A is the area of the Vecat bag within the lines of the heat seal, in^2
1.11866 is a constant that involves the universal gas constant and the density of the gas

Note: the constant 1.11866 is calculated from the quantity $RT\rho_0/M$. R is the universal gas constant, 82.05 atm•cm^3/mole•K. T is the aging temperature, 305.4 K (90°F). M/ρ_o is the molar volume, 22,400 cm^3/mole.

K_{He} will have the units of cc/100 in^2•day•atm. Approximately equal values of K_{He} should be obtained for the three panels.

27. For each panel, calculate the permeance of the Vecat bag to dry air from

$$K_{air} = \frac{b_{air}}{b_{He}} K_{He} = \frac{K_{He}}{\gamma}$$

Task IV. Predict the Pressure versus Time Curve for Powder-Evacuated Panels

1. Estimate the total exposed surface area (in square inches) and the free internal volume (in cm^3) of a typical powder evacuated panel. Unless decided otherwise by the steering committee, assume the following PEP characteristics:

> Area = 1152 square inches (corresponds to both sides of a 2 foot square panel)
> Free volume = 8495 cm^3 (corresponds to 2 foot square by 1 inch thick panel with 90% void volume)

2. Assume an initial pressure of 0 torr (an idealized number, could be changed to a more realistic value).

3. Calculate the estimated pressure versus time from the relationship

$$P = P_{atm} + (P_o - P_{atm}) \times e^{(-408.3\ K_{air}\ A\ t\ /\ V)}$$

In this equation, P_{atm} is the assumed atmospheric pressure in torr (assume this to be the standard value of 760 torr), K_{air} is the permeability to air in units of cc/100 in^2•day•atm, A is the exposed area of the Vecat film (in units of 100 in^2, or 11.52 for this example), V is the free volume in cm^3 (8495 cm^3 in this example), and t is the aging time in years. Tabulate P versus time at yearly intervals for 20 years, as shown in Table 1.

> Note: the constant, 408.3 is equal to the constant of 1.11866 (from Step 26 of Task III) multiplied by 365 (number of days in year).

Task V. Predict Thermal Resistivity versus Time.

1. Using the pressures listed in Table 1, pick off thermal resistivities from the graph in Figure 1. Finish filling out the column of thermal resistivities in Table 1.

Figure 1.

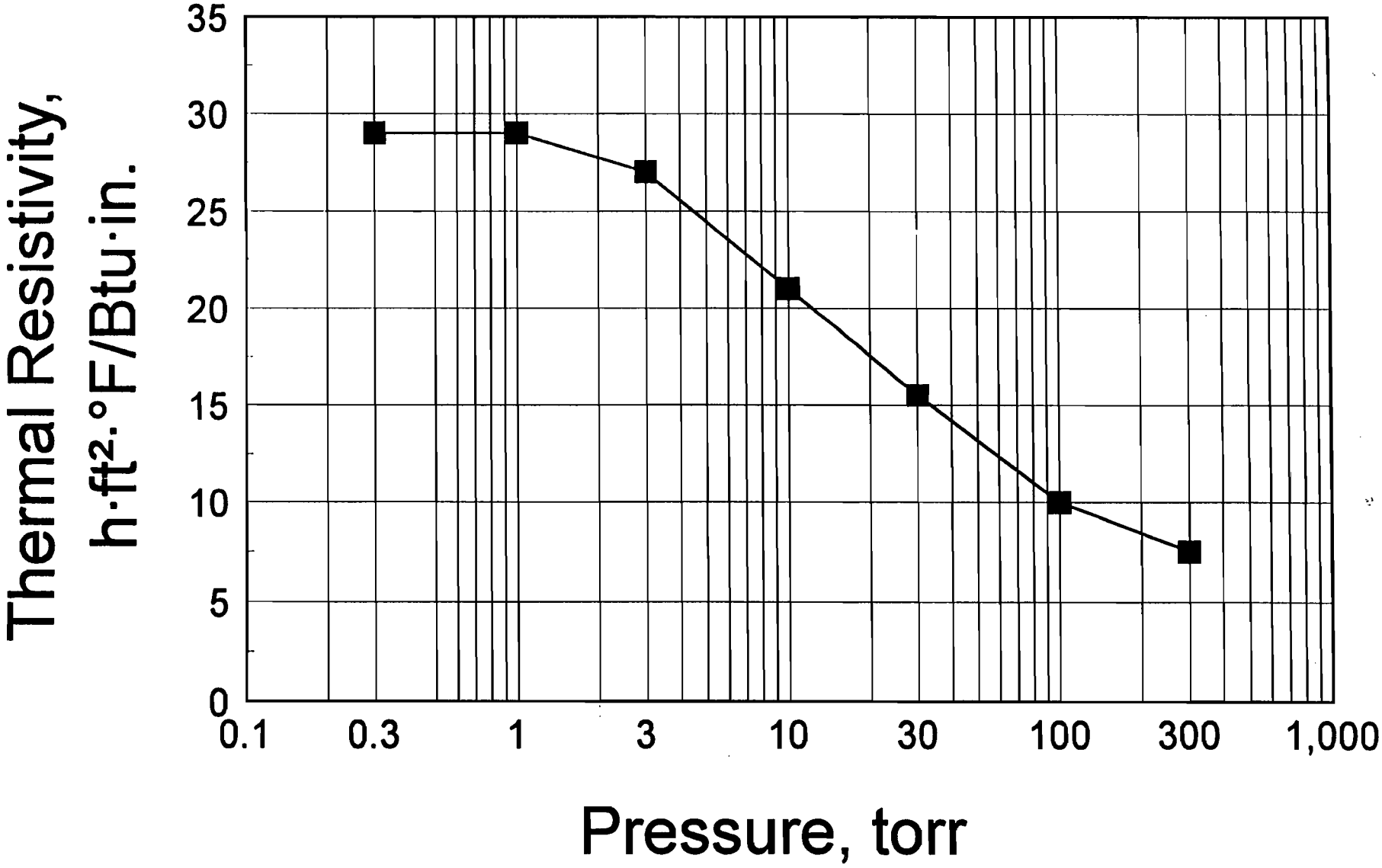
Thermal Resistivity,
h·ft².°F/Btu·in.
35
30
25
20
15
10
5
0
0.1
0.3
1
3
10
30
100
300
1,000
Pressure, torr

Figure 2. Example of Filled-In Data Sheet for Aging Study in Dry Air

Participant ORNL

Aging of Panel No. 1 in dry air at 90°F and 785 torr.

Panel Area 316.9 in²

Volume of Holes 3.59 cm³

Date	Time removed from gas	Accumulated Time in Gas, hours	Pressure, torr	ln[(P-Pg)/(Po-Pg)] (See footnote)	Time replaced in gas
5-20-94	-	0	8.5	0.000	3:30 pm
5-31-94	11:00 am	259.5	12.0	-0.00452	11:15 am
6-14-94	8:30 am	592.75	14.5	-0.00776	8:45 am
6-27-94	9:45 am	905.75	15.5	-0.00906	10:00 am
7-15-94	3:45 pm	1343.0	19.5	-0.01427	4:00 pm
8-3-94	3:15 pm	1797.75	22.2	-0.01780	3:30 pm

P = internal pressure within panel
Po = initial internal pressure
Pg = pressure of gas in environmental chamber

Figure 3. Aging in Air

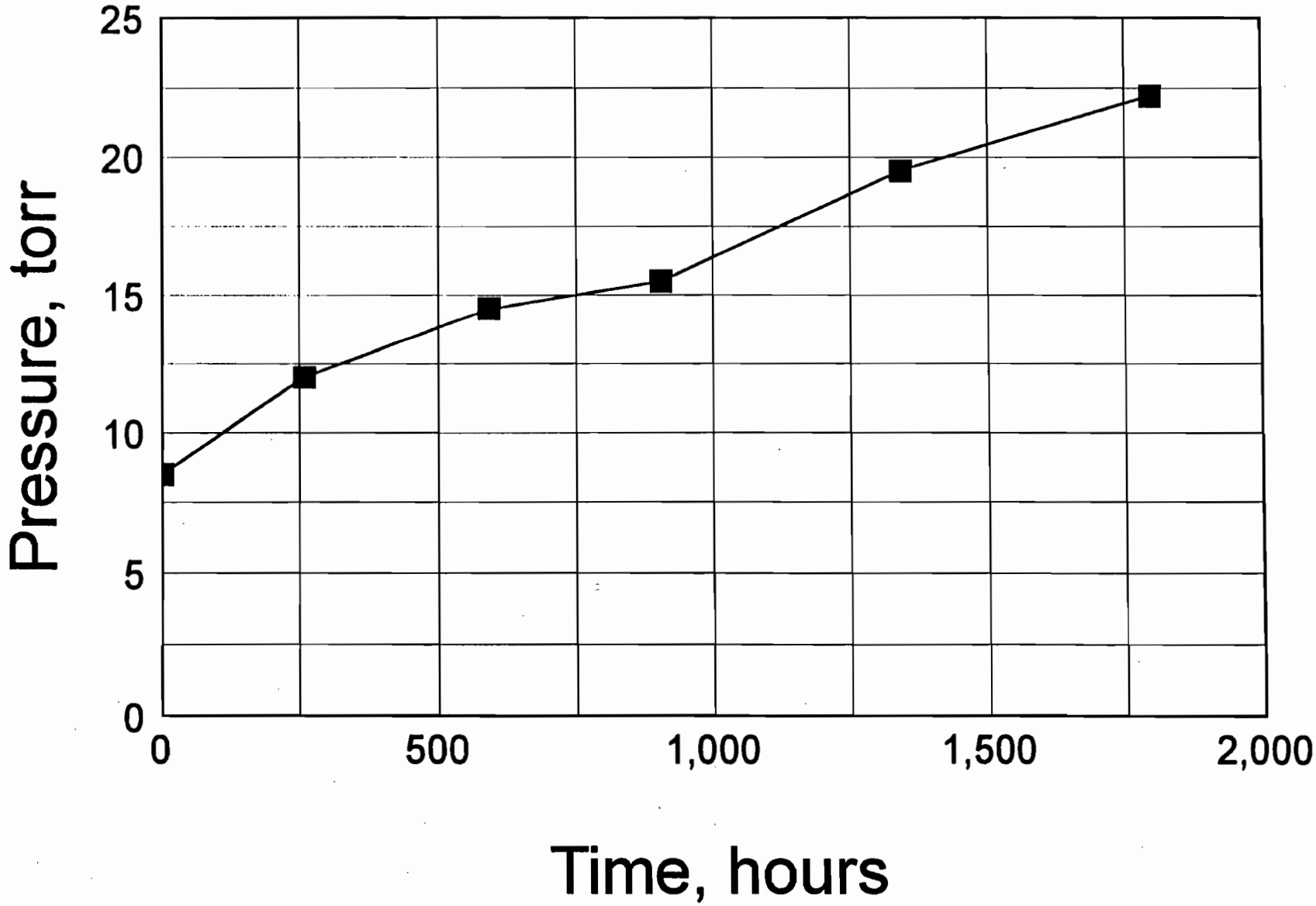

Figure 4. Aging in Air

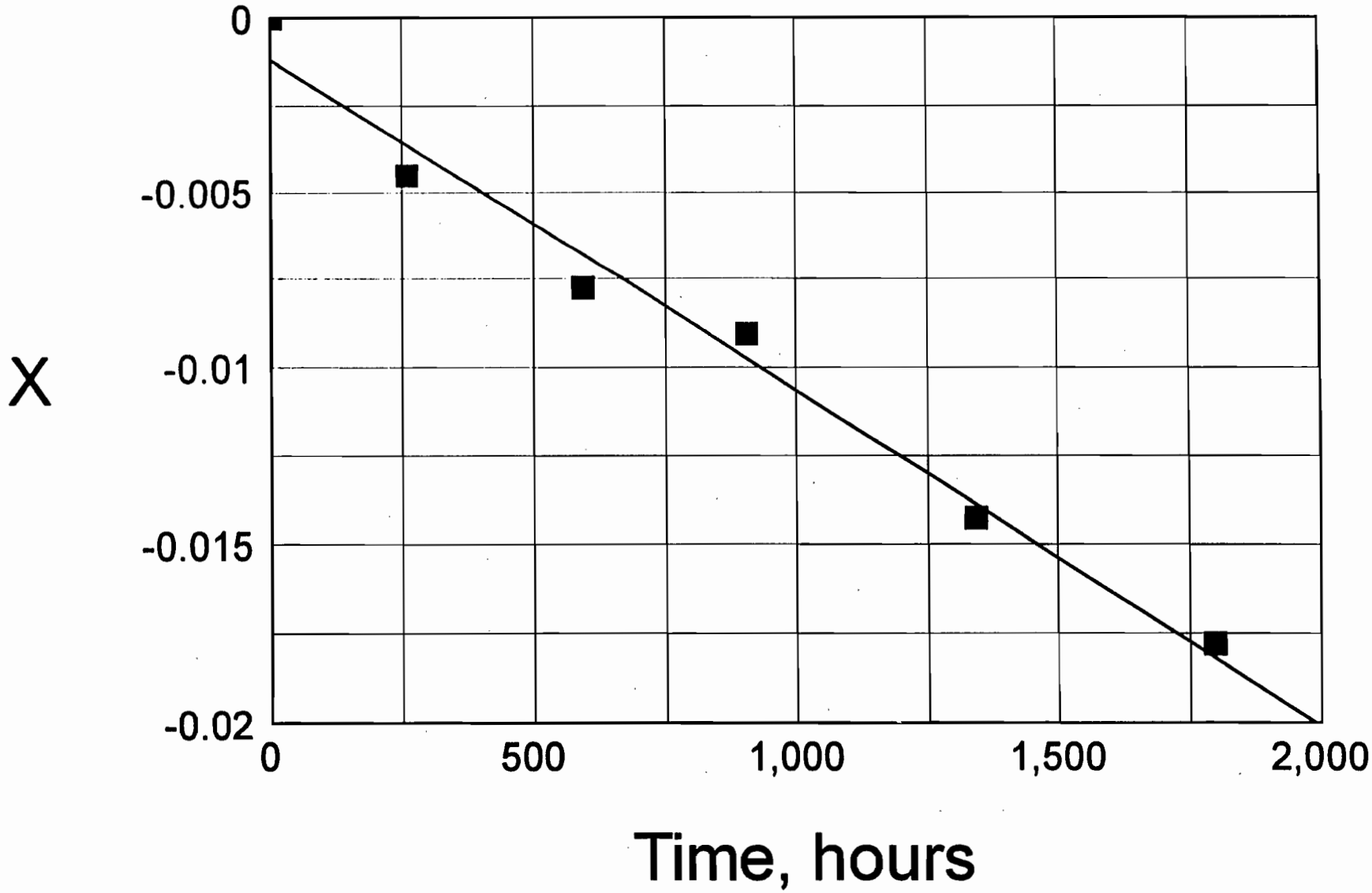

Figure 5. Example of Filled-In Data Sheet for Aging Study in Helium

Participant ORNL

Aging of Panel No. 1 in helium at 90°F and 785 torr.

Panel Area 316.9 in²

Volume of Holes 3.59 cm³

Date	Time removed from gas	Accumulated Time in Gas, hours	Pressure, torr	ln[(P-Pg)/(Po-Pg)] (See footnote)	Time replaced in gas
10-21-94	-	0	50	0.000	9:00 am
10-21-94	3:00 pm	6	141	-0.1322	3:15 pm
10-22-94	9:15 am	24	350	-0.5245	9:30 am
10-23-94	9:30 am	48	528	-1.0508	9:45 am
10-24-94	9:45 am	72	634	-1.5826	10:00 am
10-25-94	10:00 am	96	695	-2.1000	-

P = internal pressure within panel
Po = initial internal pressure
Pg = pressure of gas in environmental chamber

Figure 6. Aging in Helium

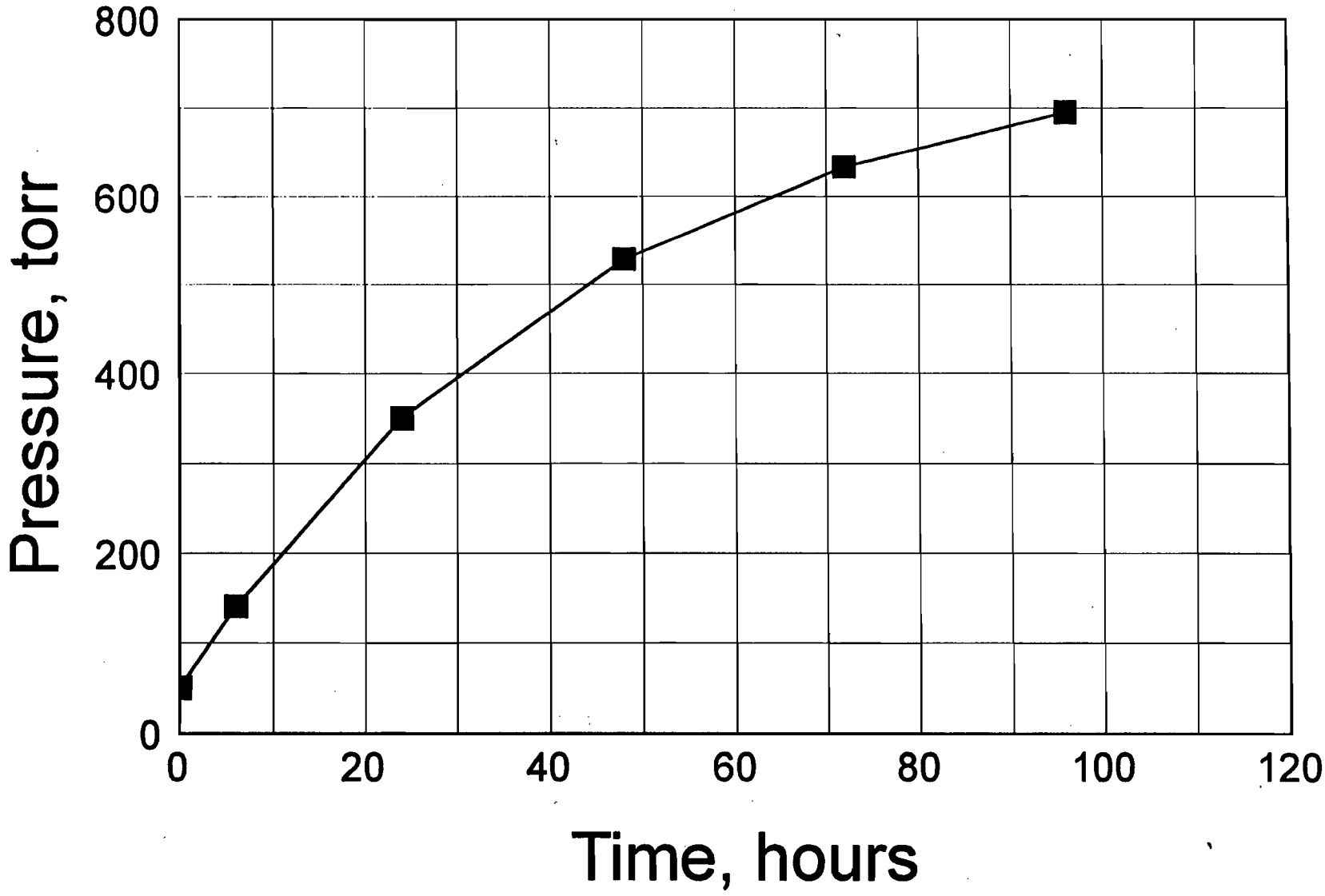

Figure 7. Aging in Helium

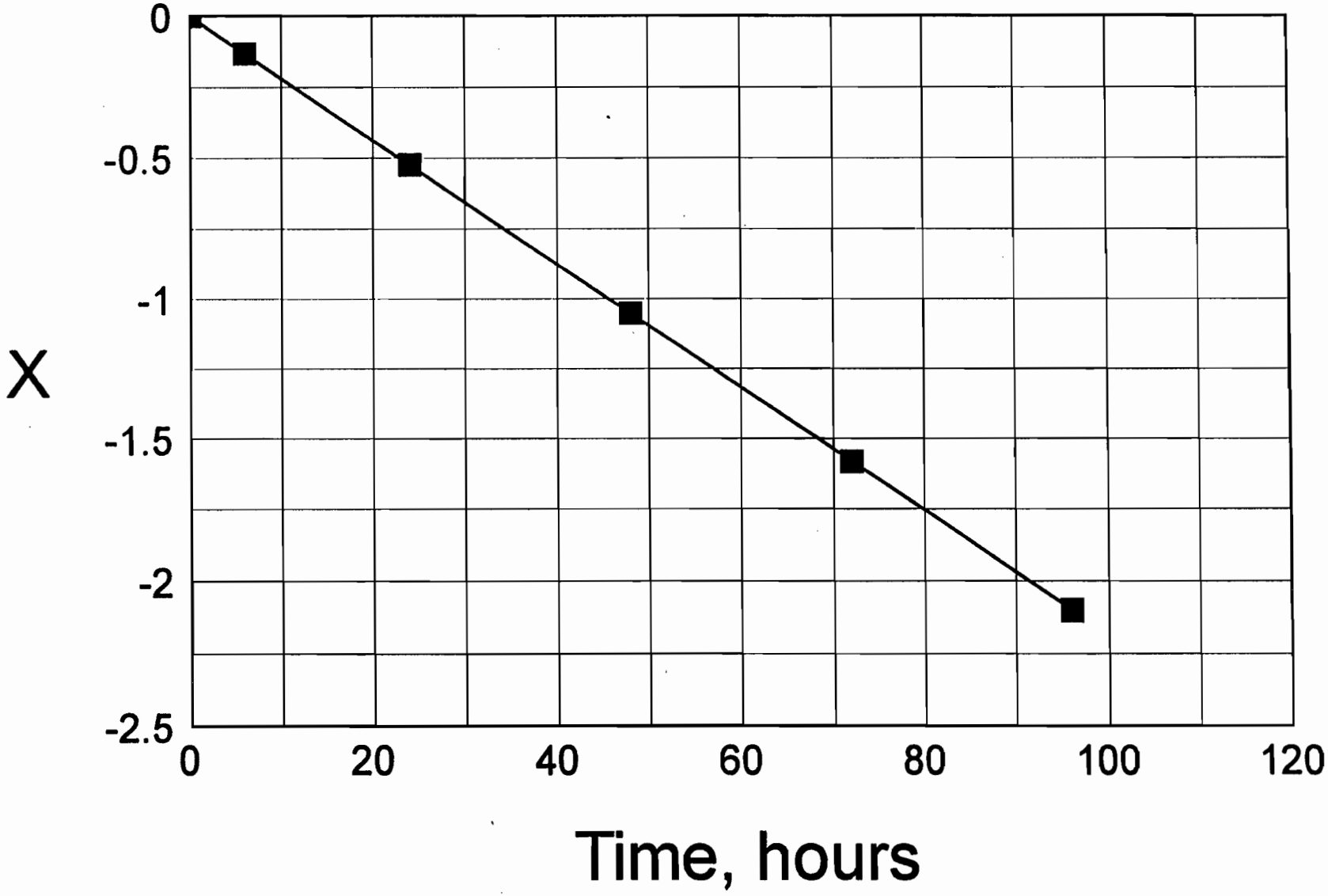

Figure 8. Determination of Volume in Tyvek

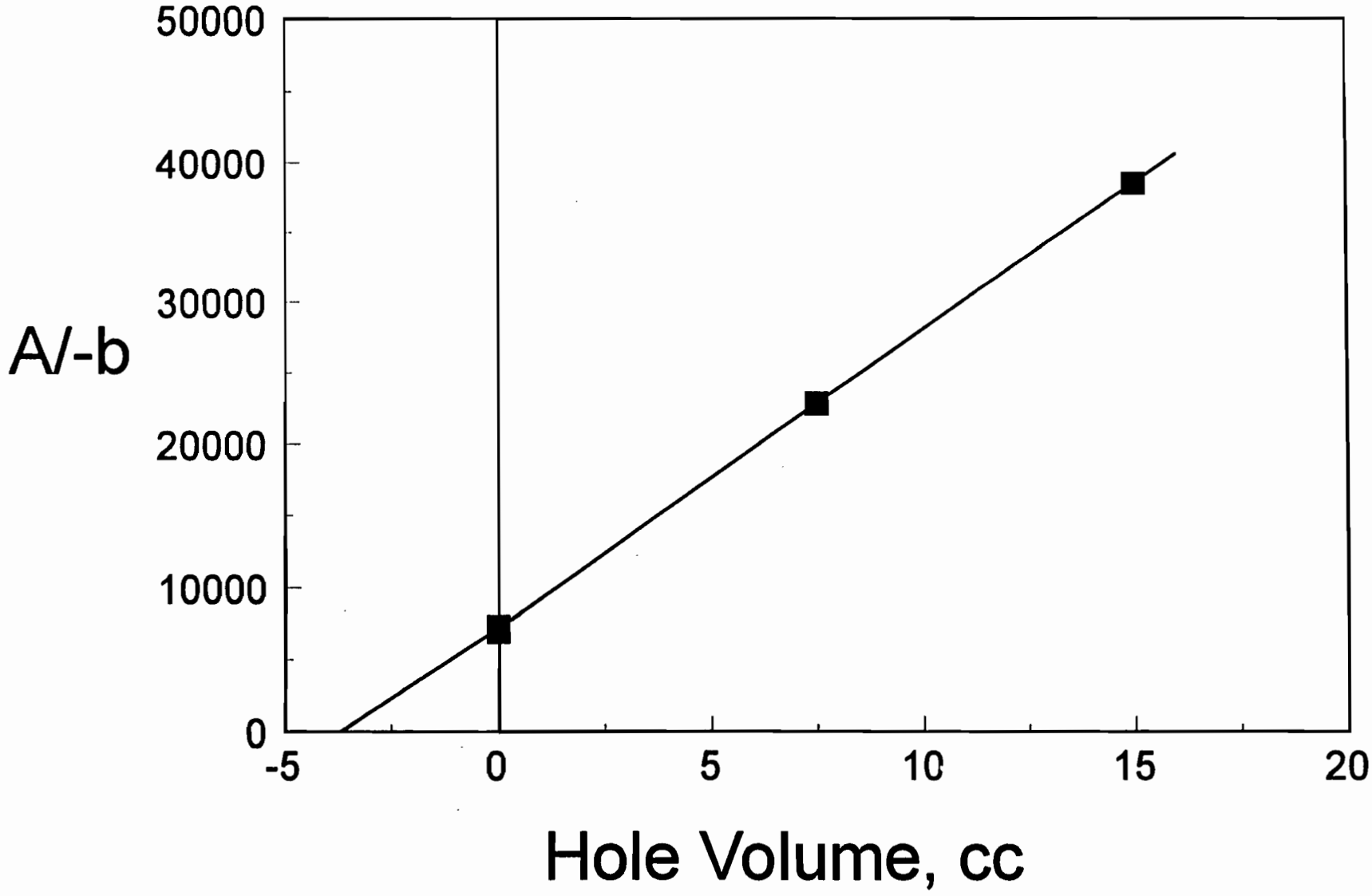

Table 1. Prediction of Resistance versus Time for Powder Evacuated Panel

Year	Pressure, torr	Thermal Resistivity, h•ft²•°F/Btu•in
0	0	29.0
1	0.3	29.0
2	0.5	29.0
3	0.6	29.0
4	0.8	29.0
5	1.0	29.0
6	1.2	28.7
7	1.4	28.4
8	1.6	28.1
9	1.8	27.8
10	1.9	27.6
11	2.1	27.4
12	2.3	27.2
13	2.5	27.0
14	2.7	26.8
15	2.9	26.6
16	3.0	26.4
17	3.2	26.2
18	3.4	26.0
19	3.6	25.8
20	3.8	25.6

APPENDIX C

INTERLABORATORY COMPARISON MEASUREMENTS OF THE THERMAL CONDUCTIVITY OF POWDER-FILLED EVACUATE

Interlaboratory Comparison Measurements of the Thermal Conductivity of Powder-Filled Evacuated Panel Superinsulation

R. S. GRAVES and T. G. KOLLIE

ABSTRACT

An interlaboratory comparison of thermal conductivity (k) measurements on Powder-filled Evacuated Panel (PEP) superinsulators is presented. Nine laboratories participated in this comparison, which is part of a Cooperative Research And Development Agreement (CRADA) between the Oak Ridge National Laboratory (ORNL) and the Appliance Research Consortium (ARC). Three different sizes of Heat Flow Meter Apparatuses (HFMAs) and specimens were employed in this work. A member of the ARC fabricated five each of the three sizes of PEPs from the same materials to approximately the same powder density and internal PEP pressure. To check the calibration of the HFMAs, an expanded polystyrene (EPS) specimen, supplied by ORNL for each size apparatus, was measured before and after measurements on the PEPs. The ASTM C 518 Test Method was employed for these measurements, which resulted in a two standard deviation (2σ) of 5.25% about the mean for the measurements by eight of the nine participating laboratories. To measure k of the PEPs, an ORNL-suggested modification of the ASTM C 518 Test Method for Heat Flow Meter Apparatuses (HFMAs) was used by all participants. Measurements on the five specimens of the two larger sized PEPs by five other laboratories and ORNL, which measured on both sizes, demonstrate a 2σ of 7.4% about the mean. When the measurements of the other three laboratories and ORNL on the five smallest sized PEPs are included, the 2σ increases to 12.9% about the mean because the ks of the smallest PEPs are higher than the other two sizes. To within experimental error, the internal pressures in the PEPs did not change during the course of this work.

Ronald S. Graves, Oak Ridge National Laboratory, P. O. Box 2008, Oak Ridge, TN 37831-6092.

Thomas G. Kollie, Oak Ridge National Laboratory, P. O. Box 2008, Oak Ridge, TN 37831-6092.

Reprinted from **THERMAL CONDUCTIVITY 22**

INTRODUCTION

In July of 1991, a Cooperative Research and Development Agreement (CRADA) was signed between the Appliance Industry-Government CFC Replacement Consortium, the Appliance Research Consortium (ARC), and the Oak Ridge National Laboratory (ORNL). The purpose of the CRADA is to develop a lifetime test procedure for Powder-filled Evacuated Panel (PEP) superinsulation in dry air. The PEPs are superinsulators, having resistivities of about 160 m·K/W. They consist of selected powders encapsulated in air barriers and evacuated to about 133 Pa (1 mm Hg) absolute pressure. A promising application of PEPs is in home refrigerator/freezers (R/F) where estimates [1] predict that about 0.6×10^{18} J (0.6×10^{15} Btu) of energy could be saved in the U.S. if PEPs replace CFC-blown foams used to insulate R/Fs. This saving is about 1% of the primary energy used in the U.S.

A major accomplishment needed before the implementation of this technology in R/Fs is the determination of the lifetimes (about 19 years) of PEPs. The procedure being developed accelerates aging of a PEP so that the test is completed in six months. The measurement of the thermal conductivity (k) of a PEP is critical to the test procedure. To determine the capability of each member of the ARC to perform this measurement, a laboratory intercomparison of measurements on k of PEPs is part of the CRADA. The results of this intercomparison are the subject of this paper.

EQUIPMENT

Nine laboratories, listed in Table I, participated in an intercomparison of the measurement of k of PEPs. Three different sizes (0.20, 0.30, and 0.61 m-square specimen openings) of Heat Flow Meter Apparatuses (HFMAs) were used. The two larger size HFMAs are capable of measuring k in accordance with the ASTM C 518 Test Method [2], but the smallest HFMAs do not operate entirely according to C 518. The details of the HFMAs are listed in Table II. The ORNL HFMA, which is the baseline apparatus for this study, is described in detail elsewhere [3]. It is a Holometrix, Inc., R-MATIC® Model R-41 HFMA having a 0.61 m-square specimen opening and a 0.25 m-square heat flux transducer (HFT) in each of its constant temperature plates.

Four participants operate Holometrix, Inc., Rapid-K® or K-Matic® HFMAs, having 0.30 m-square specimen openings and either 0.05 or 0.10 m-square HFTs in only one bounding surface. One participant operates a HFMA with a specimen opening greater than 0.61 m-square which was custom built by Holometrix, Inc. Three participants use Anacon Model 88 apparatuses with 0.20 m-square specimen openings. This type device does not measure the temperatures of the bounding plates directly and the plates are not constructed of high-conductivity rigid metal; both of these methodologies are required by ASTM C 518.

A HFMA establishes a steady-state, unidirectional heat flow through a test specimen placed between two parallel plates at constant but different

temperatures. Normally, heat flux transducers (HFT) are mounted in one or both of the two plates and are calibrated using standards [4] by the equation

$$S = \frac{k\,(T_h - T_c)}{V\,L} \quad , \tag{1}$$

where S is the HFT sensitivity in W/m^2 -V, k is the thermal conductivity of the standard in W/m-K, T_h and T_c are the temperatures of the two plates in K, L is the thickness of the standard in m, and V is the output of the HFT in V. The quantities measured during a routine test of a specimen with unknown k are the same as those measured during a calibration. The k of the unknown is computed from

$$k = \frac{(S\,V)\,L}{(T_h - T_c)} \quad . \tag{2}$$

For Eq. 2 to be valid strictly, the test specimen must be homogenous, as is required by C 518. In performing the interlaboratory comparison, however, it was necessary to sandwich the specimens between two sheets of silicone sponge rubber to accommodate variations in thicknesses of the PEP specimens. Also, because the ORNL HFMA has a 0.61 m-square specimen opening, measurements on the two smaller size specimens required placing the specimens in a "picture frame" constructed from fiberglass insulation. This type of composite specimen reduces extraneous heat losses from the edges of the specimen. For the two smaller size specimens, a smaller HFT than those mounted in the two parallel plates was used to ensure that the area of the specimen being measured was in a unidirectional heat flow regime. This supplementary HFT was inserted between the bottom plate and the specimen composite. For the intermediate sized specimens, a 6 x 5 array [5] of approximately 0.1 m-square HFTs was used; this HFT is nominally 0.9 mm thick and is masked on two sides by .05 m of a polymer board. For the smallest specimens, a 0.025 m-square HFT was employed [6]; this HFT is nominally 4.9 mm thick and is surrounded by masking material to create a 0.61 m-square rigid insert for the HFMA. A Type K thermocouple is attached so that the junction is at the surface of the HFT.

The internal pressures, P, of the PEPs were measured nondestructively by a gauge invented at ORNL [7]. To measure P, the gauge head supplies a vacuum to the outer surface of the PEP. When the P in the PEP exceeds that supplied by the gauge head, the polymer film encapsulating the powder deflects. This deflection is sensed by a fiber optic light system. A pressure transducer mounted in the gauge measures P_i at the interface of the film and the gauge head. The internal pressure in the PEP equals P_i when the light signal changes in intensity.

The bulk density of each PEP was estimated by measuring its weight and its physical dimensions. Weights and thicknesses of the polymer film were determined and subtracted appropriately. An ORNL proprietary technique was

used to determine more accurately the density of samples of the two smaller sized PEPs used in this study. (An application for a patent for this device is being prepared for submission to the U. S. Patent Office.)

The thickness of each specimen was determined by the ORNL Inspection Engineering Department using a dial gauge and gauge block system. These measurements were made over the center 70% of the surface of the specimen. In performing these measurements, wrinkles and other undulations in the polymer film were avoided. Members of the ARC performed measurements at the thickness provided by ORNL to eliminate this variable from the intercomparison. The reported ks, therefore, were for the PEP plus silicone foam rubber composite.

TABLE I. LABORATORIES PARTICIPATING IN THE INTERCOMPARISON OF THERMAL CONDUCTIVITY MEASUREMENTS OF PEPs.

Admiral Company - Galesburg, IL
Amana Refrigeration - Burlington, MA
Frigidaire Company - Greenville, MI
GE Appliances - Louisville, KY
Oak Ridge National Laboratory - Oak Ridge, TN
Sanyo E&E Corporation - San Diego, CA
Sub-Zero Freezer Company - Madison, WI
W. C. Wood Company - Guelph, Canada
Whirlpool Corporation - Evansville, IN

SPECIMENS

A total of fifteen PEP specimens were manufactured by the ARC for the interlaboratory comparison - five each for the three different sized HFMAs. All PEPs were constructed by the ARC using the same precipitated silica filler, the same type polymer-composite barrier, and the same semi-permeable inner bag material. They were manufactured using identical fabrication sequences to achieve the same internal pressure and powder density. The actual specimen sizes for the 0.20, 0.30, and 0.61 m-square specimen openings in the HFMAs are: 0.15 x 0.15 x 0.019 m, 0.24 x 0.24 x 0.019 m, and 0.55 x 0.55 x 0.019 m, respectively. The thicknesses of the specimens used in the calculations were the average of twelve determinations equally spaced over the area influencing heat flow to the HFTs. To avoid the effect of sloped edges, all thicknesses were determined at least 0.0254 m from the edges. To within experimental uncertainty ($\pm$270 Pa), the internal pressures in the PEPs did not change during the course of the interlaboratory comparison. The densities of two each of the two smaller sized PEPs were measured by an ORNL proprietary technique and found to be identical (197 kg/m^3) to within the experimental uncertainty ($\pm$1 kg/m^3). Measurements of the bulk densities of the two larger sized PEPs also showed minor variations, when the significantly larger experimental uncertainties are taken into account.

Because the HFMAs used in the interlaboratory comparisons are

TABLE II. THREE SIZES OF HFMAS USED IN THE LABORATORY INTERCOMPARISON OF THE MEASUREMENT OF k.

PART.	APPARATUS	SIZE	HOT PLATE	COLD PLATE	HFT SIZE	HFT LOCATION	CAL. STD.
A	Anacon Model 88	0.20 x 0.20 m	Top (37.8°C)	Bottom (10°C)	50.8 mm dia.	Top	SRM 1449 NIST FG
B	Anacon Model 88	0.20 x 0.20 m	Top (37.8°C)	Bottom (10°C)	50.8 mm dia.	Top	SRM 1449 PUR
C	Anacon Model 88	0.20 x 0.20 m	Top (37.8°C)	Bottom (10°C)	50.8 mm dia.	Top	High Density FG
D	Holometrix, R-Matic	0.61 x 0.61 m	Top (35°C) Bottom (35°C)	Bottom (12.8°C) Top (12.8°C)	254 x 254 mm	Bottom/Top	SRM 1450b SRM 1451 SRM 1449
E	Holometrix, Rapid-K	0.30 x 0.30 m	Top (35°C)	Bottom (12.8°C)	50.8 x 50.8 mm	Bottom	SRM 1450b
F	Holometrix, K-Matic	0.30 x 0.30 m	Bottom (35°C)	Top (12.8°C)	101.6 x 101.6 mm	Bottom	SRM 1450b
G	Holometrix, K-Matic	0.30 x 0.30 m	Top (35°C)	Bottom (12.8°C)	101.6 x 101.6 mm	Bottom	SRM 1450b
H	Holometrix, K-Matic	0.30 x 0.30 m	Top (37.8°C)	Bottom (10°C)	101.6 x 101.6 mm	Bottom	Styrofoam
I	Holometrix, Custom	0.61 x 0.91 m	Bottom (37.8°C)	Top (10°C)	101.6 x 101.6 mm (array)	Bottom	SRM 1450b SRM 1449

constructed to measure on specimens with much higher thermal conductivities than the PEPs, an expanded polystyrene (EPS) specimen of known thermal conductivity was included in the test. Three 0.61 m-square EPS specimens were measured in the ORNL HFMA and yielded an average k of 35.32 mW/m·K with a two standard deviation (2σ) of 1.83% about the mean*. Specimens 0.20 and 0.30 m-square respectively were cut from the center of two of the larger 0.61 m-square specimens which had been tested previously. These 0.20, 0.30 and 0.61 m-square specimens were then used as "transfer standards" for this interlaboratory comparison. A previous study [8] where four laboratories measured on polyisocyanurate boards yielded k-values that have a 2σ of 2.2% about the mean.

The nine participating laboratories measured the k of the EPS "transfer standard" before measuring the PEPs. In addition, most of the participants remeasured the EPS after completing the measurements on the PEPs. One laboratory reported ks that were considered outliers and these data were not included in the analysis. The eight remaining participants reported ks that averaged 35.35 mW/m·K with a 2σ of 5.25% about the mean.

PROCEDURE

Upon receipt at ORNL, the internal P and thicknesses of all the PEPs were measured; however, only the ks of the 0.55 m-square PEPs were measured upon receipt. Then the PEPs were sent to the ARC members, who measured the k of each PEP. Upon return to ORNL, the internal P and k of each PEP were measured. Data analyses were performed at ORNL.

Before measuring the k of the PEPs, the ORNL HFMA was calibrated using National Institute of Standards and Technology (NIST) standard reference materials (SRMs) and transfer standards. For operation without the HFT inserts, the HFMA was calibrated using fibrous glass board (SRM 1450b), fibrous glass blanket (SRM 1451) and transfer standards of high density fibrous glass blanket and EPS. This calibration was accomplished over a thickness range of 0.025 to 0.152 m. The HFT array and the 0.025 m-square HFT were calibrated with 0.025, 0.076 and 0.127 m thicknesses of SRM 1450b. Equation 1 was used to compute the HFT sensitivity (S), which is commonly referred to as the calibration factor.

For measurement of k of the five largest PEPs (#5, 6, 7, 8, and 10) at ORNL, the PEPs were placed between two sheets of silicone sponge rubber to accommodate variations in thicknesses of the PEPs caused by wrinkles and undulations in the polymer film encapsulating the PEP. The 3.2 mm thick silicone foam rubber used at the interfaces is very compressible but also recovers to its full thickness which allows for repeated usage. This composite specimen was placed in the HFMA and allowed to equilibrate at least six hours.

---

*In this study, the standard deviation (σ) is determined by $\sigma = \sqrt{\Sigma\,(X-\bar{X})^2/(N-1)}$, where X is a measured value and $\bar{X}$ is the mean of the N measured values.

Several tests were run for up to 24 hours to determine that six hours is adequate for steady-state to be achieved. Equation 2 was used to compute k of the specimen from the data recorded by the HFMA.

Because the ORNL HFMA has a 0.61 m-square specimen opening, measurements on the two smaller size specimens at ORNL required placing the specimens in a "picture frame" constructed from fiberglass insulation. High density (36 kg/m^3) fiberglass blanket was used for the border material. Material was removed from the central area of each of the two fiberglass boards over an area equal to the PEP area to accommodate one-half the thickness of the PEP. After insertion of the PEP in the boards, every surface within the HFMA specimen chamber was in contact with the fiberglass. The two fiberglass boards served both as a mask for the PEP and as a medium to accommodate PEP surface variations. In each test, a Type K thermocouple was taped to the center of each major surface to measure the temperature difference across the PEP.

The EPS and PEP specimens were sent to the members of the ARC with the following instructions:

1. Wipe moisture (if any) from the cold plate of your HFMA.
2. Position the ORNL-supplied silicone sponge rubber on the bottom plate.
3. Install the specimen as suggested to minimize orientation effects.
4. Insert the second ORNL-supplied silicone sponge rubber sheet between the upper plate and the specimen.
5. Close plates to compress the rubber.
6. Set the composite specimen thickness to that suggested by ORNL.
7. Allow at least six hours for steady-state to be achieved.
8. Test with a temperature difference of the plates of 22 to 28°C, with a mean temperature of 23.9°C.

The general instruction was to first calibrate the HFMA as per your usual practice, measure the k of the EPS specimen, measure the k of the five PEPs, and then repeat the measurement of the k of the EPS. Only raw data were reported to ORNL for calculation of k and analyses of the results.

RESULTS

The k measurements obtained in the laboratory intercomparison are listed in Tables III to V. Figure 1 shows that the measurements by eight of nine laboratories had a 2σ of 5.25% for the EPS "transfer standard." One laboratory was considered an outlier because its measurement of the k of the EPS specimen was more than 3σ below the mean of the other eight laboratories measurements. This result demonstrates that the HFMAs were calibrated correctly and would yield reasonably accurate measurements on specimens for which the HFMAs were designed. Besides ORNL, only one ARC member (I) was capable of measuring on the largest PEPs whereas four ARC members measured on the middle size specimens. These results are shown plotted in Fig. 2, showing a 2σ of 7.4%. The ORNL measurements on these two size

TABLE III. MEASUREMENTS ON 0.15 x 0.15 x 0.019 m PEP SPECIMENS BY THREE ARC LABORATORIES (A, B, C) AND ORNL (D).

	k (mW/m·K)						
Lab	EPS (2-3)	PEP (23)	PEP (24)	PEP (28)	PEP (29)	PEP (30)	EPS (2-3)
A	35.92	7.189	7.349	7.111	6.998	7.249	36.49
B	34.90	7.078	7.125	7.000	6.775	7.137	34.90
C	37.07	6.828	6.801	6.794	6.512	6.768	
D	35.74	6.798	6.623	6.730	6.633	6.871	
D	35.73						
D	36.13						

TABLE IV. MEASUREMENTS ON 0.24 x 0.24 x 0.019 m PEP SPECIMENS BY FOUR ARC LABORATORIES (E, F, G, H) AND ORNL (D).

	k (mW/m·K)						
Lab	EPS (7-8)	PEP (13)	PEP (14)	PEP (15)	PEP (17)	PEP (18)	EPS (7-8)
E	34.36	5.748	5.918	5.834	5.906	6.093	34.46
F	35.77	6.352	6.541	6.447	6.530	6.716	35.77
G	35.05	6.196	6.292	6.179	6.388	6.492	34.90
H	32.31	5.901	6.162	6.108	6.041	6.315	32.31
D	35.08	6.134	6.245	6.091	6.270	6.444	
D	35.14						
D	35.02						

TABLE V. MEASUREMENTS ON 0.55 x 0.55 x 0.019 m PEP SPECIMENS BY ONE ARC LABORATORY (I) AND ORNL (D).

	k (mW/m·K)						
Lab	EPS (1)	PEP (05)	PEP (06)	PEP (07)	PEP (08)	PEP (10)	EPS (1)
I	34.14	6.067	5.840	6.159	6.318	6.168	33.69
D	35.08	6.385	6.257	6.528	6.450	6.336	
D	35.15						

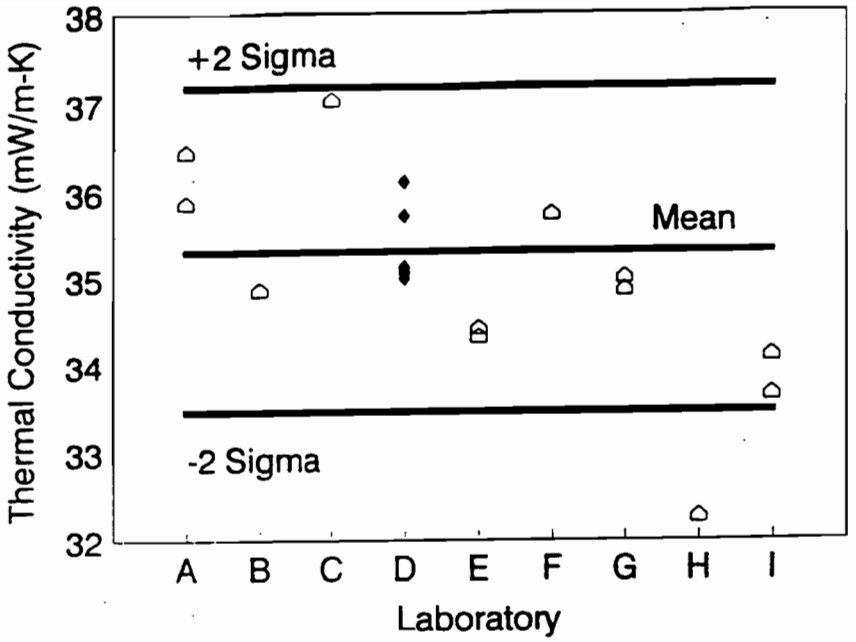

Fig. 1. Thermal tests on expanded polystyrene (EPS) show an average k of 35.35 mW/m·K with a two standard deviation of 5.25% about the mean.

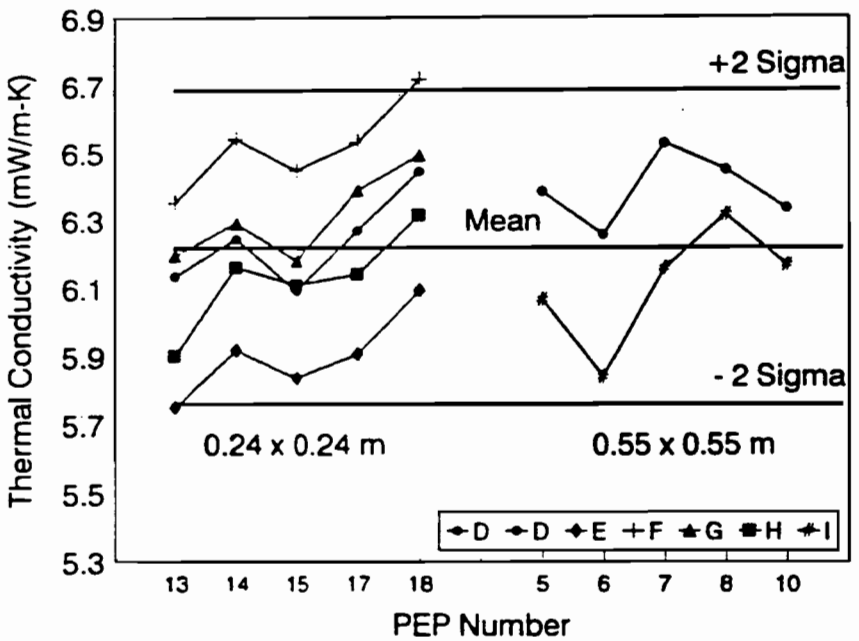

Fig. 2. Measurements by participating laboratories on two sizes of PEPs show a 2σ of 7.4% about the mean.

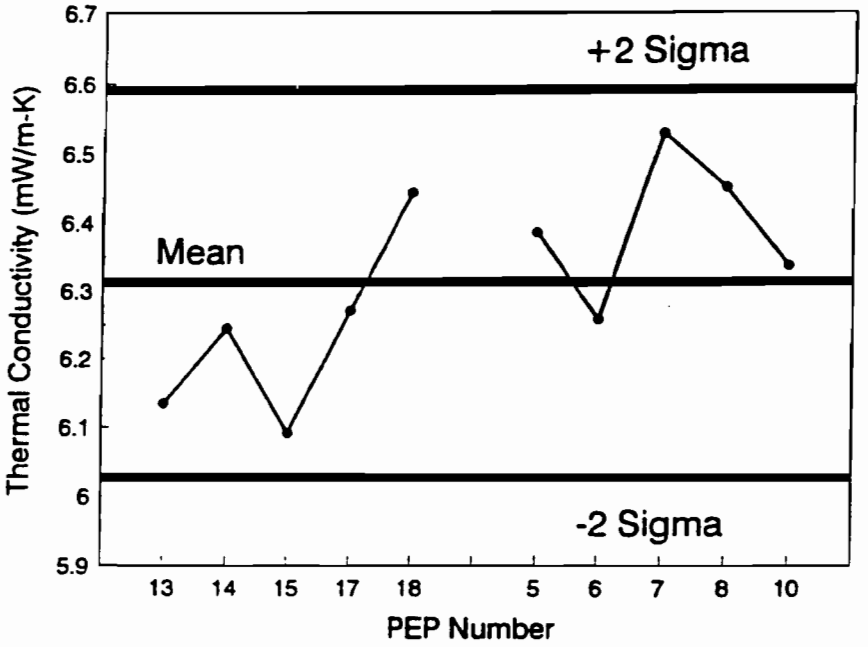

Fig. 3. Measurements by ORNL on two sizes of PEPs show a 2σ of 4.5% about the mean.

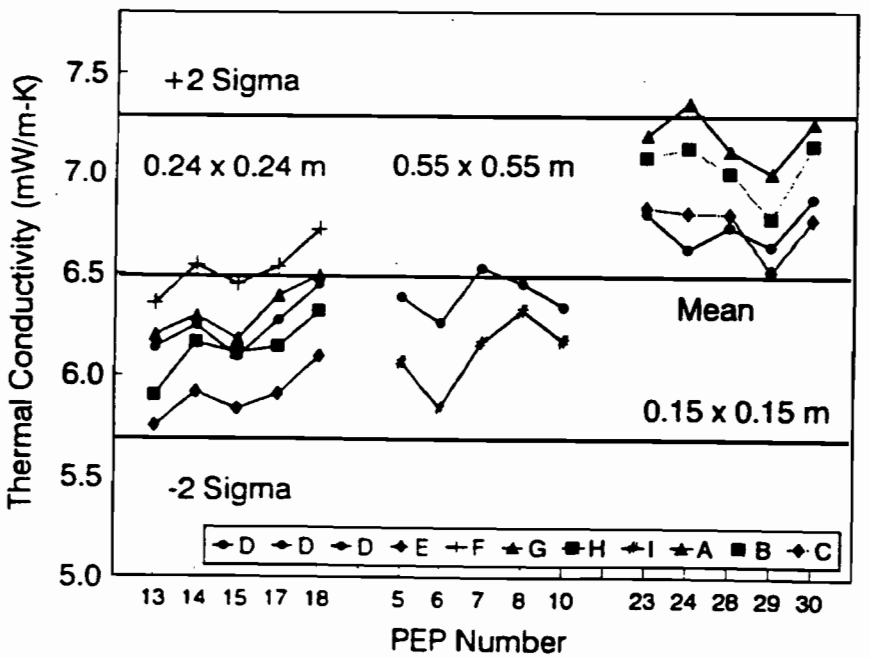

Fig. 4. Measurements by all laboratories on the three sizes of PEPs show a 2σ of 12.9% about the mean.

PEPs, which are shown in Fig. 3, had a 2σ of 4.5%. Approximately half of this measured difference in k of these specimens is estimated to be due to true variations in k of the specimen, not to experimental imprecision of the HFMAs.

Figure 4 shows the measurements on the three size PEPs by all nine laboratories. Inclusion of the measurements on the smallest size PEPs increased the 2σ to 12.9%. From Fig. 4, it is obvious that the k of the smallest panels is higher than that of the other two sizes. The reasons for these differences are not known and were not expected. Measurements of the density of the lowest and highest k PEPs from the two smaller sizes were the same to within the experimental uncertainty (± 1 kg/m^3) of the ORNL technique. If the differences in k shown in Fig. 4 are caused by differences in PEP density, the densities would have to be significantly different than ± 1 kg/m^3. Excluding the values for the smallest PEPs, the average k of the PEPs is 6.22 mW/m·K.

CONCLUSIONS

The k measurements on the three sized PEPs of this laboratory intercomparison had a 2σ of 12.9%. The measurements by eight laboratories had a 2σ of 5.25% for the EPS "transfer standard." For the two largest sized PEPs, the k measurements agreed to a 2σ of 7.4% as compared to the ORNL only measurement 2σ of 4.5%. The reason that the k of the smallest panels is higher than that of the other two sizes is not known. Excluding the values for the smallest PEPs, the average k of the PEPs is 6.22 mW/m·K.

ACKNOWLEDGEMENTS

The authors wish to thank Drs. K. E. Wilkes and D. W. Yarbrough for their review of this manuscript. Mr. F. C. Weaver is acknowledged for his assistance in performing the measurements at ORNL. Ms. Linda Parker prepared this manuscript for publication. This research was sponsored by Building Systems and Materials Division, Office of Buildings Energy Research, U.S. Department of Energy, under contract NO. DE-AC05-84OR21400 with the Martin Marietta Energy Systems, Inc., and by the ARC through ORNL CRADA 91-0042 with Martin Marietta Energy Systems, Inc.

REFERENCES

1. T. R. Curlee, Materials and Science 12(1), 1-45, (1988).

2. C 518-91, "Standard Test Method for Steady-State Heat Flux Measurements and Thermal Transmission Properties by Means of the Heat Flow Meter Apparatus," in 1992 Annual Book of ASTM Standards, Vol. 04.06 (American Society for Testing and Materials, Philadelphia, 1992), pp. 153-164.

3. R. S. Graves, et al., Review of Scientific Instruments 64 (7), 1961-1970, (1993).

4. C 1132-89, "Standard Practice for Calibration of the Heat Flow Meter Apparatus," in 1992 Annual Book of ASTM Standards, Vol. 04-06 (American Society for Testing and Materials, Philadelphia, 1992), pp. 630-633.

5. Isover Saint-Gobain, CRIR, Centre Engineering, B.D. 19, Rantigny, France.

6. International Thermal Instruments Company, Del Mar, CA.

7. T. G. Kollie and L. H. Thacker, Review of Scientific Instruments 63 (12), 5774-5779, (1992). (Patent applied for this gauge.)

8. R. S. Graves, et al., ORNL/TM-1170, 1991.

DISTRIBUTION LIST

1-10. Kenneth E. Wilkes, Principal Investigator, Bldg. 4508, MS 6092

11. Brian B. Bovee, OTT Business Manager, Bldg. 701SCA, MS 8242

12. William Painter, Science Technology Partnerships Office, Bldg. 5002, MS 6416

13-37. Association of Home Appliance Manufacturers, Appliance Research Consortium, 20 Wacker Drive, Chicago, IL 60606

38. John Talbott, Department of Energy, EE-421, 5E-098/FORS, 1000 Independence Ave., S. W., Washington DC 20585

39-40. DOE, Office of Scientific and Technical Information, Office of Information Service, P.O. Box 62, Oak Ridge, TN 37831

41. Robert M. Poteat, Office of Patent Counsel, Bldg. FED, MS 8751

42. Pamela L. Gorman, DOE-ORNL Site Office, Bldg. 4500-N, MS 6269

43. Laboratory Records, Bldg. 4500-N, MS 6285

44-48. M&C Records Office, Bldg. 4508, MS 6094